



RESEARCH MEMORANDUM

INVESTIGATION OF STRESSES DUE TO THERMAL GRADIENTS

IN TYPICAL AIRCRAFT STRUCTURES

By Martin E. Barzelay and James C. Boison

Syracuse University

NATIONAL ADVISORY COMMITTEE
FOR AERONAUTICS

WASHINGTON

January 25, 1952

NACA LIBRARY
LIBRARY AERONAUTICAL LABORATORY
Langley Field, Va.



3 1176 01434 3777

iM

NACA RM 51K06

NATIONAL ADVISORY COMMITTEE FOR AERONAUTICS

RESEARCH MEMORANDUM

INVESTIGATION OF STRESSES DUE TO THERMAL GRADIENTS
IN TYPICAL AIRCRAFT STRUCTURES

By Martin E. Barzelay and James C. Boison

SUMMARY

A series of five 75S-T6 aluminum-alloy elementary skin and spar-cap combinations with skin varying from 0.051 to 0.500 inch in thickness was investigated to determine the temperature and stress gradients resulting from the application of heat to the surface. The tests consisted of measuring the temperatures with thermocouples and the strains with bonded wire strain gages at selected points of the structure for three heating rates varying from 26,500 to 55,900 Btu per hour. The data are presented in the form of tables of the measured temperatures and stresses calculated from the measured strains. Curves are presented showing the effect of varying heating rate and skin thickness on the temperature and stress variation with time, on temperature variation with stress, on chordwise temperature and stress distributions, and on the temperature and stress differences between skin and spar cap.

INTRODUCTION

As pointed out in reference 1, new problems have been created for the aircraft designer by the advent of flight in the transonic and supersonic speed ranges, one of which is the determination of the magnitude of thermal stresses due to temperature gradients in the structure. In reference 1 measurements of temperature distributions were made throughout an aircraft wing for various heating rates in dive tests and a method presented for predicting the resultant stresses. It is pointed out, however, that "correlation between observed or estimated temperature gradients and the resultant thermal stresses is very difficult because of the limited test data available on the subject and because of the fact that the intricacies of an aircraft structure are not readily amenable to the analytic approach." Since few analytic solutions are available for temperature distribution, and these for but a few cross-sectional shapes, and since, furthermore, very little attempt has been

made to extend known temperature-distribution solutions to a determination of stress distribution, and in view of the meager experimental data available, the work described herein was undertaken. It was the purpose of this investigation to measure the temperature and stress gradients for a series of skin-thickness and spar-cap combinations for various heating rates in order to provide data which, when used in conjunction with further similar data, will permit a fundamental understanding of the phenomena involved, leading to an adequate theory for the prediction of thermal stresses in structures of the type investigated.

This investigation, conducted at Syracuse University, was sponsored by and conducted with the financial assistance of the National Advisory Committee for Aeronautics. The authors wish to thank Professor L. R. Parkinson for his advice in supervising this work.

SYMBOLS

ΔT_t	local temperature of plate above datum, °F
Δd_t	deflection of oscillograph galvanometer above datum due to transient heating, inches
Δd_c	deflection of oscillograph galvanometer above datum due to uniform heating, inches
Δd	deflection difference due to stress induced by transient heating, inches ($\Delta d_t - \Delta d_c$)
ϵ	strain, inches per inch
E_t	Young's modulus of elasticity at local temperature of plate, psi
σ	stress, psi
R	resistance, ohms
R_g	wire-strain-gage resistance, ohms
R_c	calibration resistance, ohms
K_g	calibration factor of wire strain gage, ohms per ohm per inch per inch

DESCRIPTION OF APPARATUS

A general view of the test installation is shown in figure 1. The Leeds and Northrup Micromaxes used for recording temperatures may be seen at A and the insulated oven with specimen in place at B. The sides and end C on which the bank of heaters D is mounted have been removed. The strain-recording installation, shown in figure 2, consisted of a 12-channel Miller Model H recording oscillograph A with Type C-2 amplifiers B and power supplies C. Low-frequency galvanometers of the D'Arsonval type were used in the oscillograph. The strain-gage bridge was supplied 6-volt (modified from normal 10 volt) 2000-cycle alternating current by the oscillator.

A close view of the insulated oven is shown in figure 3. Removable side and end panels such as those at A facilitated mounting of the specimen B and attachment of strain gage and thermocouple leads C. Strain gages are seen at D and thermocouples at E. The bank of 20 strip heaters faced the specimen at a distance of $1\frac{1}{2}$ inches when the oven end was in place. The 20 strip heaters, each rated 1000 watts at 230 volts, were connected in parallel and series groups so the 450-volt input to the oven would give approximately 820 watts output per strip, or a total of 16,400 watts when no external resistance was utilized. By switching in external resistances the wattage could be reduced to get the heating rates used in testing, computed from average data, as follows:

Heating rate	Amperes	Volts	Kilowatts	Btu/hr = Kw \times 3415
A	36.5	448	16.35	55,900
B	27.8	345	9.60	32,750
C	24.9	310	7.72	26,500

The temperature in the oven could also be held constant for calibration through the use of pyrometer controller A of figure 4 and a circuit-breaker arrangement. Heat input to the oven was controlled by the setting of knob B and amperage was read at C. The oven was also provided with a circulating-air system which, by means of the vacuum pump E of figure 1, evacuated air through a rake F of figure 3 at the lower edge of the specimen, and returned the air through a similar rake at the top of the specimen. This resulted in a constant temperature across the skin face as checked on a uniform-thickness plate. An air-cooled conduit G (fig. 3) for strain-gage leads was found desirable to minimize errors due to heating of the leads, and the short lengths of exposed lead from

the conduit to the gages were covered with ceramic insulators coated with silicone rubber. A similar conduit installation on the back face of the skin is not shown.

Strain-Gage Calibrator

In order to check strain-gage calibration at elevated temperatures, a constant bending moment could be applied to a 75S-T6 aluminum-alloy beam with bonded strain gage, and both this stressed beam and a corresponding unstressed beam with gage could be heated in the small oven A of figure 5. Loads were applied to the stressed beam ends B by means of the lever and cable system C and deformation of the beam center was read on the dial gage D. The sapphire rod E which transmitted this deformation reading through the oven wall was considered to expand a negligible amount at the temperatures involved. From known relationships for a constant-bending-moment beam and for the dimensions involved, the strain corresponding to dial-gage readings could be calculated and compared with oscillograph readings to calculate gage calibration factors.

TEST PROCEDURE

Description of Specimens

The test specimens consisted of skin and spar-cap combinations of 75S-T6 aluminum alloy simulating simplified wing cross sections at the main-spar location of representative types of aircraft, as shown in figure 6(a). The specimens were assembled with Al7S-T rivets countersunk at the skin face. Dimensions were chosen to give a series of skin thicknesses increasing by five approximately equal steps, in combination with a constant spar-cap and web thickness. Machining tolerances were held insofar as possible to give the same thermal bond for all mating surfaces and thus eliminate this factor as a variable. Free surfaces were left in the "as received" condition. The specimen was made oversize in that the skin was of sufficiently large area that measurements confined to the central portion were relatively free of heat-loss effects from the edges of the skin and the ends of the spar cap. The specimen was mounted in the oven with the axis of the spar cap vertical. Since the spar cap was made to overhang the skin at the end slightly the specimen rested on the spar-cap end. No restraint was provided the specimen beyond the negligible amount provided by positioning angles at the skin edges to which attachment was made through oversize bolt holes.

Strain Gages and Thermocouples

The strain gages and thermocouples were installed at the locations shown in figure 6(b). Gages G3 through G6 and thermocouples T3 through T6 gave stress and temperature measurements at intervals from the center line of the spar cap to a point 6 inches from this center line on the face of the specimen. Gages G7, G8, and G9 and thermocouples T7, T8, and T9 were located on the back of the skin away from the heater and G10, G11, T10, and T11 were on the side of the spar cap. Gages G1, G3, and G12 and thermocouples T1, T3, and T12 were so located to check on the symmetry of the data about the center line. All gages and thermocouples lay along a line perpendicular to the longitudinal axis of the spar cap, thus providing approximately uniaxial strain data for a two-dimensional cross section of the specimen. Strain gages were standard SR-4, Type AB-3, Bakelite wire resistance-type gages cemented to the specimen, using the manufacturer's recommended baking cycle. Jigs were constructed to apply pressure through silicone rubber pads over the gages during baking.

Washer-type thermocouples, attached to the specimen with screws, were used after some experimentation with both rolled and spot-welded types. It was found that a thin brass washer, when screwed tightly to the aluminum, gave an average temperature over the small area it covered, and that temperature differences, due to cement-layer thicknesses in the case of rolled-type thermocouples and due to nonuniform welds and localized hot spots in the case of the spot-welded types, would be eliminated. Heat-lag effects due to the mass of the washer will have small effect on the results, provided each washer is identical, since temperature differences between points at identical times are being determined rather than absolute values. Protection of the thermocouple junction with silicone rubber paste which hardened in place minimized errors due to direct heating of the junction.

The temperature-recording equipment was calibrated and adjusted prior to testing in accordance with the manufacturer's manual. In addition, prior to each installation of the thermocouples on a specimen, a calibration of each thermocouple and associated recording equipment was made at known temperatures.

Strain-Measurement Technique

As pointed out in reference 2, the use of strain gages to measure stress variation in structures subject to temperature changes gives rise to the problem of differentiating the strains due to stresses from those due to thermal expansion of the structures. Additional apparent strains due to heating of leads, change in resistance of gages, and change in gage calibration factor at elevated temperatures must be considered.

The commonly used method of compensating for these effects by utilizing a dummy gage at the same temperature as the active gage was not considered feasible, since the transient nature of the temperatures would involve applying the same transient temperature experienced by the active gage, without thermal stresses, to the dummy gage. The strain-measuring circuit and calibration procedure described in the following paragraph were therefore utilized to obviate this difficulty.

The strain-measuring circuit consisted of the two-leg bridge shown in figure 7(a). One leg consisted of the active gage bonded to the test specimen and the other consisted of a dummy leg bonded to a heavy bar of 75S-T6 aluminum D of figure 2. Since the accuracy of this method depends on the constancy of temperature at the dummy gage, the voltage across the bridge was kept as low as possible by utilizing a 6-volt circuit which resulted in 0.0748 watt to be dissipated at the dummy gage. In addition, a careful check was made to ascertain that the heavy bar to which the dummy gages were bonded did not change in temperature because of ambient-air-temperature changes during a test run. The temperature of this bar was found to be constant within $\pm 1^{\circ}$ F during all tests. It should perhaps be mentioned that the room in which the tests were conducted was an engine test cell with thick concrete walls and the ambient-air temperature varied only several degrees on any given day and remained within $\pm 6^{\circ}$ F for a period of several months.

For calibration a series of constant temperatures ranging from room temperature to approximately 320° F was held in the oven, and readings were taken of temperature and deformation. (The modification of the strain-measuring circuit for calibration is shown in fig. 7(b).) In this process the specimens were heat-soaked for at least 2 hours to insure constant temperature and therefore a thermal-stress-free condition throughout and readings were taken on the cooling cycle. As an additional precaution, data were taken for each strain-gage and thermocouple pair individually to allow for minor variations in thermocouple and strain-gage output, as well as minor variations in local plate temperatures. These data were then plotted as oscillograph deflection above datum against temperature above datum for each thermocouple and strain-gage pair; figure 8 is a typical plot of these data. The strain-recording bridge was balanced at room temperature by the schematic circuit shown in figure 7(a); the oscillograph deflection recorded at a given elevated temperature thus represented the output of the active gage due to thermal expansion, due to change in gage resistance with temperature, and due to any change in gage calibration factor with temperature, since the dummy gage remained at the constant room temperature. It should be noted that since the strain-gage leads, except for a short length (from 1 to 6 in. depending on location), were maintained at essentially room temperature in an air-cooled conduit the change in lead resistance, included in the aforementioned recorded deflection,

could be neglected. The small amount of apparent strain due to the exposed strain-gage leads between the conduit and the gages would cause error in the final results proportionate to the relative temperature difference of a given lead during a calibration and during a transient run. This error was calculated and found to be negligible.

During a transient run the strain-recording bridge was balanced at room temperature; the oscillograph deflection recorded at a given local elevated temperature (time synchronization of strain and temperature measurements enabled readings of both to be taken simultaneously at a given location on the specimen) thus represented the output of the active gage due to thermal expansion, due to change in gage resistance with temperature, due to change in gage calibration factor with temperature, and due to strain induced by thermal gradients. Subtraction of this reading from the calibration reading at the same temperature above datum yielded the galvanometer deflection, proportional to strain, due to induced thermal stress. This difference was then converted to a strain reading through calculations based on the oscillograph calibration described in appendix A. To convert strain to stress, Young's modulus of elasticity must be known. Since its value varies with temperature, corrections were made for the modulus at the local temperature of the plate by utilizing figure 9 which is replotted from reference 3 in a more convenient form. The room-temperature base used for figure 9 was taken from reference 4. The deviation of the room temperatures of the present investigation from this base gave a negligible change in the modulus. There is some indication that exposure time at temperature affects the modulus, but this effect was considered negligible on the basis of comparison with data presented for 24S-T3 aluminum alloy in reference 5. In addition, two-dimensional effects were neglected in the stress calculations.

The procedure outlined above is illustrated by an example in appendix B. As an alternative procedure, instead of utilizing a calibration curve for each gage of each specimen, the calibration data could have been averaged, yielding a single curve of strain against temperature which would be applicable for all gages. The former method was deemed more accurate, however, and was the method used, despite the increased calculation time involved.

Conduct of Tests

The transient tests were conducted by simultaneously starting the oven, the temperature recorders, and the oscillograph. During a test run the oscillograph was stopped and again started at intervals read on an accurate stop watch. The temperature-recording instruments took readings of each thermocouple every 14.4 seconds; this printing interval was carefully checked to insure time synchronization of the data.

At each heating rate for each specimen the transient run was repeated from two to three times to insure reliability and reproducibility of the data. The resultant temperature and galvanometer deflection readings for each series of runs were averaged, as shown in table I, prior to calculation of the stresses.

PRECISION OF DATA

The accuracy of the temperature measurements could not be precisely determined because of the effect of thermal lag, although as discussed elsewhere in this report the errors involved are not considered to be appreciable. Since the temperatures were recorded on equipment which was not continuously balancing and on which printed readings could vary $\pm 1^\circ$ F through mechanical misalignment or human reading error, the overall error was estimated to be $\pm 3^\circ$ F for transient runs and $\pm 2^\circ$ F for calibration runs.

A precise determination of the accuracy of the stress data was not practicable because of the large number of variables involved. Evaluation of some of the known precisions such as $\pm \frac{1}{2}$ percent for decade resistances used for calibration, $\pm \frac{1}{2}$ percent for gage resistances, and ± 1 percent for gage factor, together with an estimate of other factors affecting the results, resulted in what is believed to be a reasonable estimate of ± 300 psi for the accuracy of the stress data.

The constancy of heat input for a test run must also be considered because of changes in resistance of the strip heaters in the initial period of heating and because of voltage fluctuations. It was considered that the first 2 minutes of transient runs at the highest heating rate and the first 4 minutes of the slower runs should be considered unreliable and therefore not presented in the results. For the remainder of the transient heating period, an accuracy of ± 2 percent in nominal output of the heaters is considered reasonable. An examination of possible heat losses indicates that the probable variation in heat input to the specimens, including the variation in output of the heaters, could reasonably be estimated as ± 3 percent of the values of British thermal units per hour given for heating rates A, B, and C.

RESULTS AND DISCUSSION

The temperatures measured on each of the five specimens at selected time intervals for heating rates A, B, and C of 55,900, 32,750, and 26,500 Btu per hour, respectively, are presented in table I. The

intervals of time shown in the table are those corresponding to the times at which strain readings were taken by the oscillograph, although the temperature was recorded during a test run every 14.4 seconds at each thermocouple location. Since more than one test run was conducted for each heating rate, the number of the run in the sequence of runs for any specimen is shown in the table for identification purposes. The channel number is used to identify both the thermocouple and gage at a given location and corresponds with the designation of gages prefaced by G and thermocouples by T as shown in figure 6(b). The temperature section of this table is completed by averaging the temperatures for like transient runs at the same heating rate.

The galvanometer readings for each run are presented and averaged in table I for each transient run. These data, not in themselves pertinent, are included for completeness since the data in the following table II are calculated from them. Some discontinuities appear in these galvanometer data, representing points at which difficulties were experienced, such as strain-gage or circuit failures and unreadable or otherwise unreliable records.

The stress data calculated from the averaged galvanometer deflection readings by methods previously discussed are presented in table II for each specimen and heating rate. These stress data may be related to the temperature data of table I by noting the specimen number, heating rate, thermocouple or gage number, and the time.

The time history of temperature is presented in figure 10 for selected thermocouple locations and heating rates for all five specimens. The stresses corresponding to these locations for the same heating rates are plotted against time in figure 11. The locations selected as being most representative of the over-all behavior of the specimen were a point on the heated side of the skin over the spar cap (T3, G3), a point on the heated side close to the edge of the spar cap (T4, G4), a point on the heated side some distance from the spar cap (T5, G5), a point some distance from the spar cap on the rear face of the skin (T8, G8), and a point on the inner side of the spar cap (T11, G11). Heating rates A and C were chosen for presentation since they represent the two extremes of the data taken.

The effect of increasing skin thickness on temperature rise may be seen in figure 10. As would be expected the smaller mass heated more rapidly and thus the point farthest from the large mass of the spar cap T5 attained the highest temperature at any given time and increased in temperature at a greater rate than any of the points shown, although this behavior becomes decreasingly evident as skin thickness increases and heating rate decreases. Point T4 close to the spar cap shows the effect of the large mass in its lowered temperature compared with T5

for all specimens, but as the skin approaches the spar cap in mass, it is noted that T₄ becomes nearly identical with T₃. The stresses of figure 11 show some correspondence in general with the temperatures of figure 10. For specimen 5, rate A, for example, the nearly identical temperatures of T₄ and T₃ result in nearly identical stresses, but at point T₅ a temperature difference of only 10° F above the temperature of T₄ and T₃ results in a stress difference of 1500 psi, an appreciable stress difference for a small thermal gradient. Thus it is seen that the local thermal gradient does not always predominate in producing stress, but the total relationship of skin and spar-cap masses, heating rate, and such presently unassessable variables as thermal bond may be involved.

The stresses at the same locations used in the curves of figures 10 and 11 are plotted against temperature above datum in figure 12. Each set of curves in this figure is plotted for heating rate A for the sequence of specimens. Thus figure 12 reveals the difference in the nature of the stress as temperature increases for various positions on the specimen. For specimen 1, heating rate A, there is a large increase in temperature and a correspondingly high compression stress at position G₅, $1\frac{1}{2}$ inches from the edge of the spar cap; while at the spar cap the skin, although subject to less than half the temperature rise of the skin at G₅, shows a tension stress reasonably close in magnitude to the compression stress at G₅, 4700 psi in tension compared with 6600 psi in compression. The stress at G₄, influenced by the proximity of the spar cap, begins to increase in tension to 1500 psi as temperature increases, but as temperature increases further and with it the compression stress far from the spar cap, this tendency is reversed and the stress at G₄ reaches a compression of 3200 psi. At position G₁₁ on the inside face of the spar cap little temperature rise and stress increase were noted, the spar-cap mass having little time in which to heat.

It is also of interest to note that as skin thickness increases the curves for G₅ and for G₈, which is directly behind G₅ on the skin, become increasingly divergent (with the exception of specimen 2) indicating an increasing stress gradient through the skin due to the temperature gradient.

Examination of the set of curves for each specimen shows that the relationship between temperatures with increasing skin thickness remains qualitatively the same, although an outstanding exception occurs at G₄ close to the spar cap. In this case, perhaps more clearly seen in figure 13 where stress against temperature is plotted for each specimen at heating rate A, the tendency of G₄ to increase in tension and then reverse sign and become compression in the thinnest specimen is no longer apparent for the thicker skins. For specimen 2, G₄ increases in

compression steadily with temperature. With further increase in skin thickness, in specimen 3, the influence of the increasing mass of skin takes effect and the compression at first slowly increases with temperature and then decreases. For specimens 4 and 5 with heavy skins the stress remains virtually constant at very low values not exceeding 500 psi, with some tendency toward increasing tension. The remaining curves of figure 13 show a decrease in stress for G3, G5, G8, and G11 with increasing skin thickness and increasing temperature. Here again the predominance of factors other than direct temperature gradients on the stresses may be clearly seen.

The curves of figure 14 plotted for the highest and lowest heating rates, A and C, for specimens 1, 3, and 5 show the chordwise temperature distribution for several time intervals at the beginning, middle, and end of typical transient test runs. The distribution on the rear face of the skin is also shown for one time. The thin-skinned specimen 1 shows a sharp drop in temperature of the skin close to the spar cap due to the strong effect of the heavy spar cap relative to the thin skin. This sharp gradient becomes steeper with increasing time as the spar temperature lags behind the skin temperature for all specimens at all heating rates, but is most noticeable in figure 14(a) for the thinnest skin at the greatest heating rate. As the mass of the skin approaches that of the spar cap the gradient becomes less pronounced until for the thickest skin and slowest heating rate, specimen 5 at rate C, an almost uniform temperature rise is seen everywhere except for the innermost part of the spar cap at T11.

The chordwise stress distribution is plotted in figure 15 for the same heating rates and specimens as figure 14, though with some points omitted because of previously mentioned discontinuities in the data. The general trend of the curves indicates that the spar cap and the skin over the spar cap are in tension, and that this tension gradually reduces in magnitude as the distance from the spar cap increases, changes in sign, and becomes an increasing compression, for all but specimen 1. In specimen 1, instead of this continuous increase in compression with distance from the spar cap center line, the compression begins to decrease at a distance of 3 inches from the spar center line and finally a state of tension is reached about 6 inches from the center line. This trend is more marked for specimen 1 at heating rate A for the 8-minute time interval, but is also apparent at 12 minutes of heating rate C. There is some indication that buckling took place in the thin skin of specimen 1 which would explain the anomalous behavior of this specimen as mentioned above. If the average stress for the thin skin is computed at points where gages are opposite on the front and back faces of the skin, the average values are -1137 psi 6 inches from the center line and -1191 psi 3 inches from the center line at 4 minutes of heating rate A. Similarly, for 8 minutes of heating rate A the average values are -1137 psi 6 inches from the center line and 5600 psi 3 inches from

the center line. A plot of average stress for specimen 1 in figure 15(a), although not included, would appear similar to those for the other specimens which did not buckle.

In figure 15(e) it may be noted that as skin thickness increases and the heat flow path to the spar cap becomes correspondingly better, the influence of the spar cap reaches farther outboard on the skin; and the tendency to reverse from compression to tension is seen about 6 inches from the center line, though not to as noticeable a degree as in specimen 1 at 3 inches from the center line. For specimen 5 the point of reversal has apparently moved still farther out from the spar cap to the extent that the compression is still increasing at the 6-inch distance for all time intervals.

The effect of differences in heating rate and specimen skin thickness on temperatures and stresses is presented in figures 16 and 17. Upon examination of figure 16 it is seen that at the highest heating rate, 55,900 Btu per hour, for the thinnest skin, 0.051 inch, the temperature difference between T5 and T3 is 107° F at 8 minutes. At 9 minutes this temperature difference (not plotted) was 128° F. Increasing the skin thickness to 0.125 inch causes a drop in temperature difference between the same two points to slightly less than half the original value and a reduction in stress difference between the two points from 10,625 to 5712 psi. This reduction in temperature difference as skin thickness increases, which is also seen in the other curves of this figure, may be attributed to the greater mass of the skin which provides more heat-absorbing capacity relative to the spar cap, as well as a larger path for heat flow to the spar cap. This reduction in thermal gradient results in a reduction in stress differences as may be seen in figure 17, where the trend of reduced stress with decreasing heat rate and increasing skin thickness follows the trend of figure 16. Thus it would appear that the tendency in some present-day aircraft designs toward heavy skin with many stringers comparable in heat capacity with the skin will to some extent alleviate the thermal stress problem, but unless the skin and stringer combination is properly proportioned from a thermal stress standpoint this problem will still be encountered.

The curves of figure 18 may be of some interest, especially in view of the linearity of the stress difference when plotted against time for the thicker-skinned specimens.

Although an attempt was made to check measured stresses at the spar cap and nearby skin with stresses calculated using the procedure suggested in reference 1 no correlation was apparent. The proposed method especially failed to predict the large magnitude of the tensile stresses over the spar cap. This lack of correlation was due in part to the difficulty in assessing proper weight to such factors as thermal bond between skin and

spar cap, restraint of the skin by the spar cap, and choice of distance from the spar cap in the selection of temperature differences to be used in the calculations. It would thus appear that the proposal of an adequate theory for the prediction of stresses in components similar to those tested requires the study of a larger body of data than that presented here. Until such theory is available it is suggested that the data of this report be utilized where it is necessary to predict temperatures and stresses for structures of the type investigated. The curves contained in this report, which may be amplified by reference to the data of tables I and II, should be of practical value since the average heating rate for a given flight condition can be calculated by known methods to a fair degree of accuracy and a reasonable choice made of the specimen configuration most nearly representative of the actual installation in spar-cap mass and skin thickness. Thermal gradients and induced stresses may then be determined by reference to the data of this report.

CONCLUSIONS

From laboratory tests of a series of five specimens of varying skin thickness and constant spar-cap dimensions subject to the three heating rates of 55,900, 32,750, and 26,500 Btu per hour the following conclusions are made:

1. Large thermal gradients exist for combinations of heavy spar cap with thin skin and these gradients are considerably increased by high heating rates corresponding to those likely to occur in high-speed aircraft.
2. Stress changes of appreciable magnitude occur as a result of these large thermal gradients, but the stress difference between skin and spar cap may also be appreciable when only small thermal gradients exist for certain combinations of dimensions and heating rate.
3. Appreciable tensile stresses exist in the skin over the spar cap which will add to those due to aerodynamic loads. The influence of the heavy mass of the spar cap in providing tensile restraining forces extended for some distance out on the skin, causing the skin close to the spar cap to remain in tension for thin specimens at high heating rates.
4. Compressive stresses appreciably higher than predicted by simple theory were found for thin skins at high heating rates at a distance from the restraining spar cap.

5. Calculations of stress gradients based on measured temperature gradients appear to be unreliable when the assumption is made that the skin and spar-cap stresses are related to the completely restrained skin stress in proportion to percentages of spar-cap thickness as proposed in TN 1675.

6. Considerably more data are required for the complete evaluation of thermal stresses created by thermal gradients due to the large number of variables involved which cannot be taken into account by simplified thermoetical considerations.

Syracuse University

Syracuse, N. Y., July 31, 1950

APPENDIX A

CALIBRATION OF OSCILLOGRAPH

The calibration of the oscillograph was carried out by the commonly used method of applying known unbalances to one leg of the strain-measuring bridge and recording the resulting galvanometer deflections. The strain corresponding to the known unbalance was then calculated using the manufacturer's values for gage resistance and sensitivity factor. To insure accuracy of results the known unbalances were provided by accurate decade boxes and the gage resistance and sensitivity used in these calculations were checked for several gages bonded to 75S-T6 bars. These latter were found in all cases to fall within the manufacturer's stated tolerances of 119.5 ± 0.5 ohms for resistance and 2.08 ± 1 percent for gage sensitivity factor.

For this calibration, the strain-measuring circuit was modified, as shown in figure 7(b), to permit the application of the known unbalance through a series of decade resistance boxes and switch arrangements across one leg of the two-leg bridge. The two legs of the bridge chosen for this purpose were two adjacent gages of the set of dummy gages used throughout the testing, which were bonded to the heavy bar (seen at D in fig. 2) to insure adequate temperature stabilization. The input connection of this two-leg bridge was then plugged into each channel of the strain-measuring equipment in turn, the series of known unbalances applied to each channel, and the corresponding galvanometer deflections recorded. The strain corresponding to a given galvanometer reading could then be found through the relationship:

$$\epsilon = \frac{R_g}{K_g(R_c + R_g)} = \frac{119.5}{2.08(R_c + 119.5)}$$

It was noted in carrying out the calibration procedure that, although each channel was closely adjusted by the means provided to equalize the attenuation of all channels, some difference was apparently inherent in each channel. A separate calibration curve was therefore used for each channel.

APPENDIX B

METHOD OF CALCULATING STRESSES

The method of calculating stresses based on the principles outlined in the section entitled "Stress Measurement Technique" is as follows:

- (1) At a given time during a transient heating cycle, say for channel 7 at 12 minutes of heating rate A on specimen 4, the average local temperature rise ΔT_t was 114°F and the average galvanometer deflection reading from the recording oscillograph Δd_t was 0.30 inch from the same room-temperature datum condition (see table I).
- (2) For this temperature rise of 114°F , the galvanometer deflection Δd_c read from the typical calibration curve of figure 8 was 0.68 inch.
- (3) The difference between the deflections of items (1) and (2) above is that due to thermal stress. This difference is taken with regard to the proper sign indicating tension or compression. A deflection in item (1) greater than in item (2) indicates tension. For this example the difference Δd between Δd_t and Δd_c is -0.38 inch, or compression.
- (4) The deflection difference, representing induced thermal stress, is then converted to a strain reading by using the calibration curves for the strain-measuring equipment. This calibration is described in appendix A of this report. The strain corresponding to a galvanometer deflection of -0.38 inch for channel 7 was -1.99×10^{-4} inch per inch.
- (5) Since Young's modulus varies with temperature, in order to calculate the stress corresponding to a given strain at a point, reference is made to figure 9 where the proper modulus value is read corresponding to the local temperature above datum for either tension or compression. For this example, $E_t = 10.19 \times 10^6$ psi.
- (6) The local stress is then computed from the known strain and the modulus at temperature. For this example,

$$\sigma = \epsilon E = -1.99 \times 10^{-4} \times 10.19 \times 10^6 = -2028 \text{ psi.}$$
The stress data thus computed are shown in table II.

REFERENCES

1. Tendeland, Thorval, and Schlaff, Bernard A.: Temperature Gradients in the Wing of a High-Speed Airplane during Dives from High Altitudes. NACA TN 1675, 1948.
2. Jones, Alun R., and Schlaff, Bernard A.: An Investigation of a Thermal Ice-Prevention System for a C-46 Cargo Airplane. VII - Effect of the Thermal System on the Wing-Structure Stresses as Established in Flight. NACA ARR 5G20, 1945.
3. Heimerl, George J., and Roberts, William M.: Determination of Plate Compressive Strengths at Elevated Temperatures. NACA Rep. 960, 1950. (Formerly TN 1806.)
4. Miller, James A.: Stress-Strain and Elongation Graphs for Alclad Aluminum-Alloy 75S-T Sheet. NACA TN 1385, 1947.
5. Roberts, William M., and Heimerl, George J.: Elevated-Temperature Compressive Stress-Strain Data for 24S-T3 Aluminum-Alloy Sheet and Comparisons with Extruded 75S-T6 Aluminum Alloy. NACA TN 1837, 1949.

TABLE I

TEMPERATURE AND OSCILLOGRAPH DEFLECTION READINGS FOR FIVE SPECIMENS AND THREE HEATING RATES

(a) Specimen 1

Channel	Heating rate A								Heating rate B								Heating rate C							
	ΔT_t (°F)				Δt_t (in.)				ΔT_t (°F)				Δt_t (in.)				ΔT_t (°F)				Δt_t (in.)			
	Run 1	Run 2	Run 7	Av.	Run 2	Run 7	Av.	Run 3	Run 4	Run 9	Av.	Run 3	Run 4	Run 9	Av.	Run 5	Run 6	Run 10	Av.	Run 5	Run 6	Av.		
	Time, 2 min.								Time, 4 min.								Time, 6 min.							
1	14	10	16	13	0.02	-0.02	0	28	34	31	31	-0.03	0.06	0.02	43	46	45	45	0.20	0.24	0.22			
2	3	2	6	4	.14	.14	.14	10	10	7	10	.34	.44	.39	16	17	18	18	.70	.72	.71			
3	4	1	5	3	.13	.13	.13	6	5	5	6	.31	.41	.36	12	16	15	14	.64	.66	.65			
4	5	5	8	6	.13	.11	.12	14	14	15	14	.86	.37	.32	23	27	27	26	.57	.56	.57			
5	10	11	14	12	.01	-.01	-.01	23	27	26	25	-.03	.04	.01	38	46	42	42	.21	.18	.20			
6	10	10	14	11	.06	.05	.06	30	33	34	32	.01	-.06	-.04	55	61	52	57	.36	.43	.42			
7	13	11	15	13	0	-.05	-.03	31	33	32	32	-.13	-.07	-.10	52	69	56	60	.03	-.03	0			
8	6	8	10	8	.02	.01	.02	20	21	24	22	.02	-.08	.05	32	42	39	38	.21	.15	.18			
9	4	3	3	3	.09	.08	.09	11	12	12	12	.17	.26	.22	20	25	20	22	.44	.43	.43			
10	0	0	3	3	.01	-.06	-.04	3	2	3	3	-.13	.01	-.06	6	8	9	8	.06	.09	.06			
11	1	1	1	1	-.01	-.08	-.05	2	2	1	2	-.13	.05	-.09	4	9	8	7	.06	.09	.06			
12	6	11	22	13	----	----	----	27	27	24	26	----	----	----	37	40	38	38	----	----	----			
	Time, 4 min.								Time, 6 min.								Time, 12 min.							
1	53	46	55	51	0.19	0.10	0.15	54	59	56	56	0.39	0.25	0.18	105	107	103	105	0.95	0.97	0.96			
2	19	19	23	20	.79	.64	.72	22	22	22	26	.84	.81	.79	49	48	53	50	1.22	1.23	1.23			
3	19	14	19	17	.78	.61	.67	13	18	20	17	.76	.76	.77	43	47	46	45	1.15	1.17	1.16			
4	27	30	33	30	.61	.46	.54	34	34	34	34	.63	.63	.63	73	73	71	72	.87	.88	.88			
5	49	50	54	51	.13	-.04	.05	55	60	58	58	.20	.11	.05	112	112	118	114	.16	.14	.15			
6	62	65	69	64	.89	.43	.66	71	74	74	73	.56	.38	.47	143	146	138	142	.88	.93	.91			
7	61	61	66	63	-.05	-.05	-.05	71	72	73	72	-.02	-.11	-.07	143	143	138	141	.13	.22	.18			
8	42	45	45	43	.14	0	.07	50	51	53	51	.18	.15	.10	101	104	103	103	.18	.17	.18			
9	25	25	28	26	.42	.33	.38	30	30	30	30	.46	.47	.39	66	67	67	67	.66	.65	.66			
10	6	6	7	6	.07	-.08	0	11	10	9	10	----	.09	.05	31	31	32	3	.29	.30	.30			
11	4	6	6	5	.06	-.09	-.02	9	9	7	8	----	.07	-.01	.03	29	29	31	30	.37	.28	.33		
12	4	4	5	5	----	----	----	52	50	46	49	----	----	----	94	96	90	93	----	----	----			
	Time, 6 min.								Time, 8 min.								Time, 18 min.							
1	103	93	106	101	0.33	0.55	0.44	81	89	84	85	0.52	0.52	0.48	0.53	164	167	160	164	0.93	0.95	0.94		
2	41	41	48	43	1.09	1.07	1.08	34	38	38	37	1.13	1.20	1.15	92	91	94	92	1.57	1.57	1.57			
3	38	35	39	37	1.09	1.06	1.06	20	31	32	28	1.09	1.13	1.09	83	86	82	84	1.49	1.50	1.50			
4	58	67	69	65	.64	.60	.62	55	57	57	56	.84	.92	.87	.88	124	121	120	122	1.01	1.02	1.02		
5	102	109	112	106	-.04	-.10	-.07	88	94	90	91	.26	.23	.14	.21	174	177	169	173	.21	.19	.20		
6	131	138	141	135	.82	1.12	.97	113	121	118	117	.73	.64	.69	.69	219	223	214	219	----	----	----		
7	131	135	139	135	.01	.01	.01	112	119	115	115	.23	.19	.08	.17	215	217	210	214	.39	.39	.39		
8	91	104	101	99	-.03	-.03	-.03	79	83	83	82	.24	.25	.18	.22	162	164	160	162	.21	.22	.22		
9	56	60	61	59	.45	.46	.46	48	52	52	51	.62	.71	.64	.66	116	114	114	115	.80	.78	.79		
10	19	17	20	19	.18	.16	.17	19	20	18	19	.28	.34	.33	.32	63	65	64	64	.53	.53	.53		
11	18	19	18	18	.12	.16	.14	17	17	17	17	.32	.32	.27	.62	62	63	62	.49	.49	.49			
12	89	92	105	95	----	----	----	76	76	74	76	----	----	----	153	156	147	152	----	----	----			
	Time, 8 min.								Time, 12 min.								Time, 20 min.							
1	152	146	167	155	1.13	0.95	1.14	140	149	144	144	1.04	0.96	0.64	0.88	184	186	179	183	1.05	1.06	1.06		
2	72	67	78	72	1.31	1.29	1.30	68	73	72	71	1.49	1.56	1.41	1.48	106	106	105	106	1.69	1.66	1.66		
3	65	59	66	64	1.26	1.29	1.28	60	63	64	62	1.42	1.56	1.47	1.47	97	100	96	98	1.58	1.58	1.58		
4	99	111	110	107	.45	.44	.45	96	104	104	101	.94	.99	.84	.92	138	141	135	139	1.06	1.05	1.06		
5	162	172	178	170	-.09	-.16	-.13	149	159	157	155	.22	----	----	----	193	195	188	192	.25	.23	.24		
6	211	222	226	219	2.03	----	----	187	203	201	197	1.22	----	----	----	238	242	232	238	----	----	----		
7	216	214	221	217	.14	.19	.17	188	199	202	196	.40	.50	----	.45	235	236	230	234	.49	.49	.49		
8	149	166	162	158	-.23	-.18	-.21	137	145	145	142	.26	.28	----	.27	181	183	177	182	.24	.29	.27		
9	95	100	105	100	.38	.38	.35	91	98	95	95	.73	.82	----	.78	131	132	129	131	.86	.84	.85		
10	34	35	38	36	.32	.34	.33	42	42	44	43	.53	.61	----	.57	76	76	76	76	.66	.61	.61		
11	34	35	34	34	.32	.31	.30	40	42	41	41	.50	.63	----	.57	73	74	73	74	.56	.56	.56		
12	133	148	162	147	----	----	----	131	135	130	132	----	----	----	.77	170	173	163	169	----	----	----		
	Time, 9 min.								Time, 14 min.								Time, 21 min.							
1	195	176	202	191	1.20	1.10	1.15	167	179	173	173	1.17	1.23	0.88	1.09	191	193	187	190	1.10	1.12	1.11		
2	84	81	94	86	1.45	1.32	1.39	86	88	90	88	1.62	1.69	1.44	1.58	113	114	111	113	1.77	1.72	1.75		
3	75	73	80	77	1.33	1.33	1.33	77	79	82	79	1.53	1.63	1.45	1.54	104	105	101	103	1.62	1.64	1.63		
4	122	135	134	131	.33	.30	.32	118	128	125	125	.99	1.02	.76	.91	147	150	143	147	1.10	1.09	1.10		
5	194	207	213	207	-.10	-.17	-.14	177	190	187	185	.28	.26	----	.27	200	202	195	199	.29	.28	.29		
6	252	262	272	262	2.74	----	----	221	239	238	233	----	----	----	----	247	251	241	246	----	----	----		
7	249	245	265	253	.28	.30	.29	218	234	236	229	.50	.61	----	.56	242	244	238	241	.54	.54	.54		
8	180	203	195	193	-.24	-.24	-.24	164	174	176	172	.26	.24	----	.22	186	191	183	187	.27	.32	.30		
9	120	125	127	124	.27	.29	.28	112	120	118	117	.75	.84	----	.80	136	139	135	137	.69	.69	.69		
10	44	42	49	45	.39	.35	.37	57	57	61	58	.61	.70	----	.66	80	83	81	81	.64	.65	.65		
11	44	46	45	45	.34	.32	.33	54	57	57	56	.57	.64	----	.61	78	80	80	79	.60	.60	.60		
12	173	177	192	181	----	----	----	156	163	157	159	----	----	----	----	177	180	170	176	----	----	----		

TABLE I

TEMPERATURE AND OSCILLOGRAPH DEFLECTION READINGS FOR FIVE SPECIMENS AND THREE HEATING RATES - Continued

(b) Specimen 2

Channel	Heating rate A										Heating rate B										Heating rate C									
	ΔT (°F)					Δd (in.)					ΔT (°F)					Δd (in.)					ΔT (°F)					Δd (in.)				
	Run 5	Run 6	Run 7	Run 16	Av.	Run 5	Run 6	Run 7	Run 16	Av.	Run 8	Run 9	Run 10	Av.	Run 8	Run 9	Run 10	Av.	Run 17	Run 18	Av.	Run 17	Run 18	Av.						
Time, 4 min.																														
1	23	25	25	32	27	0.07	0.05	0.08	—	0.07	17	14	14	15	0.02	0.02	0.04	29	30	30	0.01	0	0.01	23	23	23				
2	15	18	18	16	16	0.21	0.23	0.23	0.23	0.23	9	7	7	8	0.16	0.11	0.14	12	13	13	0.23	0.22	0.23	13	13	13				
3	18	17	16	18	16	0.17	0.19	0.18	0.20	0.18	9	6	6	7	0.14	0.07	0.12	10	13	12	0.18	0.20	0.19	13	12	12				
4	18	22	22	22	21	0.26	0.13	0.14	0.19	0.18	4	12	9	8	0.09	0.05	0.06	19	20	20	0.16	0.19	0.18	20	20	20				
5	29	31	31	32	31	0.02	0.02	0.02	0.04	0	20	16	14	17	0.01	0.02	0.01	26	26	27	0.07	0.06	0.06	27	27	27				
6	27	34	32	36	32	0.01	0.01	0.04	0.07	0.03	23	22	20	20	0.03	0.01	0.02	32	33	33	0.07	0.06	0.07	33	33	33				
7	26	33	31	34	32	0.09	0.09	0.02	0	0.03	22	15	13	17	0.01	0.03	0.01	30	32	31	0.02	0.02	0.02	32	31	32				
8	22	25	24	25	24	0	0	0	0	0	13	12	12	12	0.01	0.02	0	21	21	22	0.09	0.08	0.09	22	22	22				
9	17	4	2	18	4	0.07	0.09	0.10	0.18	0.11	10	9	8	9	0.07	0.03	0.03	13	20	19	0.22	0.33	0.23	20	19	20				
10	4	2	3	4	3	0.11	0.10	0.10	0.11	0.10	1	1	1	1	0.06	0.03	0.03	4	5	5	0.09	0.11	0.10	5	5	5				
11	2	3	3	2	2	0.10	0.07	0.09	0.10	0.09	0	1	1	1	0.06	0.01	0.05	4	5	5	0.09	0.09	0.09	5	5	5				
12	19	25	19	26	22	0.09	0.04	0.07	—	0.09	13	9	16	11	0.05	0.02	0.04	22	25	24	0	0.01	0.01	25	24	24				
Time, 6 min.																														
1	35	63	60	68	63	0.10	0.07	0.07	—	0.08	53	49	—	51	0.11	0.08	0.12	75	79	77	0.07	0.06	0.07	75	75	75				
2	34	39	38	38	37	0.47	0.35	0.36	0.44	0.38	32	31	31	31	0.46	0.42	0.42	44	47	45	0.39	0.39	0.39	45	45	45				
3	26	38	36	36	35	0.39	0.36	0.37	0.39	0.39	31	29	29	29	0.37	0.32	0.32	33	36	35	0.36	0.36	0.36	36	36	36				
4	41	41	41	41	41	0.37	0.22	0.22	0.28	0.27	42	40	38	38	0.28	0.23	0.23	43	47	45	0.33	0.33	0.33	45	45	45				
5	65	68	65	65	65	0.06	0.06	0.09	0.04	0.04	62	62	62	62	0.04	0.03	0.01	80	81	80	0.01	0.01	0.01	80	80	80				
6	73	73	73	73	73	0	0	0	0	0	73	69	66	66	0.04	0.03	0.03	98	100	99	0.04	0.04	0.04	98	98	98				
7	72	86	77	77	77	0	0	0	0	0	62	62	62	62	0.04	0.03	0.03	98	100	99	0.04	0.04	0.04	98	98	98				
8	53	53	53	53	53	0	0	0	0	0	47	47	47	47	0.06	0.03	0.07	70	73	72	0.17	0.17	0.17	72	72	72				
9	42	45	45	45	45	0.19	0.21	0.20	0.27	0.27	35	37	37	37	0.23	0.23	0.23	53	55	55	0.36	0.36	0.36	55	55	55				
10	15	15	15	15	15	0.31	0.27	0.29	0.29	0.29	15	13	13	13	0.23	0.19	0.21	26	28	28	0.36	0.36	0.36	28	28	28				
11	11	14	14	14	14	0.28	0.22	0.22	0.27	0.27	13	12	12	12	0.20	0.16	0.19	26	28	27	0.35	0.35	0.35	28	27	28				
12	49	53	49	58	53	0.08	0.04	0.04	—	0.04	49	42	43	43	0.13	0.09	0.12	66	68	67	0.06	0.07	0.07	67	67	67				
Time, 12 min.																														
1	99	106	99	112	104	0.11	—	0.07	—	0.09	96	93	96	93	0.17	0.15	0.17	127	132	129	0.15	0.15	0.15	127	127	127				
2	62	68	68	66	66	0.72	0.72	0.74	0.69	0.73	63	63	63	63	0.74	0.74	0.74	86	88	87	0.94	0.94	0.94	87	87	87				
3	34	64	61	62	62	0.66	0.66	0.63	0.63	0.62	60	59	59	59	0.63	0.63	0.63	86	90	88	0.90	0.83	0.83	88	88	88				
4	73	84	81	90	83	0.25	0.25	0.26	0.34	0.28	78	77	77	77	0.36	0.36	0.36	107	111	109	0.71	0.71	0.71	109	109	109				
5	109	113	109	122	113	0.11	0.11	0.11	0.05	0.10	104	104	104	104	0.11	0.08	0.09	127	132	129	0.15	0.15	0.15	127	127	127				
6	118	133	128	134	128	0.05	0.03	0.04	0.13	0.07	128	124	127	126	0.11	0.08	0.09	127	132	129	0.15	0.15	0.15	127	127	127				
7	126	139	123	136	129	0.25	0.25	0.23	0.34	0.28	128	124	127	126	0.11	0.08	0.09	127	132	129	0.15	0.15	0.15	127	127	127				
8	94	99	99	106	99	0.01	0.01	0.01	0.01	0.01	91	91	91	91	0.04	0.04	0.04	122	128	125	0.06	0.06	0.06	122	122	122				
9	73	73	71	81	73	0.38	0.36	0.36	0.33	0.36	70	73	70	71	0.45	0.42	0.45	99	113	106	0.86	0.86	0.86	106	106	106				
10	89	92	90	92	91	0.31	0.36	0.44	0.33	0.31	38	37	37	37	0.49	0.44	0.47	60	66	63	0.66	0.66	0.66	63	63	63				
11	27	31	29	31	29	0.34	0.44	0.43	0.47	0.47	34	33	34	34	0.43	0.38	0.41	38	64	61	0.61	0.61	0.61	61	61	61				
12	86	92	89	97	91	0.05	0.03	0.03	—	0.01	90	89	89	89	0.16	0.16	0.16	115	122	119	0.17	0.17	0.17	119	119	119				
Time, 16 min.																														
1	146	141	143	160	148	0.06	0.01	0.03	—	0.03	141	141	141	142	0.24	0.21	0.23	173	180	177	0.34	0.32	0.33	177	177	177				
2	93	99	92	102	97	1.09	0.99	1.01	0.97	1.02	97	93	96	93	1.09	1.09	1.09	127	132	129	1.28	1.28	1.28	127	127	127				
3	89	97	90	103	94	0.90	0.82	0.81	0.83	0.84	94	94	94	96	0.91	0.90	0.91	127	132	129	1.09	1.11	1.10	127	127	127				
4	115	126	120	132	123	0	0.26	0.27	0.36	0.30	119	119	119	119	0.53	0.53	0.53	158	158	159	0.94	1.01	1.00	158	158	158				
5	159	163	156	172	163	0.07	0.11	0.10	0.03	0.08	150	150	152	151	0.06	0.06	0.06	184	193	189	0.38	0.37	0.38	189	189	189				
6	175	192	183	188	184	0.36	0.36	0.35	0.67	0.54	181	180	181	181	0.27	0.27	0.27	215	220	217	0.57	0.63	0.61	217	217	217				
7	184	186	179	196	186	0.36	0.36	0.35	0.69	0.66	176	177	177	176	0.32	0.32	0.32	209	216	213	0.68	0.74	0.70	213	213	213				
8	141	147	139	154	143	—	—	—	—	—	135	137	140	137	0.10	0.07	0.09	169	169	169	0.38	0.40	0.40	169	169	169				
9	115	115	108	123	115	0.45	0.39	0.41	0.38	0.41	109	111	112	111	0.62	0.61	0.62	143	153	143	1.03	1.03	1.03	143	143	143				
10	87	90	89	99	90	0.78	0.69	0.71	0.69	0.69	63	62	63	62	0.71	0.65	0.67	97	101	99	0.84	0.84	0.84	99	99	99				
11	47	50	49	58	54	0	0	0	0	0	47	47	47	47	0.22	0.22	0.22	62	66	65	0.37	0.37	0.37	65	65	65				
12	132	135	127	141	134	0	0.07	0.08	—	0.02	133	124	132	130	0.28	0.25	0.26	161	166	163	0.37	0.37	0.37	163	163	163				
Time, 20 min.																														
1	187	202	195	213	199	0.16	—	0.12	—	0.12	183	186	189	185	0.38	0.38	0.38	201	207	204	0.44	0.50	0.47	204	204	204				
2	185	196	193	213	197	1.03	1.22	1.23	1.03	1.23	134	134	134	134	1.14	1.14	1.14	185	195	185	1.33	1.33	1.33	185	185	185				
3	123	137	130	147	134	1.03	1.03	1.03	1.03	1.03	130	130	132	131	1.13	1.17	1.17	196	198	198	1.32	1.32	1.32	198	198	198				
4	192	170	161	181	171	0.31	0.41	0.41	0.36	0.36	158	160	160	160	0.78	0.78	0.78	177	179	178	1.09	1.09	1.09	178	178	178				
5	204	224	214	244	214	—	—	—	—	—	193	198	198	194	0.24	0.27	0.26	212	221	217	0.49	0.55	0.52	217	217	217				
6	238	250	244	264	244	1.23	1.59	1.69	1.28	1.28	230	234	234	231	0.70	0.88	0.88	241	249	245	0.73	0.82	0.78	245	245	245				
7	231	254	243	283	243	1.23	1.04	1.01	1.23	1.23	224	228	228	224	0.33	0.33	0.33	236	244	241	0.55	0.62	0.59	241	241	241				
8	182	201	1																											

TABLE I
TEMPERATURE AND OSCILLOGRAPH DEFLECTION READINGS FOR FIVE SPECIMENS AND THREE HEATING RATES - Continued

(c) Specimen 3

Channel	Heating rate A								Heating rate B								Heating rate C									
	ΔT_c (°F)				ΔT_c (in.)				ΔT_c (°F)				ΔT_c (in.)				ΔT_c (°F)				ΔT_c (in.)					
	Run 1	Run 2	Run 3	Av.	Run 1	Run 2	Run 3	Av.	Run 3	Run 4	Av.	Run 3	Run 4	Av.	Run 5	Run 6	Run 9	Av.	Run 5	Run 6	Run 9	Av.	Run 5	Run 6	Run 9	Av.
Time, 4 min.																										
1	14	16	14	15	0.01	0	-0.05	-0.01	18	21	20	0.02	0.04	0.03	15	11	12	13	0.03	0.03	0.03	0.03	0.03	0.03	0.03	0.03
2	10	11	12	11	0.06	0.07	0.05	0.06	13	18	16	0.12	0.13	0.13	10	9	9	9	0.11	0.09	0.06	0.09	0.06	0.09	0.06	0.09
3	8	13	10	10	0.07	0.06	0.05	0.06	13	15	14	0.10	0.10	0.10	10	10	6	9	0.08	0.06	0.05	0.07	0.04	0.06	0.05	0.07
4	10	13	11	11	0.07	0.05	0.03	0.05	15	18	17	0.08	0.09	0.09	12	10	8	10	0.07	0.07	0.04	0.03	0.03	0.03	0.03	0.03
5	13	18	17	16	0.02	0	-0.01	0	22	23	24	0.02	0.03	0.03	15	15	11	14	0.02	0.03	0.02	0.02	0.02	0.02	0.02	0.02
6	23	22	18	21	0	0.01	0.03	0.01	26	31	29	0.05	0.05	0.05	19	17	14	17	0.03	0.04	0.03	0.01	0.01	0.01	0.01	0.01
7	12	17	13	14	0.01	0.02	0.01	0.01	22	26	24	0.01	0.03	0.02	14	13	11	13	0.02	0.02	0.01	0.01	0.01	0.01	0.01	0.01
8	8	12	9	10	0.04	0.02	0	0.02	17	23	20	0.02	0.04	0.03	11	9	9	10	0.03	0.02	0.01	0.02	0.02	0.02	0.02	0.02
9	6	10	7	8	0.05	0.05	0.05	0.05	12	13	13	0.07	0.09	0.08	7	8	7	7	0.07	0.06	0.03	0.05	0.03	0.05	0.03	0.05
10	0	3	2	2	0.10	0.11	0.09	0.10	6	7	7	0.11	0.12	0.12	3	2	2	2	0.09	0.10	0.04	0.08	0.04	0.08	0.04	0.08
11	1	1	3	2	0.10	0.06	0.09	0.09	6	7	6	0.11	0.12	0.12	2	1	2	2	0.09	0.03	0.05	0.06	0.05	0.06	0.05	0.06
12	7	10	9	9	0	-0.01	0	0	15	16	16	0.02	0.04	0.03	11	7	6	8	0.03	0.07	0.03	0.04	0.03	0.04	0.03	0.04
Time, 6 min.																										
1	70	67	56	64	0.13	0.12	0.20	0.15	68	73	71	0.20	0.22	0.21	51	47	38	45	0.17	0.14	0.24	0.18	0.18	0.18	0.18	0.18
2	52	49	49	50	0.36	0.39	0.38	0.39	62	61	61	0.47	0.50	0.49	40	39	33	37	0.36	0.36	0.33	0.30	0.30	0.30	0.30	0.30
3	50	53	45	49	0.30	0.35	0.33	0.33	54	57	56	0.40	0.42	0.41	39	37	28	35	0.30	0.30	0.29	0.30	0.29	0.30	0.29	0.30
4	53	53	46	51	0.29	0.31	0.31	0.30	56	61	59	0.38	0.42	0.40	42	39	32	38	0.31	0.30	0.29	0.30	0.29	0.30	0.29	0.30
5	74	71	58	71	0.08	0.07	0.10	0.08	90	95	93	0.15	0.17	0.16	66	63	59	63	0.13	0.13	0.15	0.16	0.15	0.16	0.15	0.16
6	74	71	58	71	0.08	0.07	0.10	0.08	77	81	79	0.11	0.13	0.12	66	63	59	63	0.13	0.13	0.15	0.16	0.15	0.16	0.15	0.16
7	78	77	57	75	0.14	0.12	0.13	0.13	66	69	68	0.18	0.21	0.20	44	42	34	40	0.16	0.15	0.15	0.15	0.15	0.15	0.15	0.15
8	46	49	40	45	0.30	0.28	0.30	0.29	54	54	53	0.35	0.39	0.37	35	35	29	34	0.28	0.28	0.29	0.28	0.28	0.28	0.28	0.28
9	23	28	24	25	0.44	0.45	0.43	0.44	35	38	37	0.46	0.48	0.47	25	21	20	22	0.35	0.33	0.31	0.33	0.31	0.33	0.31	0.33
10	23	24	22	23	0.37	0.40	0.39	0.39	35	37	36	0.40	0.42	0.41	24	20	22	20	0.28	0.28	0.25	0.27	0.25	0.27	0.25	0.27
11	51	56	45	50	0.12	0.14	0.20	0.15	58	62	60	0.22	0.24	0.24	43	39	32	38	0.17	0.16	0.20	0.18	0.20	0.18	0.20	0.18
12	51	56	45	50	0.12	0.14	0.20	0.15	58	62	60	0.22	0.24	0.24	43	39	32	38	0.17	0.16	0.20	0.18	0.20	0.18	0.20	0.18
Time, 8 min.																										
1	70	67	56	64	0.13	0.12	0.20	0.15	68	73	71	0.20	0.22	0.21	51	47	38	45	0.17	0.14	0.24	0.18	0.18	0.18	0.18	0.18
2	52	49	49	50	0.36	0.39	0.38	0.39	62	61	61	0.47	0.50	0.49	40	39	33	37	0.36	0.36	0.33	0.30	0.30	0.30	0.30	0.30
3	50	53	45	49	0.30	0.35	0.33	0.33	54	57	56	0.40	0.42	0.41	39	37	28	35	0.30	0.30	0.29	0.30	0.29	0.30	0.29	0.30
4	53	53	46	51	0.29	0.31	0.31	0.30	56	61	59	0.38	0.42	0.40	42	39	32	38	0.31	0.30	0.29	0.30	0.29	0.30	0.29	0.30
5	74	71	58	71	0.08	0.07	0.10	0.08	90	95	93	0.15	0.17	0.16	66	63	59	63	0.13	0.13	0.15	0.16	0.15	0.16	0.15	0.16
6	74	71	58	71	0.08	0.07	0.10	0.08	77	81	79	0.11	0.13	0.12	66	63	59	63	0.13	0.13	0.15	0.16	0.15	0.16	0.15	0.16
7	78	77	57	75	0.14	0.12	0.13	0.13	66	69	68	0.18	0.21	0.20	44	42	34	40	0.16	0.15	0.15	0.15	0.15	0.15	0.15	0.15
8	46	49	40	45	0.30	0.28	0.30	0.29	54	54	53	0.35	0.39	0.37	35	35	29	34	0.28	0.28	0.29	0.28	0.28	0.28	0.28	0.28
9	23	28	24	25	0.44	0.45	0.43	0.44	35	38	37	0.46	0.48	0.47	25	21	20	22	0.35	0.33	0.31	0.33	0.31	0.33	0.31	0.33
10	23	24	22	23	0.37	0.40	0.39	0.39	35	37	36	0.40	0.42	0.41	24	20	22	20	0.28	0.28	0.25	0.27	0.25	0.27	0.25	0.27
11	51	56	45	50	0.12	0.14	0.20	0.15	58	62	60	0.22	0.24	0.24	43	39	32	38	0.17	0.16	0.20	0.18	0.20	0.18	0.20	0.18
12	51	56	45	50	0.12	0.14	0.20	0.15	58	62	60	0.22	0.24	0.24	43	39	32	38	0.17	0.16	0.20	0.18	0.20	0.18	0.20	0.18
Time, 10 min.																										
1	97	100	86	94	0.24	0.19	0.24	0.22	107	115	111	0.35	0.36	0.36	97	90	78	88	0.36	0.36	0.36	0.36	0.36	0.36	0.36	0.36
2	82	82	74	79	0.59	0.59	0.54	0.57	91	96	94	0.76	0.78	0.77	81	76	67	75	0.72	0.68	0.63	0.68	0.63	0.68	0.63	0.68
3	76	76	66	73	0.73	0.73	0.64	0.68	87	91	89	0.69	0.66	0.68	79	73	65	73	0.60	0.58	0.53	0.57	0.53	0.57	0.53	0.57
4	82	81	78	78	0.48	0.48	0.41	0.46	91	97	94	0.63	0.67	0.65	82	77	65	73	0.63	0.61	0.57	0.60	0.57	0.60	0.57	0.60
5	104	105	92	100	0.16	0.15	0.14	0.15	112	116	114	0.30	0.33	0.32	96	93	76	89	0.32	0.35	0.33	0.33	0.33	0.33	0.33	0.33
6	137	129	111	126	0.11	0.09	0.11	0.10	137	142	140	0.26	0.27	0.27	118	112	92	107	0.27	0.31	0.30	0.29	0.29	0.29	0.29	0.29
7	103	98	91	97	0.11	0.08	0.08	0.10	121	126	124	0.20	0.21	0.21	104	100	81	95	0.24	0.23	0.21	0.23	0.21	0.23	0.21	0.23
8	89	86	76	84	0.22	0.20	0.17	0.20	100	104	102	0.34	0.35	0.35	86	81	69	79	0.37	0.34	0.31	0.34	0.31	0.34	0.31	0.34
9	72	76	64	74	0.48	0.47	0.40	0.45	85	86	86	0.59	0.62	0.61	75	71	59	68	0.59	0.56	0.57	0.57	0.57	0.57	0.57	0.57
10	41	45	40	42	0.66	0.66	0.59	0.64	62	66	64	0.72	0.72	0.72	58	56	46	53	0.65	0.61	0.54	0.60	0.54	0.60	0.54	0.60
11	40	42	38	40	0.58	0.57	0.51	0.55	61	63	62	0.61	0.62	0.62	55	52	45	51	0.56	0.53	0.47	0.53	0.47	0.53	0.47	0.53
12	80	87	72	80	0.25	0.24	0.23	0.24	95	100	98	0.41	0.42	0.42	87	79	67	77	0.40	0.39	0.39	0.39	0.39	0.39	0.39	0.39
Time, 12 min.																										
1	134	137	120	131	0.35	0.29	0.29	0.31	147	153	150	0.53	0.57	0.55	142	134	132	136	0.50	0.57	0.51	0.55	0.51	0.55	0.51	0.55
2	113	113	105	110	0.84	0.84	0.79	0.79	128	133	131	1.05	1.08	1.07	125	118	115	119	1.05	0.99	0.90	0.98	0.90	0.98	0.90	0.98
3	107	110	98	105	0.70	0.70	0.65	0.65	125	128	127	0.86	0.90	0.88	121	114	108	115	0.86	0.83	0.75	0.81	0.75	0.81	0.75	0.81
4	115	113	101	110	0.68	0.71	0.65	0.65	128	134	1															

TABLE I

TEMPERATURE AND OSCILLOGRAPH DEFLECTION READINGS FOR FIVE SPECIMENS AND THREE HEATING RATES - Continued.

(a) Specimen 4

Channel	Heating rate A								Heating rate B								Heating rate C							
	ΔT (°F)				Δd (in.)				ΔT (°F)				Δd (in.)				ΔT (°F)				Δd (in.)			
	Run 3	Run 4	Run 11	Av.	Run 3	Run 4	Run 11	Av.	Run 1	Run 2	Run 9	Av.	Run 1	Run 2	Run 9	Av.	Run 3	Run 6	Run 8	Av.	Run 3	Run 6	Run 8	Av.
Time, 4 min.																								
1	15	15	16	15	0.02	0.01	0.01		29	30	30	0.06	0.09	0.15	0.10		21	24	23	23	0.06	0.05	0.10	0.07
2	14	12	12	12	.07	.07	.07	.07	28	29	29	.19	.21	.21	.21	.21	20	21	20	.15	.15	.15	.15	
3	10	10	12	11	.07	.06	.06	.06	23	23	23	.16	.18	.19	.19	.19	17	16	15	.12	.12	.12	.12	
4	11	12	13	12	.08	.07	.06	.07	23	26	24	.17	.19	.21	.19	.19	20	20	19	.14	.22	.14	.17	
5	13	14	14	14	.05	.03	.04	.04	28	29	29	.10	.11	.13	.11	.11	22	21	21	.10	.09	.09	.09	
6	14	16	19	16	.04	.04	.05	.04	32	35	35	.10	.11	.11	.11	.11	22	25	24	.09	.06	.10	.09	
7	9	10	11	10	.03	.03	.03	.03	21	27	27	.19	.09	.08	.12	.12	17	20	18	.07	.04	.07	.06	
8	6	7	7	7	.05	.05	.05	.05	20	20	20	.12	.13	.13	.13	.13	15	17	15	.09	.06	.06	.06	
9	5	5	5	5	.05	.05	.05	.05	15	17	17	.15	.15	.15	.15	.15	15	14	13	.10	.10	.11	.11	
10	3	3	3	3	.05	.05	.05	.05	10	9	10	.19	.19	.19	.19	.19	9	9	9	.11	.11	.12	.11	
11	3	3	3	3	.05	.05	.05	.05	6	9	8	.17	.17	.17	.17	.17	5	7	7	.10	.11	.11	.11	
12	6	9	9	9	.04	.02	.02	.03	22	21	22	.10	.12	.12	.11	.11	16	17	16	.08	.07	.07	.07	
Time, 8 min.																								
1	62	63	64	63	0.11	0.10	0.12	0.11	32	63	61	0.17	0.22	0.26	0.22		69	72	72	71	0.27	0.28	0.27	0.27
2	62	63	64	63	.36	.36	.36	.36	32	32	32	.43	.47	.47	.47	.47	63	66	68	.54	.57	.57	.56	
3	48	49	50	49	.31	.32	.33	.32	49	49	49	.37	.40	.40	.40	.40	59	59	59	.46	.47	.47	.47	
4	49	50	51	50	.34	.34	.34	.34	50	51	51	.36	.43	.43	.43	.43	60	62	62	.52	.53	.52	.52	
5	47	47	47	47	.18	.17	.18	.18	36	36	36	.23	.26	.27	.27	.27	62	67	67	.53	.53	.53	.53	
6	69	72	71	71	.15	.13	.15	.14	67	70	70	.24	.22	.23	.23	.23	80	76	76	.31	.31	.31	.31	
7	30	30	32	31	.15	.15	.15	.15	45	45	45	.29	.21	.18	.23	.23	63	67	68	.46	.45	.45	.45	
8	42	42	42	42	.21	.21	.21	.21	44	44	44	.26	.29	.29	.29	.29	57	57	57	.36	.35	.35	.35	
9	39	39	40	39	.27	.28	.28	.28	39	39	39	.42	.34	.34	.33	.34	49	53	53	.40	.43	.43	.44	
10	22	22	23	22	.37	.34	.36	.36	26	26	26	.39	.41	.41	.41	.41	36	40	39	.42	.43	.43	.44	
11	22	19	24	22	.34	.34	.34	.34	24	24	24	.29	.32	.32	.32	.32	35	37	38	.38	.38	.38	.38	
12	49	51	48	49	.19	.17	.17	.18	51	51	51	.24	.27	.27	.27	.27	60	61	61	.33	.37	.34	.35	
Time, 12 min.																								
1	128	129	129	129	0.25	0.26	0.29	0.27	117	120	115	0.38	0.44	0.54	0.45		124	129	131	128	0.59	0.59	0.53	0.54
2	120	117	121	119	.77	.81	.79	.79	107	107	112	.83	.88	.88	.88	.88	116	119	123	1.01	1.02	1.02	1.02	
3	101	104	105	103	.67	.70	.70	.69	97	101	94	.97	.76	.76	.74	.73	105	108	112	.84	.89	.83	.83	
4	104	107	106	106	.73	.71	.76	.73	96	101	99	.99	.76	.83	.83	.83	101	108	111	.89	.97	.83	.96	
5	116	117	116	116	.39	.38	.43	.40	107	112	110	.46	.44	.44	.44	.44	117	120	125	.69	.63	.64	.64	
6	142	147	141	143	.29	.28	.32	.30	123	131	127	.48	.44	.44	.44	.44	140	143	144	.39	.37	.36	.37	
7	112	117	113	114	.29	.31	.31	.30	103	112	106	.48	.43	.43	.43	.43	120	124	128	.30	.29	.29	.29	
8	93	96	98	96	.44	.46	.46	.46	93	95	94	.50	.51	.50	.50	.50	106	109	113	.66	.66	.66	.66	
9	84	89	89	87	.59	.62	.61	.61	84	89	87	.63	.62	.62	.62	.62	98	101	107	.75	.78	.78	.77	
10	59	58	61	59	.77	.76	.78	.77	65	67	66	.72	.77	.77	.77	.77	80	82	86	.83	.81	.81	.80	
11	59	54	57	57	.70	.70	.70	.70	61	66	66	.63	.64	.64	.64	.64	80	83	83	.70	.67	.67	.69	
12	106	110	110	109	.43	.42	.40	.42	102	102	102	.52	.57	.52	.52	.52	112	114	117	.68	.72	.66	.69	
Time, 16 min.																								
1	200	200	196	199	0.62	0.52	0.59	0.57	170	176	169	0.63	0.73	0.78	0.71		177	182	182	0.83	0.91	0.84	0.85	
2	184	181	184	183	1.30	1.37	1.34	1.34	159	164	159	1.22	1.32	1.32	1.27	1.27	165	169	176	1.38	1.50	1.44	1.44	
3	162	164	165	164	1.04	1.15	1.10	1.10	137	138	134	1.04	1.14	1.06	1.08	1.03	153	157	163	1.19	1.33	1.19	1.23	
4	163	170	168	167	1.23	1.20	1.19	1.21	148	154	149	1.50	1.37	1.25	1.25	1.25	159	162	170	1.36	1.46	1.40	1.41	
5	185	186	181	184	.70	.73	.73	.71	161	167	162	.63	.70	.79	.80	.76	169	173	179	.93	.99	.94	.99	
6	219	222	215	219	.56	.67	.58	.60	184	192	183	.66	.72	.69	.66	.66	196	198	202	.86	.94	.87	.89	
7	185	188	182	185	.58	.64	.64	.62	158	169	163	.63	.72	.69	.66	.66	172	178	186	.79	.83	.78	.79	
8	159	161	160	160	.79	.80	.77	.77	145	150	144	.76	.86	.86	.86	.86	156	161	165	.93	1.02	.93	.96	
9	144	149	144	146	.98	1.03	.98	1.00	133	141	137	.94	1.01	.99	.99	.99	145	150	157	1.08	1.18	1.10	1.12	
10	107	109	109	108	1.17	1.20	1.09	1.13	110	115	109	1.11	1.04	1.12	1.02	1.06	125	130	134	1.09	1.22	1.14	1.14	
11	106	104	106	105	1.04	1.04	1.05	1.05	111	106	108	1.08	1.12	1.12	1.08	.88	122	128	130	1.27	.99	.94	.97	
12	173	176	172	174	.82	.82	.71	.78	154	177	156	.84	.92	.77	.77	.77	163	172	166	1.02	1.14	1.02	1.06	
Time, 24 min.																								
1	236	234	233	234	0.85	0.72	0.69	0.73	224	230	220	0.92	1.09	1.12	1.04		221	228	236	1.13	1.24	1.18	1.18	
2	215	215	215	215	1.74	1.67	1.61	1.61	203	214	201	1.61	1.76	1.76	1.70	1.70	209	215	224	1.76	1.93	1.74	1.83	
3	195	196	195	195	1.51	1.49	1.46	1.46	196	204	196	1.53	1.73	1.68	1.67	1.67	209	212	220	1.48	1.67	1.54	1.77	
4	196	202	197	198	1.68	1.49	1.46	1.46	196	204	196	1.53	1.73	1.68	1.67	1.67	209	212	220	1.48	1.67	1.54	1.77	
5	217	222	213	217	1.03	.90	.90	.90	214	219	213	.93	1.15	1.13	1.09	1.09	208	217	209	1.73	1.90	1.68	1.82	
6	247	261	252	253	.91	.88	.78	.86	235	249	237	.82	1.09	1.00	1.05	1.05	235	244	244	1.11	1.27	1.23	1.21	
7	222	225	216	221	.93	.83	.72	.83	212	223	214	1.02	1.06	.89	.99	.99	223	235	226	1.02	1.13	.94	1.03	
8	195	193	193	193	1.10	1.00	.96	1.02	192	202	195	1.07	1.20	1.08	1.12		207	214	207	1.21	1.34	1.23	1.43	
9	176	181	178	178	1.16	1.10	1.04	1.12	182	184	183	1.06	1.27	1.17	1.34	1.32	190	196	207	1.38	1.52	1.43	1.65	
10	137	137	137	137	1.32	1.14	1.14	1.38	157	162	153	1.38	1.33	1.46	1.37	1.39	169	174	180	1.71	1.92	1.72	1.95	
11	135	131	132	133	1.33	1.18	1.18	1.18	158	159	153	1.35	1.34	1.46	1.37	1.34	165	171	177	1.71	1.92	1.72	1.95	
12	207	212	209	209	1.22	1.07	.89	1.06	204	209	206	1.22	1.33	1.12	1.12	1.12	208	211	219	1.35	1.54	1.42	1.44	
Time, 43 min.																								
1	247	255	252	253	1.53	1.32	1.40	1.40	247	255	252	1.53	1.72	1.68	1.68		247	255	252	1.53	1.72	1.68	1.68	
2	236	240	238	239	2.03	2.20	2.23	2.23	236	240	238	2.03	2.20	2.23	2.23	2.23	236	240	238	2.03	2.20	2.23	2.23	
3	226	230	228	229	2.03	2.20	2.23	2.23	226	230	228	2.03	2.20	2.23	2.23	2.23	226	230	228	2.03	2.20	2.23	2.23	
4	214	217	215	216																				

TABLE I
TEMPERATURE AND OSCILLOGRAPH DEFLECTION READINGS FOR FIVE SPECIMENS AND THREE HEATING RATES - Concluded

(e) Specimen 5

Channel	Heating rate A										Heating rate B										Heating rate C										
	ΔT_c (°F)					ΔT_c (in.)					ΔT_c (°F)					ΔT_c (in.)					ΔT_c (°F)					ΔT_c (in.)					
	Run 2	Run 5	Run 9	Av.	Run 2	Run 5	Run 9	Av.	Run 3	Run 4	Run 10	Av.	Run 3	Run 4	Run 10	Av.	Run 5	Run 6	Run 7	Av.	Run 6	Run 7	Av.	Run 6	Run 7	Av.					
	Time, 8 min.										Time, 8 min.										Time, 8 min.										
1	54	56	54	55	0.13	0.15	0.15	0.14	27	27	26	27	0.06	0.10	0.11	0.09	22	19	21	0.09	0.06	0.08	0.08	0.08	0.08	0.08					
2	47	49	49	48	.33	.33	.33	.33	23	23	23	23	.14	.19	.18	.17	17	15	16	.14	.13	.14	.14	.14	.14	.14					
3	44	47	45	45	.23	.26	.23	.24	20	22	18	20	.09	.14	.14	.12	16	14	15	.11	.09	.11	.10	.10	.10	.10					
4	43	41	42	42	.30	.32	.34	.32	20	20	21	20	.14	.19	.19	.17	16	13	15	.15	.11	.13	.11	.10	.10	.10					
5	50	50	51	50	.20	.22	.20	.21	23	25	26	25	.11	.13	.13	.12	21	17	19	.11	.08	.10	.08	.08	.08	.08					
6	62	62	62	62	.17	.17	.17	.17	29	29	32	30	.11	.13	.14	.13	24	22	23	.12	.10	.11	.10	.10	.10	.10					
7	41	41	45	42	.14	.14	.14	.14	20	20	24	21	.08	.12	.07	.09	17	16	17	.09	.06	.08	.08	.08	.08	.08					
8	38	36	38	37	.22	.24	.22	.23	17	17	18	18	.10	.14	.11	.12	13	12	13	.10	.08	.09	.09	.09	.09	.09					
9	35	36	36	36	.27	.28	.26	.27	15	17	16	16	.14	.16	.12	.14	12	11	12	.11	.09	.10	.10	.10	.10	.10					
10	19	16	19	18	.31	.24	.27	.27	7	7	9	8	.11	.14	.10	.12	5	6	6	.11	.09	.10	.10	.10	.10	.10					
11	17	18	18	18	.25	.25	.25	.25	7	7	7	7	.08	.13	.12	.12	5	3	4	.11	.09	.10	.10	.10	.10	.10					
12	43	42	42	42	---	---	---	---	19	19	19	19	---	---	---	---	14	13	15	---	---	---	---	---	---	---					
Time, 12 min.																															
1	111	112	109	111	0.36	0.36	0.35	0.36	83	85	83	84	0.34	0.36	0.37	0.36	67	63	65	0.27	0.30	0.29	0.29	0.29	0.29	0.29					
2	99	101	100	100	.72	.70	.68	.70	73	75	73	74	.60	.62	.61	.61	58	54	56	.49	.49	.49	.49	.49	.49	.49					
3	94	96	95	95	.53	.58	.51	.54	70	72	70	70	.46	.49	.48	.48	55	52	54	.37	.38	.38	.38	.38	.38	.38					
4	91	90	91	91	.67	.70	.65	.67	69	69	70	70	.58	.61	.61	.60	55	49	52	.47	.47	.47	.47	.47	.47	.47					
5	104	102	104	103	.43	.45	.42	.43	76	78	79	78	.41	.42	.44	.42	62	57	60	.33	.34	.34	.34	.34	.34	.34					
6	124	124	125	124	.36	.37	.34	.36	90	91	94	92	.37	.38	.39	.38	78	67	70	.31	.33	.33	.33	.33	.33	.33					
7	95	93	95	94	.30	.30	.30	.30	72	72	76	73	.28	.28	.28	.28	58	54	56	.24	.24	.24	.24	.24	.24	.24					
8	86	82	84	84	.44	.48	.45	.46	65	67	67	66	.38	.43	.39	.40	50	47	49	.32	.31	.31	.31	.31	.31	.31					
9	80	80	80	80	.57	.57	.56	.56	62	63	63	63	.48	.51	.46	.48	49	47	49	.39	.36	.36	.36	.36	.36	.36					
10	49	50	50	50	.71	.70	.69	.69	42	44	44	43	.48	.48	.48	.48	33	32	33	.37	.34	.34	.34	.34	.34	.34					
11	48	49	49	49	.54	.52	.54	.52	42	43	44	42	.37	.40	.36	.38	33	29	31	.31	.29	.29	.29	.29	.29	.29					
12	95	93	93	94	---	---	---	---	76	74	72	74	---	---	---	---	---	---	---	---	---	---	---	---	---	---					
Time, 16 min.																															
1	172	173	170	172	0.62	0.63	0.63	0.63	149	149	148	149	0.74	0.68	0.71	0.71	120	112	116	0.55	0.56	0.56	0.56	0.56	0.56	0.56					
2	155	158	157	157	1.12	1.11	1.13	1.12	138	137	136	137	1.12	1.10	1.08	1.08	107	101	104	.86	.86	.86	.86	.86	.86	.86					
3	149	151	150	150	.80	.80	.80	.80	132	134	132	134	.89	.89	.87	.88	105	99	102	.71	.70	.70	.70	.70	.70	.70					
4	147	146	147	147	1.06	1.08	1.06	1.07	130	130	131	130	1.09	1.07	1.07	1.06	103	96	100	.84	.84	.84	.84	.84	.84	.84					
5	164	161	162	162	.68	.68	.69	.68	141	141	142	141	.76	.73	.76	.75	113	106	110	.61	.59	.60	.60	.60	.60	.60					
6	189	189	190	189	.79	.61	.59	.60	158	158	161	159	.74	.69	.71	.71	126	120	123	.57	.57	.57	.57	.57	.57	.57					
7	155	155	155	155	.52	.52	.52	.52	135	137	139	137	.55	.54	.55	.55	109	102	106	.44	.42	.42	.42	.42	.42	.42					
8	141	138	139	139	.80	.72	.70	.74	125	125	127	126	.71	.74	.72	.72	98	93	96	.57	.54	.54	.54	.54	.54	.54					
9	134	132	134	133	.89	.88	.87	.88	122	122	122	122	.88	.87	.83	.86	96	89	93	.67	.67	.67	.67	.67	.67	.67					
10	92	92	93	93	1.10	.96	1.02	1.03	94	97	96	95	.90	1.04	.96	.90	73	70	72	.69	.67	.68	.68	.68	.68	.68					
11	93	92	93	93	.84	.79	.83	.83	94	94	94	94	.71	.65	.69	.69	73	68	71	.53	.53	.53	.53	.53	.53	.53					
12	153	152	151	152	---	---	---	---	137	136	133	133	---	---	---	---	106	111	109	---	---	---	---	---	---	---					
Time, 18 min.																															
1	201	204	202	202	0.76	0.79	0.79	0.78	212	211	209	210	1.10	1.06	1.11	1.09	170	161	166	0.84	0.81	0.83	0.83	0.83	0.83	0.83					
2	185	185	186	185	1.35	1.33	1.32	1.33	197	196	194	195	1.27	1.26	1.26	1.26	156	147	152	1.23	1.19	1.21	1.21	1.21	1.21	1.21					
3	178	180	178	179	1.05	1.07	1.06	1.06	191	192	185	189	1.26	1.20	1.28	1.28	144	144	148	1.00	.96	.96	.96	.96	.96	.96					
4	176	173	176	176	1.29	1.28	1.28	1.29	189	191	191	190	1.25	1.24	1.24	1.25	142	142	147	1.22	1.19	1.21	1.21	1.21	1.21	1.21					
5	191	191	191	191	.81	.82	.82	.82	202	201	201	201	1.12	1.09	1.13	1.13	152	153	158	.87	.85	.86	.86	.86	.86	.86					
6	221	220	221	221	.77	.77	.77	.77	222	221	223	222	1.10	1.07	1.09	1.09	177	170	174	.85	.84	.85	.85	.85	.85	.85					
7	185	185	186	185	.63	.63	.63	.63	199	198	199	199	.89	.87	.87	.86	156	150	154	.64	.63	.64	.64	.64	.64	.64					
8	168	168	168	168	.86	.89	.87	.87	185	183	185	184	.86	1.09	1.06	1.07	145	138	142	.83	.80	.82	.82	.82	.82	.82					
9	162	161	161	161	1.07	1.07	1.06	1.07	180	181	180	180	1.24	1.26	1.21	1.21	124	124	130	.93	.92	.93	.93	.93	.93	.93					
10	118	119	119	119	1.29	1.14	1.20	1.21	190	192	191	191	1.31	1.27	1.22	1.22	119	118	126	.97	.96	.97	.97	.97	.97	.97					
11	116	116	116	116	.99	.94	.96	.96	146	148	150	149	.99	1.02	.95	.97	111	111	114	.75	.73	.74	.74	.74	.74	.74					
12	183	182	181	182	---	---	---	---	198	196	194	196	---	---	---	---	156	151	154	---	---	---	---	---	---	---					
Time, 20 min.																															
1	233	234	231	233	1.00	1.01	1.03	1.01	239	238	237	236	1.29	1.29	1.29	1.29	216	205	211	1.11	1.11	1.10	1.11	1.11	1.11	1.11					
2	213	215	214	214	1.61	1.60	1.60	1.60	226	224	222	224	1.79	1.81	1.79	1.80	201	190	196	1.56	1.53	1.53	1.53	1.53	1.53	1.53					
3	206	208	207	207	1.89	1.82	1.88	1.87	219	219	217	218	1.48	1.48	1.48	1.48	198	187	192	1.69	1.66	1.66	1.66	1.66	1.66	1.66					
4	200	204	205	205	1.57	1.58	1.56	1.57	219	218	216	218	1.80	1.79	1.80	1.80	197	189	191	1.58	1.54	1.54	1.54	1.54	1.54	1.54					
5	222	221	221	221	1.06	1.01	1.02	1.00	226	228	228	228	1.30	1.29	1.30	1.30	200	197	203	1.18	1.16	1.16	1.16	1.16	1.16	1.16					
6	224	222	222	223	.99	.99	.98	.98	250	249	249	249	1.29	1.29	1.29	1.29	224	216	218	1.18	1.12	1.12	1.12	1.12	1.12	1.12					
7	217	215	215	216	.80	.82	.84	.82	226	224	226	226	1.06	1.06	1.06	1.06	202	193	198	.87	.85	.85	.85	.85	.85	.85					
8	198	198	198	198	1.05	1.07	1.06	1.06	212	210	213	212	1.26	1.26	1.26	1.26	187	180	183	1.08	1.04	1.04	1.04	1.04	1.04	1.04					
9	190	190	190	190	1.26	1.26	1.26	1.26	206	206	207	207	1.40	1.40	1.40	1.40	188	177	183	1.21	1.19	1.19	1.19	1.19	1.19	1.19					
10	141	143	143	143	1.48	1.32	1.39	1.40	179	176	176	177	1.61	1.61	1.61	1.61	161	153	157	1.23											

TABLE II
CALCULATED STRESSES FOR FIVE SPECIMENS AT THREE HEATING RATES

(a) Specimen 1

Gage	Heating rate A					Heating rate B					Heating rate C				
	Time (min)					Time (min)					Time (min)				
	2	4	6	8	9	4	6	8	12	14	6	12	18	20	21
1	-315	-522	-257	1405	985	-682	0	608	890	1212	51	302	673	804	846
2	484	2585	3588	3760	3775	1411	2936	4061	4626	4554	2606	4059	4424	4428	4590
3	585	3028	4517	4845	4680	1679	3492	4888	5860	5730	2925	4724	5430	5400	5698
4	209	1461	786	-1040	-2190	968	1717	2146	1066	362	1669	1693	893	559	396
5	-483	-1380	-3740	-5780	-6630	-782	-1126	-1641	-3412	-3977	-241	-2698	-4057	-4330	-4237
6	-51	-197	512	2341	-----	-1189	51	-192	1194	-----	337	92	-----	-----	-----
7	-556	-2076	-3711	-4815	-----	-1478	-2444	-2395	-2980	-3227	-1740	-2980	-3705	3626	-3594
8	-191	-1002	-3074	-5420	-6280	-430	-904	-1472	-2850	-3660	-336	-2237	-3598	-3762	3833
9	340	973	240	-1573	-2641	682	1118	1483	620	0	1360	959	50	-191	-189
10	-216	-215	266	529	475	-433	0	1056	1573	1564	160	530	682	682	782
11	-304	-253	198	596	444	-556	-52	894	1727	1534	196	844	786	785	834
12	----	----	----	----	----	----	----	----	----	----	----	----	----	----	----

NACA

TABLE II

CALCULATED STRESSES FOR FIVE SPECIMENS AT THREE HEATING RATES - Continued

(b) Specimen 2

Gage	Heating rate A					Heating rate B					Heating rate C				
	Time (min)					Time (min)					Time (min)				
	4	6	8	10	12	4	8	12	16	20	6	12	18	24	28
1	-420	-1355	-2516	-3867	-4178	-210	-951	-1854	-2730	-3066	-839	-1818	-2389	-3085	-3103
2	484	879	1142	1463	1383	350	1008	1480	1750	1972	616	1149	1399	1355	1328
3	585	1054	1562	1888	1857	370	1111	1829	2262	2401	690	1569	1965	2223	2257
4	-44	-681	-2051	-3400	-4497	-86	-511	-1403	-2308	-2799	0	-380	-1196	-1759	-195
5	-1022	-2470	-4150	-5474	-----	-541	-1825	-3283	-4291	-4469	-541	-2077	-3330	-3696	-3650
6	-991	-2442	-3838	-3251	-2479	-607	-2113	-3636	-4046	-3634	-795	-2644	-3869	-3862	-3587
7	-1049	-3197	-5499	-8706	-11617	-612	-2394	-4710	-3346	-8111	-829	-3066	-4925	-5809	-6388
8	-625	-1522	-3118	-5319	-7470	-336	-1204	-2608	-3537	-4400	-241	-1331	-2558	-3080	-3354
9	98	-99	-244	-1011	-2156	0	194	336	142	-282	895	1083	1384	747	902
10	424	952	1626	2234	2576	212	585	1213	1561	1746	319	1006	1409	1391	1420
11	349	845	1524	2019	2150	149	545	1132	1233	1751	299	993	1378	1493	1491
12	-459	-1411	-2526	-3869	-----	-168	-869	-1758	-2644	-3110	-670	-1719	-2677	-3047	-3069



TABLE II
CALCULATED STRESSES FOR FIVE SPECIMENS AT THREE HEATING RATES - Continued

(c) Specimen 3

Gage	Heating rate A							Heating rate B					Heating rate C				
	Time (min)							Time (min)					Time (min)				
	4	8	10	12	14	^a 15	6	12	16	20	24	6	12	18	24	30	34
1	-525	-989	-1546	-1966	-2254	-2107	-420	-884	-1225	-1290	-1389	-158	-366	-465	-953	-1016	-612
2	-44	131	130	170	251	650	90	347	560	718	776	132	483	741	680	830	2986
3	53	369	472	411	558	947	160	581	989	965	1088	113	584	888	923	992	1389
4	-126	-256	-379	-499	-568	-400	-128	-42	-41	39	115	-42	123	289	201	236	459
5	-483	-1416	-2099	-2660	-2968	-3106	-542	-1131	-1508	-1630	-1725	-304	-539	-708	-1324	-1210	-1082
6	-546	-2138	-3080	-3912	-4695	-4809	-647	-1949	-2670	-3152	-3375	-346	-125	-1737	-2490	-2700	-2546
7	-446	-1643	-2420	-3387	-3940	-3941	-669	-1713	-7530	-2966	-3152	-388	-993	-1617	-2345	-2119	-2328
8	-242	-1045	-1647	-2258	-2554	-2505	-480	-1041	-1398	-1770	-1713	-242	-524	-758	-1295	-1421	-1220
9	0	-52	-198	-340	-332	-50	-99	0	97	50	0	0	339	446	330	932	539
10	478	1576	2087	2428	2848	3250	-586	1419	1879	2097	2312	371	1112	1565	1757	1750	1919
11	394	1339	1676	2011	2381	2598	-496	1090	1431	1495	1434	249	793	1229	1265	1143	1358
12	-210	-623	-1027	-1132	-1542	-1320	-25	-540	-698	-802	-719	0	-168	-330	-682	-637	-456

^aPrecisely, 15 min and 7 sec.



TABLE II

CALCULATED STRESSES FOR FIVE SPECIMENS AT THREE HEATING RATES - Continued

(d) Specimen 4

Gage	Heating rate A					Heating rate B					Heating rate C					
	Time (min)					Time (min)					Time (min)					
	4	8	12	16	18	8	12	18	24	30	8	16	24	32	40	45
1	-368	-1146	-2068	-2508	-2834	-315	-469	-865	-975	-1205	-262	-520	-656	-484	-646	-807
2	-178	-313	-218	241	586	-43	174	429	577	792	0	391	810	1027	1098	998
3	-56	106	413	645	1101	160	422	777	896	1137	212	638	1030	1430	1517	1427
4	-87	-127	-85	117	302	86	251	453	792	795	166	458	692	977	898	656
5	-301	-955	-1619	-2022	-2073	-420	-536	-875	-1066	-1170	-301	-179	-406	-388	-427	-776
6	-298	-1466	-2720	-3235	-3290	-497	-936	-1616	-1990	-2020	298	-884	-1371	-1144	-1335	-1989
7	-168	-826	-2028	-2463	-2632	-114	-442	-1247	-1542	-1664	-223	-770	-1316	-1423	-1789	-1510
8	0	-286	-752	-1120	-1002	96	-144	-515	-591	-695	-96	-49	-234	-315	-302	-503
9	0	193	288	415	628	194	388	480	604	755	-978	435	619	781	840	644
10	319	1164	2126	2475	3028	637	1163	1765	1930	2002	319	1053	1550	1710	1649	1616
11	298	1092	1768	2030	1850	595	845	1327	1152	1120	348	788	1077	1049	831	804
12	-126	-622	-1216	-1429	-1242	-168	-418	-531	-746	-562	-168	-249	-244	-118	75	107

NACA

TABLE II

CALCULATED STRESSES FOR FIVE SPECIMENS AT THREE HEATING RATES - Concluded

(e) Specimen 5

Gage	Heating rate A					Heating rate B					Heating rate C					
	Time (min)					Time (min)					Time (min)					
	8	12	16	18	20	8	16	24	32	36	8	16	24	32	40	48
1	-1020	-1532	-1999	-2173	-2249	-368	-725	-243	-987	-1188	-210	-520	-713	-833	-893	-1233
2	-89	0	82	123	195	0	347	588	718	504	133	392	515	623	639	305
3	-110	-54	-52	50	191	0	419	610	774	563	108	368	572	603	675	324
4	84	83	80	116	150	124	414	603	689	445	84	416	615	634	687	365
5	-300	-942	-1406	-1523	-1693	-62	-1796	-287	-272	-424	-62	0	-176	-228	-379	-726
6	-1209	-2244	-2976	-3181	-3461	-354	-1170	-1627	-1888	-2036	-198	-688	-1194	-1409	-1530	-1766
7	-501	-1196	-1859	-2020	-2150	-113	-716	-1152	-1330	-1408	-58	-387	-917	-1148	-1350	-1726
8	48	-191	-365	-624	-606	95	0	-140	-1338	-172	50	142	-48	-138	-263	-297
9	197	239	186	226	310	194	386	376	448	393	98	388	382	232	222	125
10	793	1671	2202	2229	2330	319	1160	1745	1554	2261	266	741	1101	1118	1095	1055
11	719	1282	1414	1397	1312	348	642	729	564	414	348	595	589	385	280	270
12	-----	-----	-----	-----	-----	----	-----	-----	-----	-----	-----	-----	-----	-----	-----	-----

NACA



Figure 1.- General view of test installation.

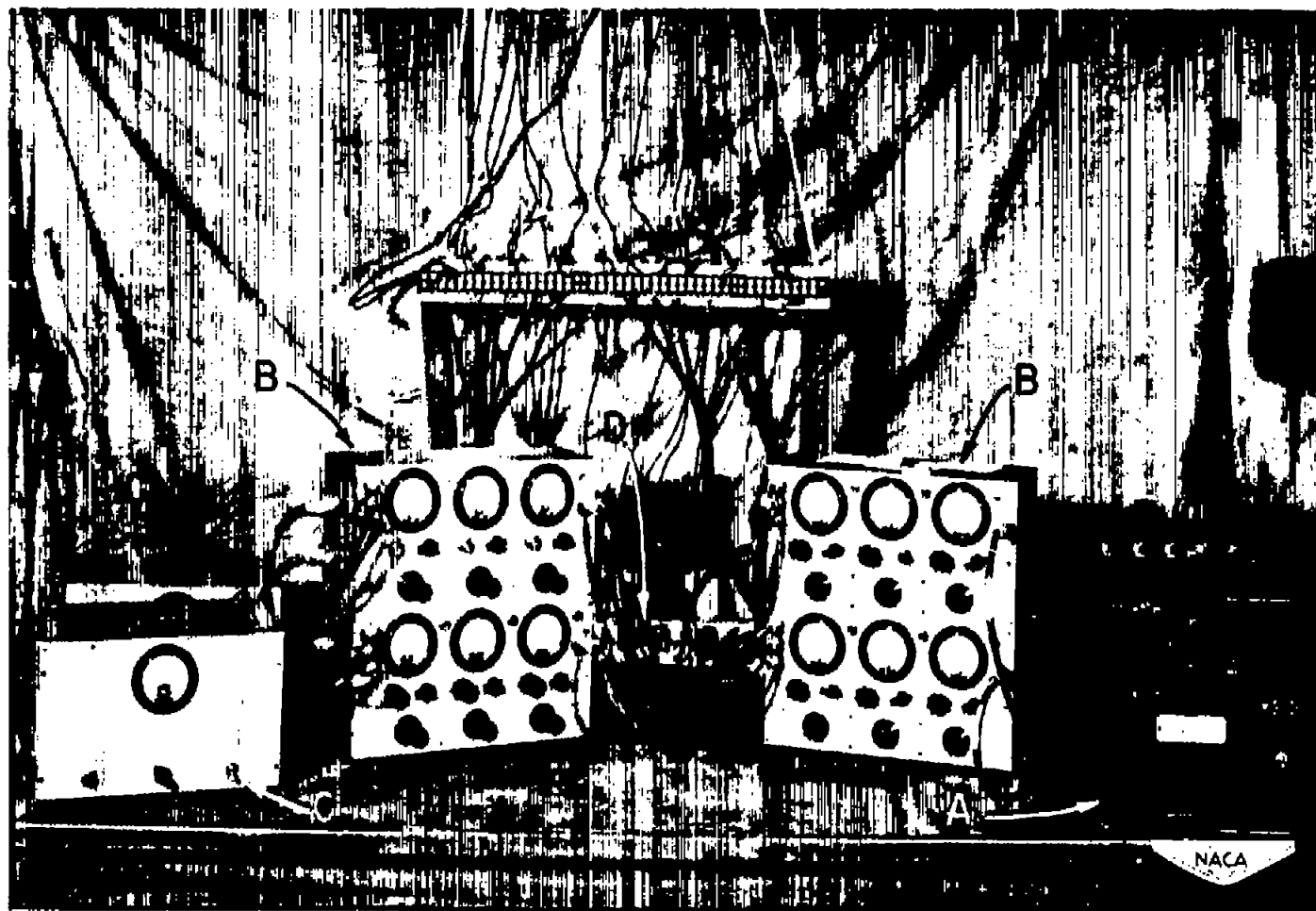


Figure 2.- Installation of strain-gage recording equipment.



Figure 3.- Test oven with specimen in place.

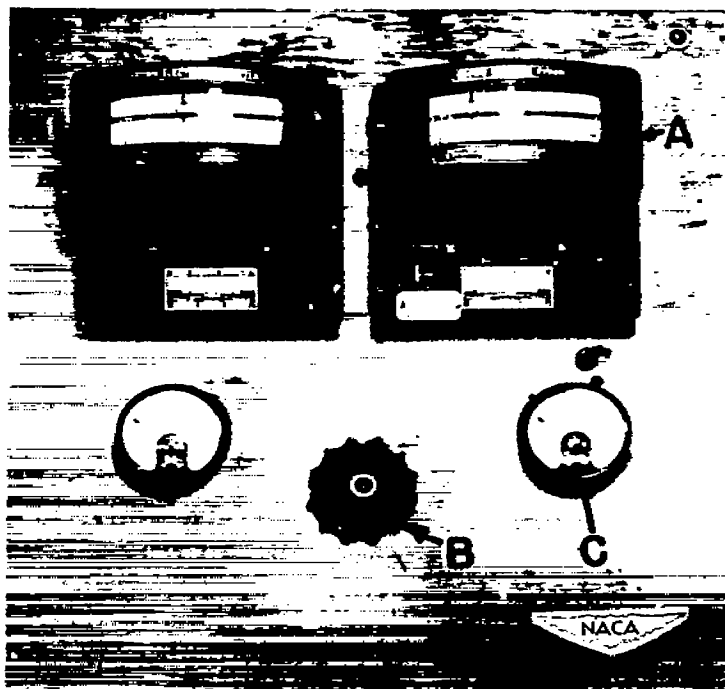


Figure 4.- Test-oven control panel.

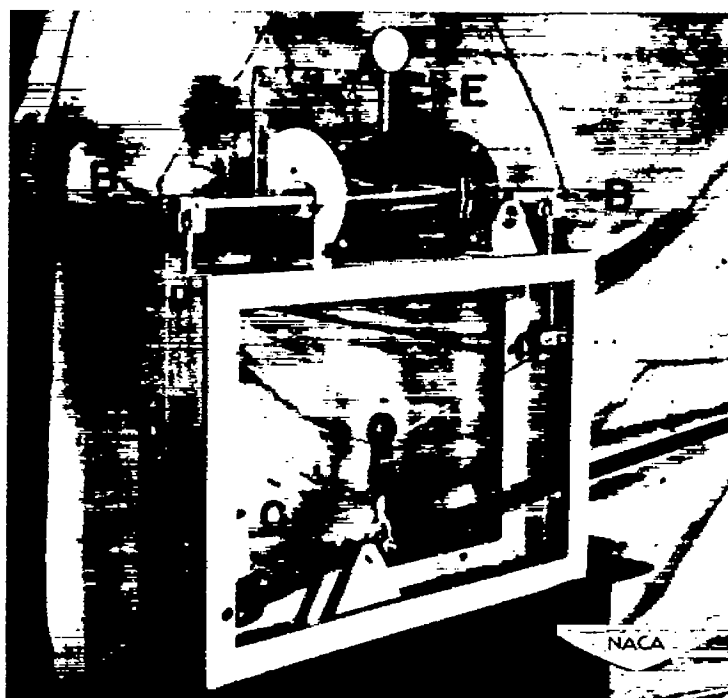
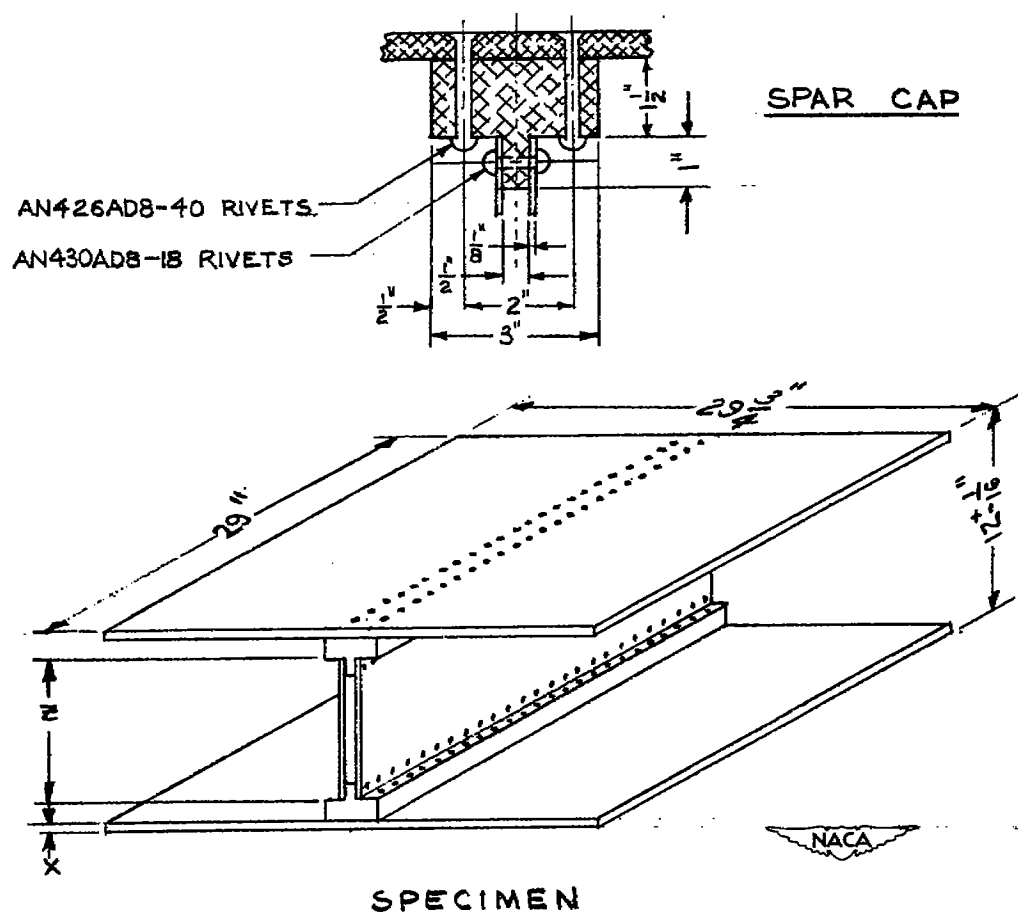


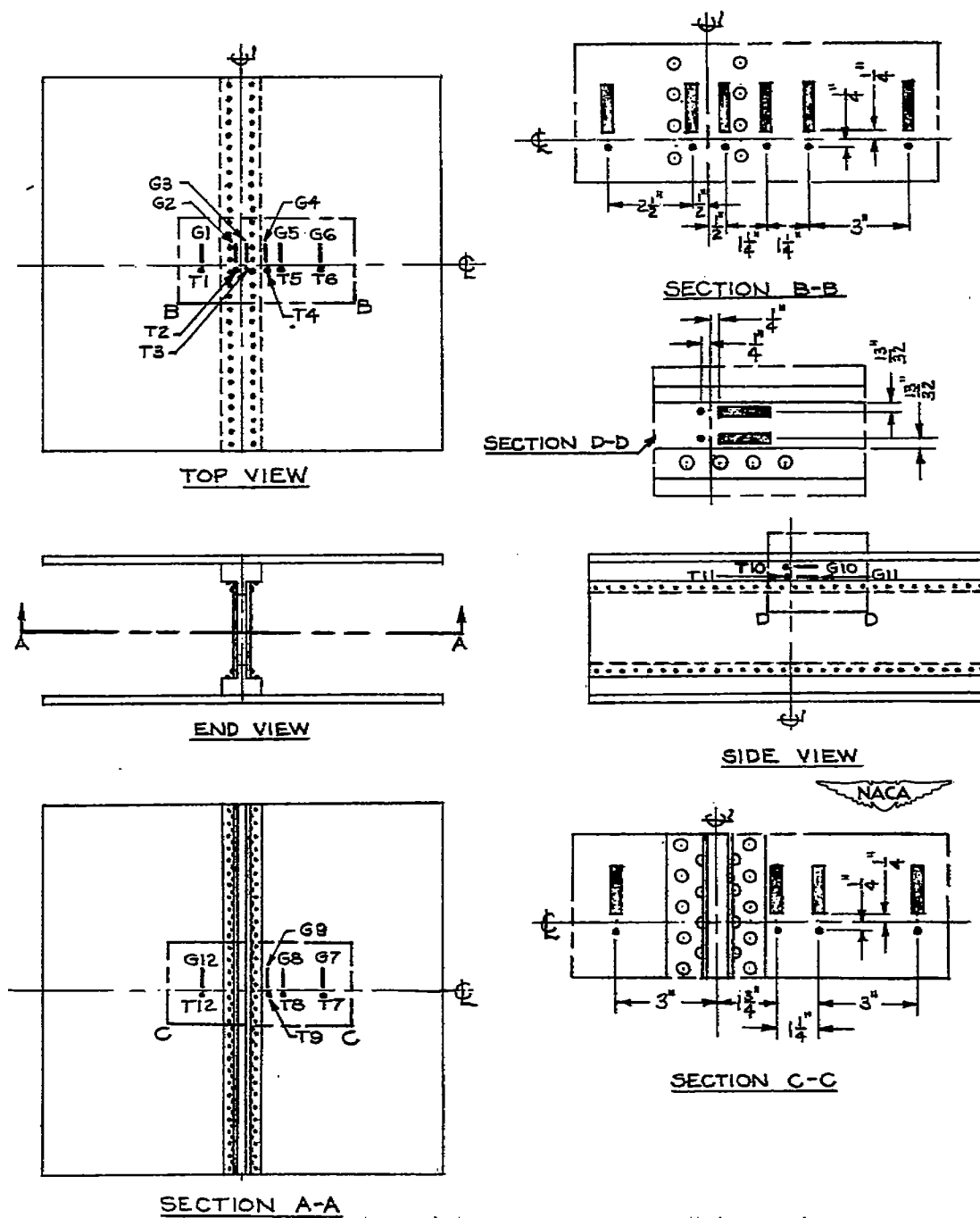
Figure 5.- Strain-gage calibrator.



Specimen	Skin thickness, x (in.)	Web dimension, z (in.)
1	0.051	8.90
2	.125	8.75
3	.250	8.50
4	.375	8.25
5	.500	8.00

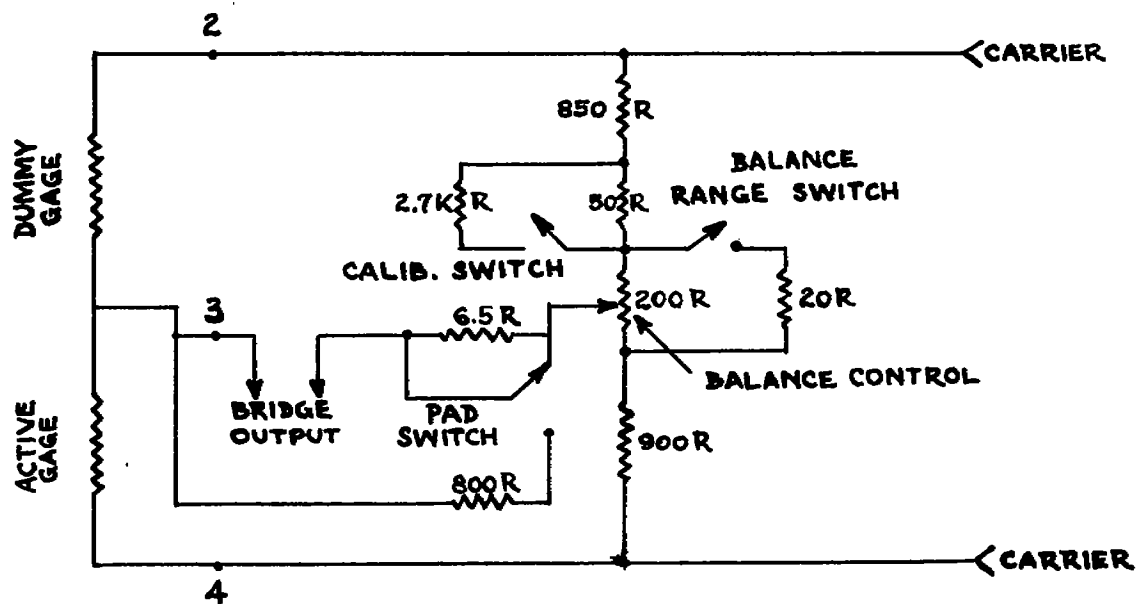
(a) Sketch and dimensions of specimens.

Figure 6.- Test-specimen configurations.

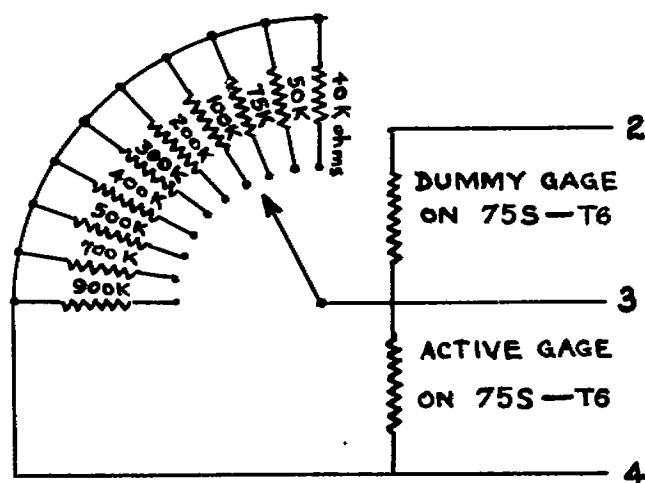


(b) Location and designation of strain gages and thermocouples on specimens.

Figure 6.- Concluded.



(a) Simplified schematic wiring diagram of strain-measuring circuit for one channel, including balancing controls in amplifier.



(b) Modification of strain-measuring circuit for calibration of oscillograph.

Figure 7.- Strain-measuring circuit.

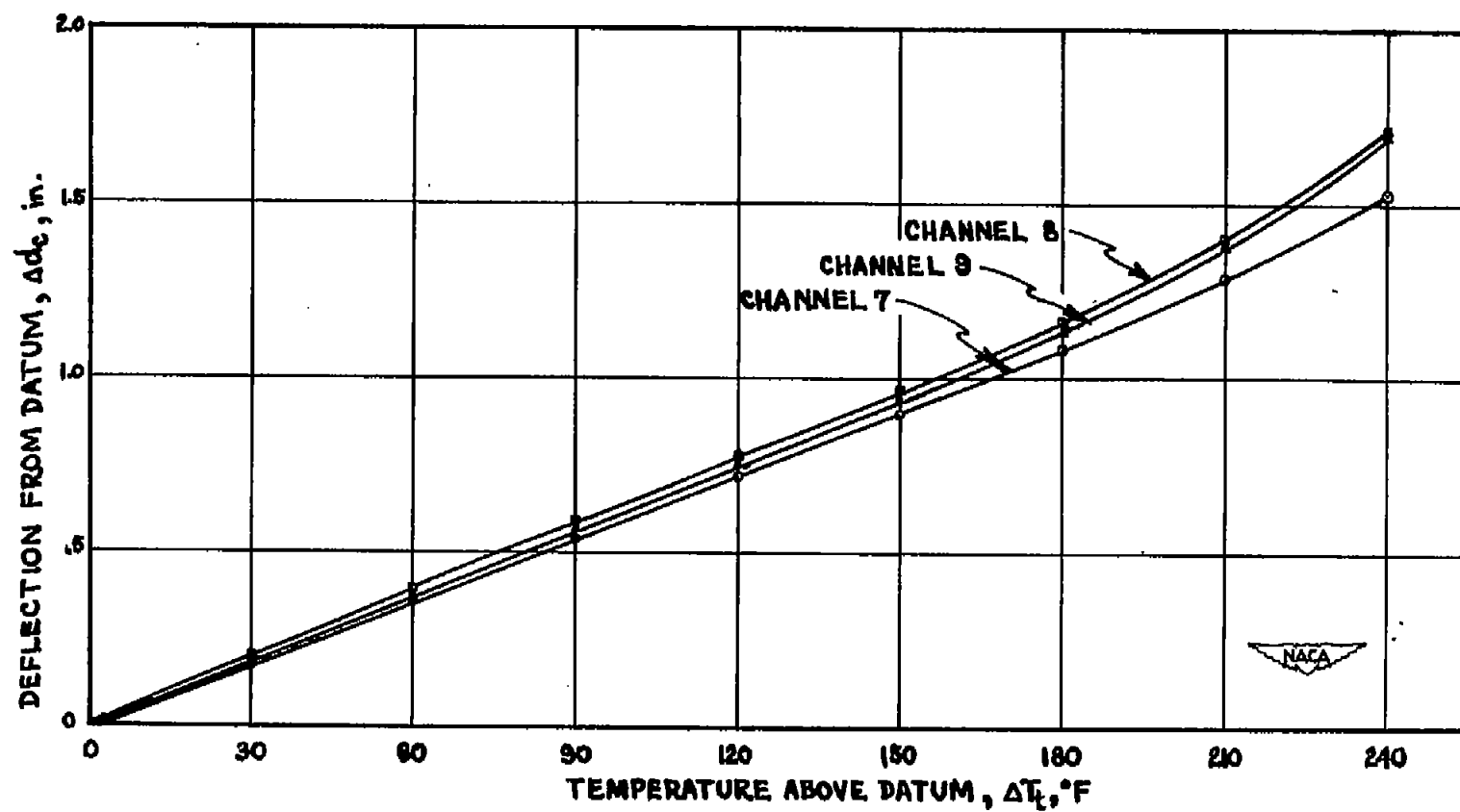


Figure 8.- Typical calibration curves of oscillograph deflection against temperature above datum for specimen 4.

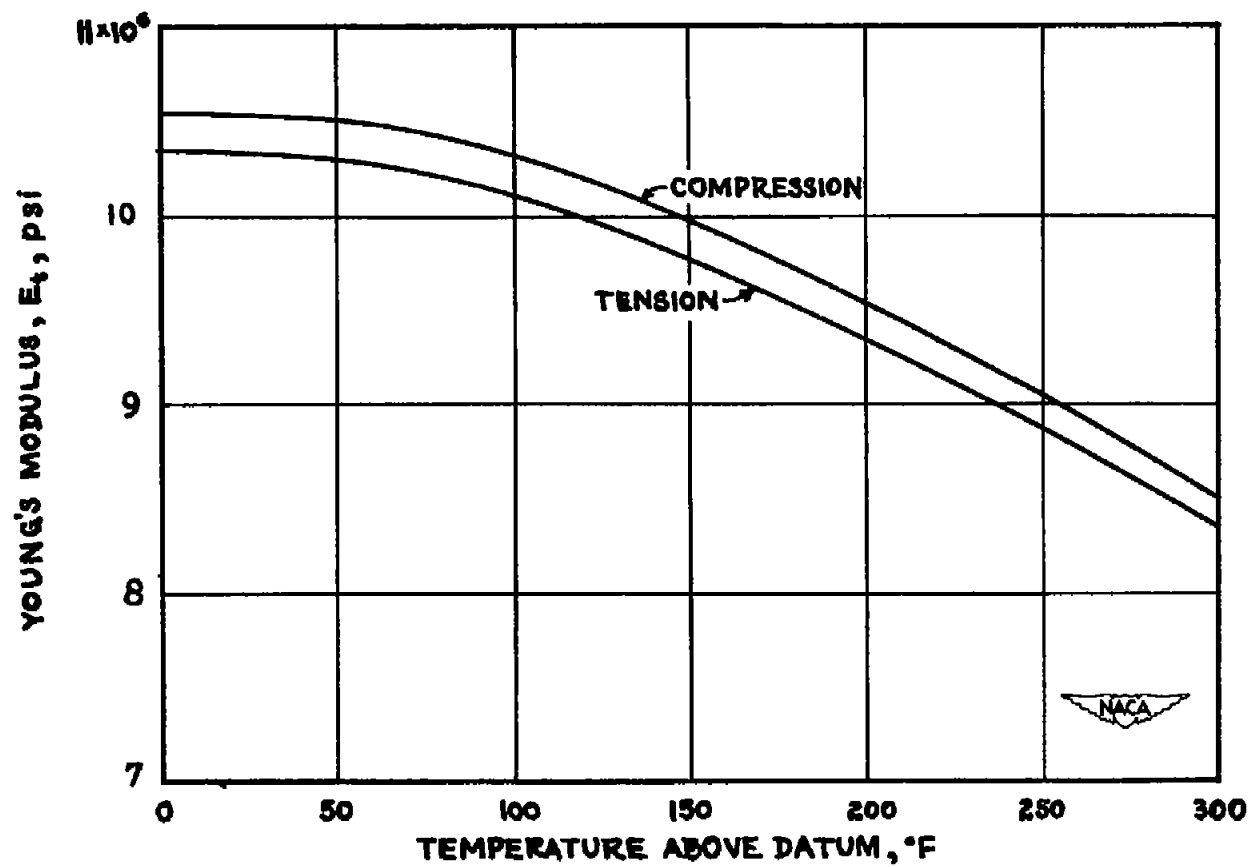
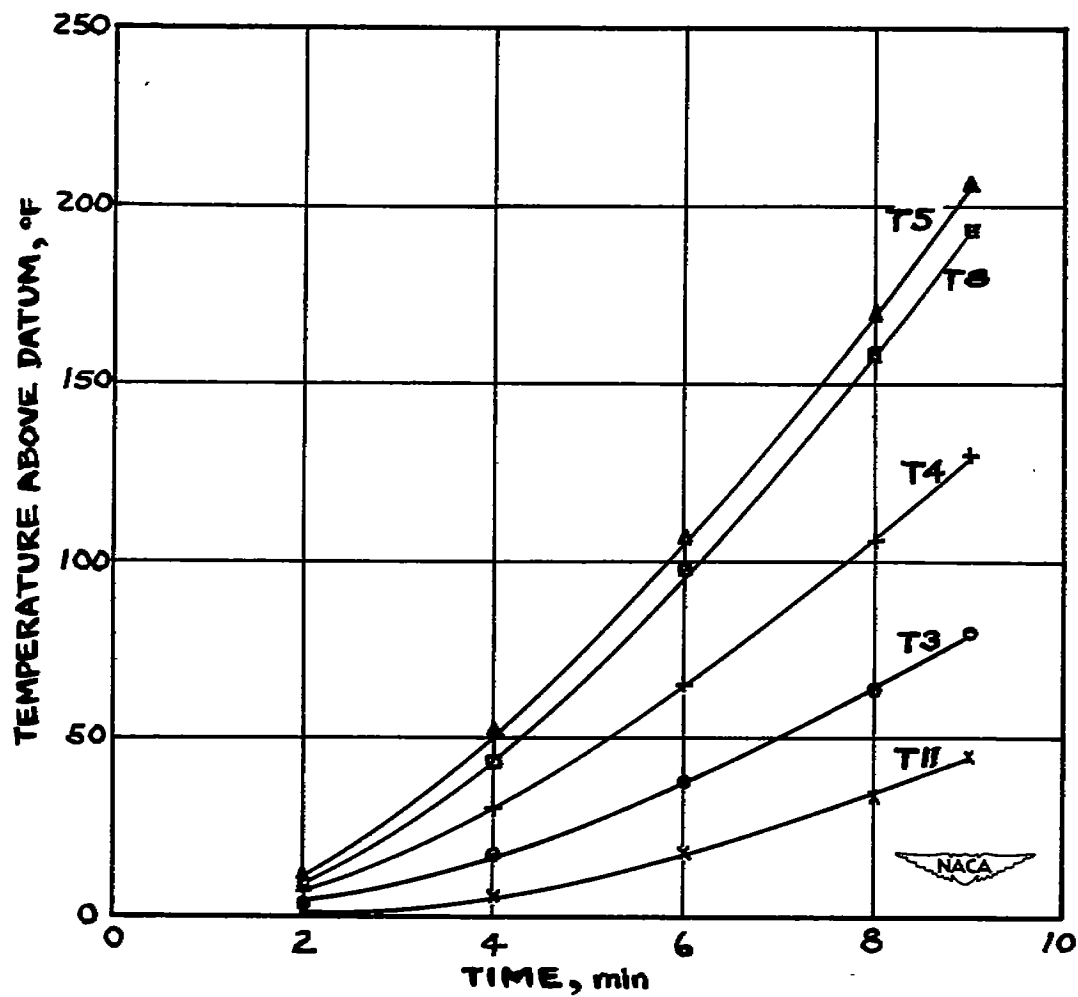
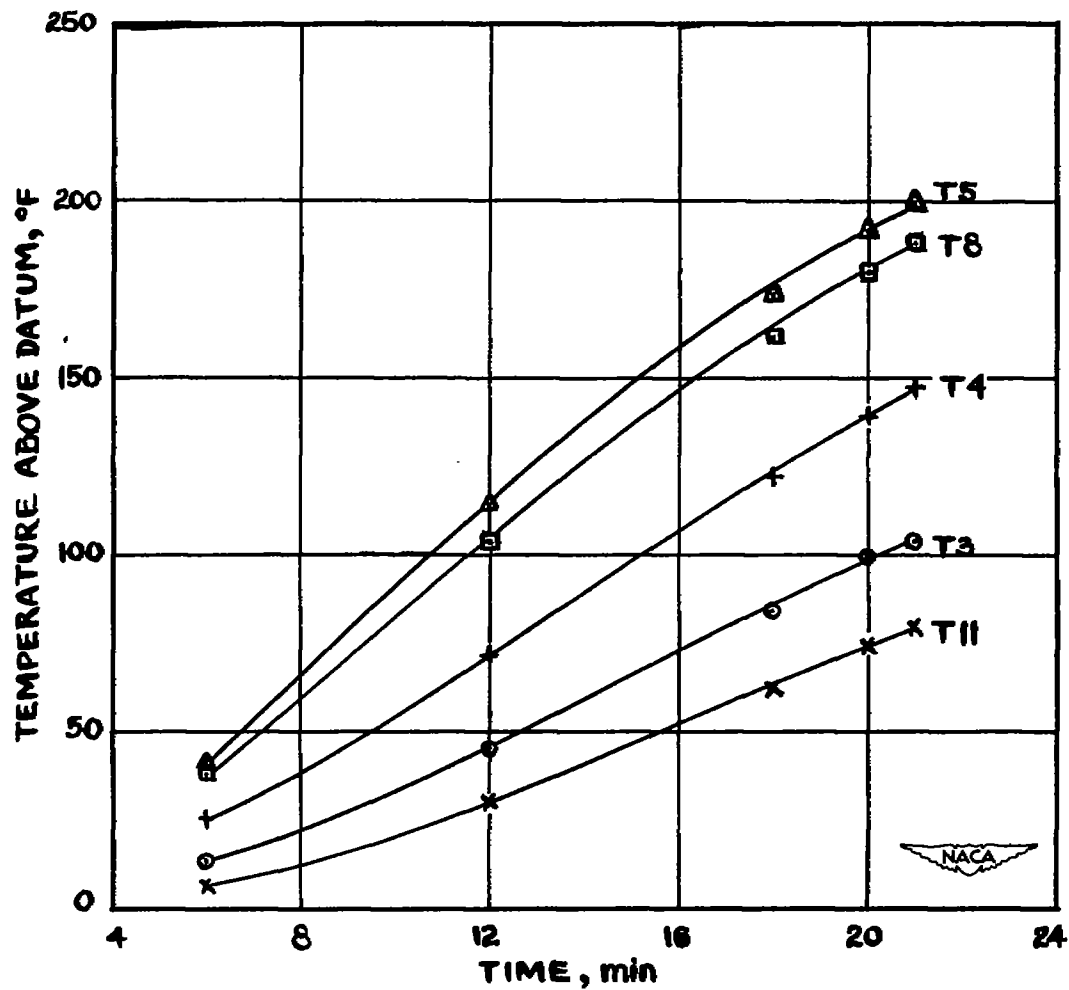


Figure 9.- Variation of Young's modulus with temperature above datum.
(Datum is 70°F .)



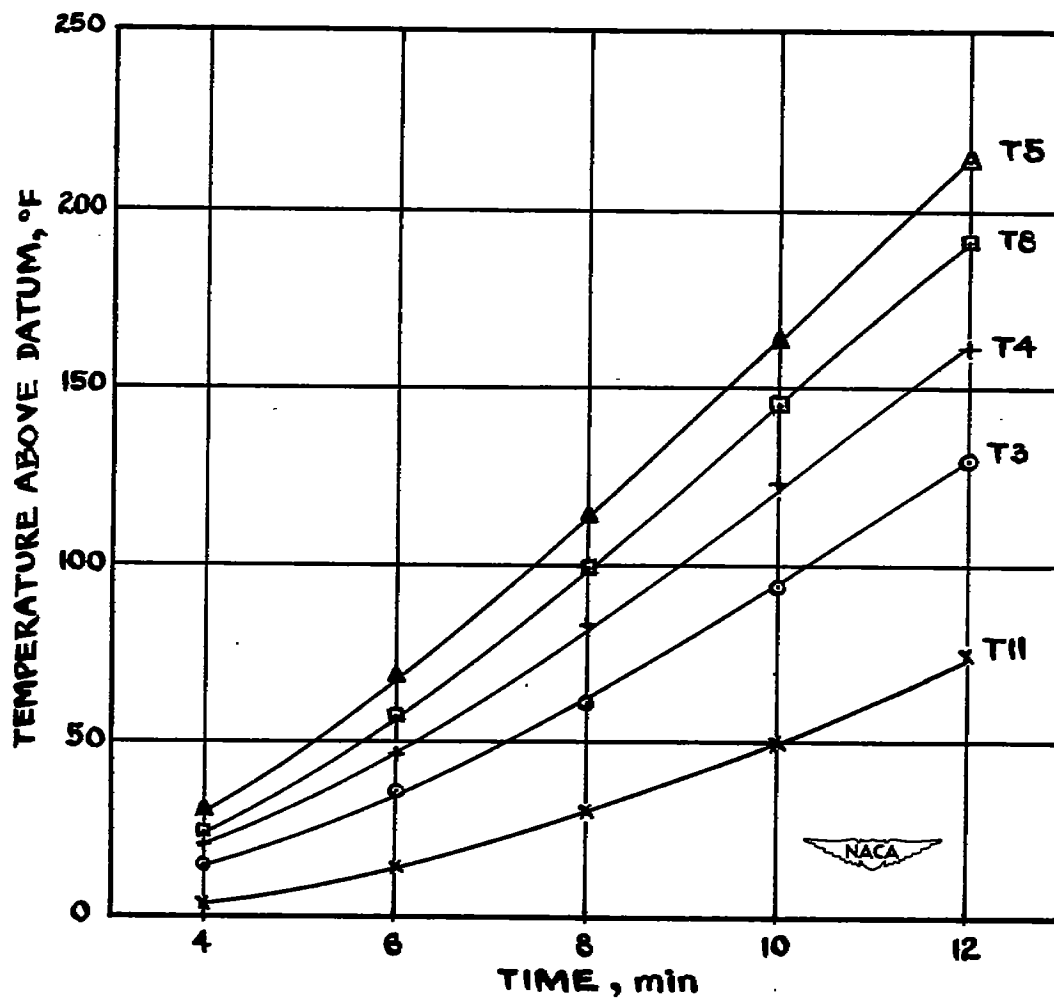
(a) Specimen 1, heating rate A.

Figure 10.- Time history of temperature for selected points on specimens.



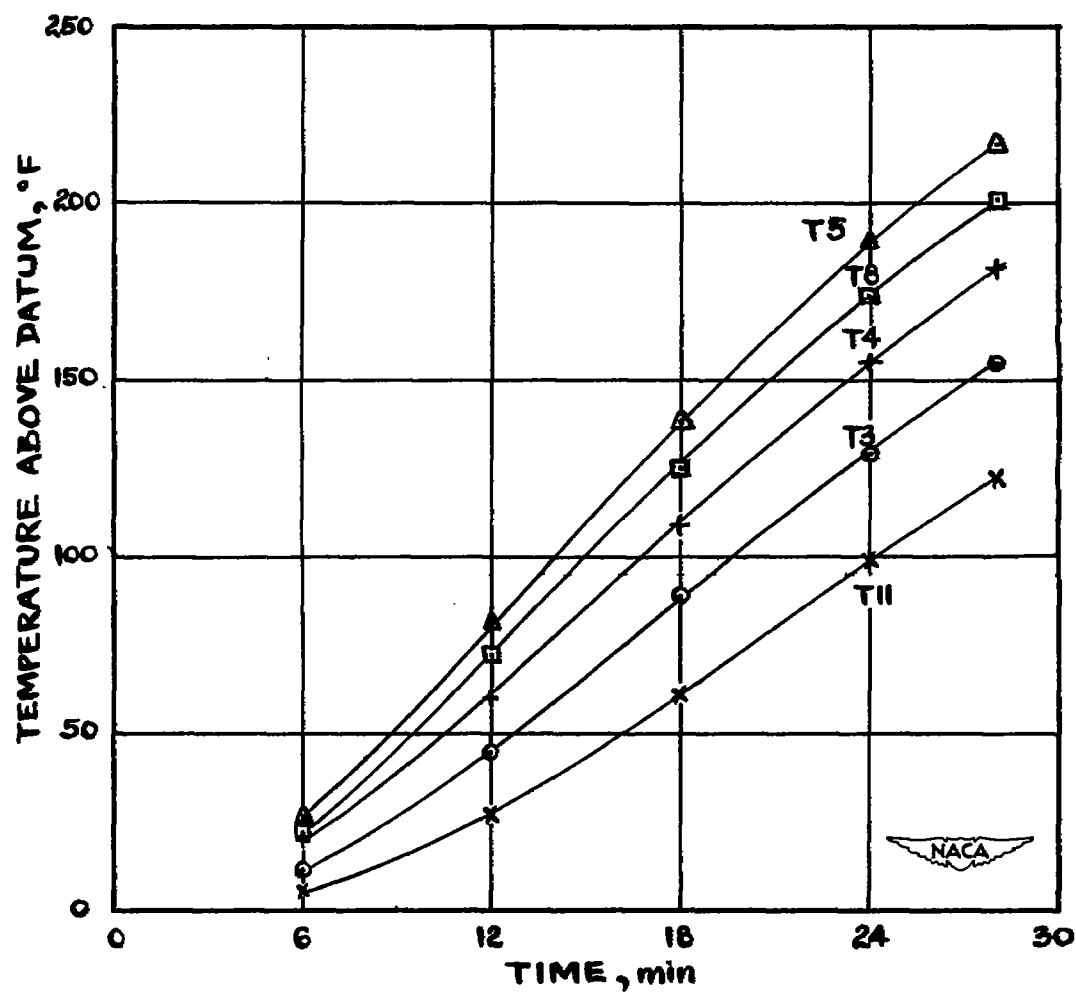
(b) Specimen 1, heating rate C.

Figure 10.- Continued.



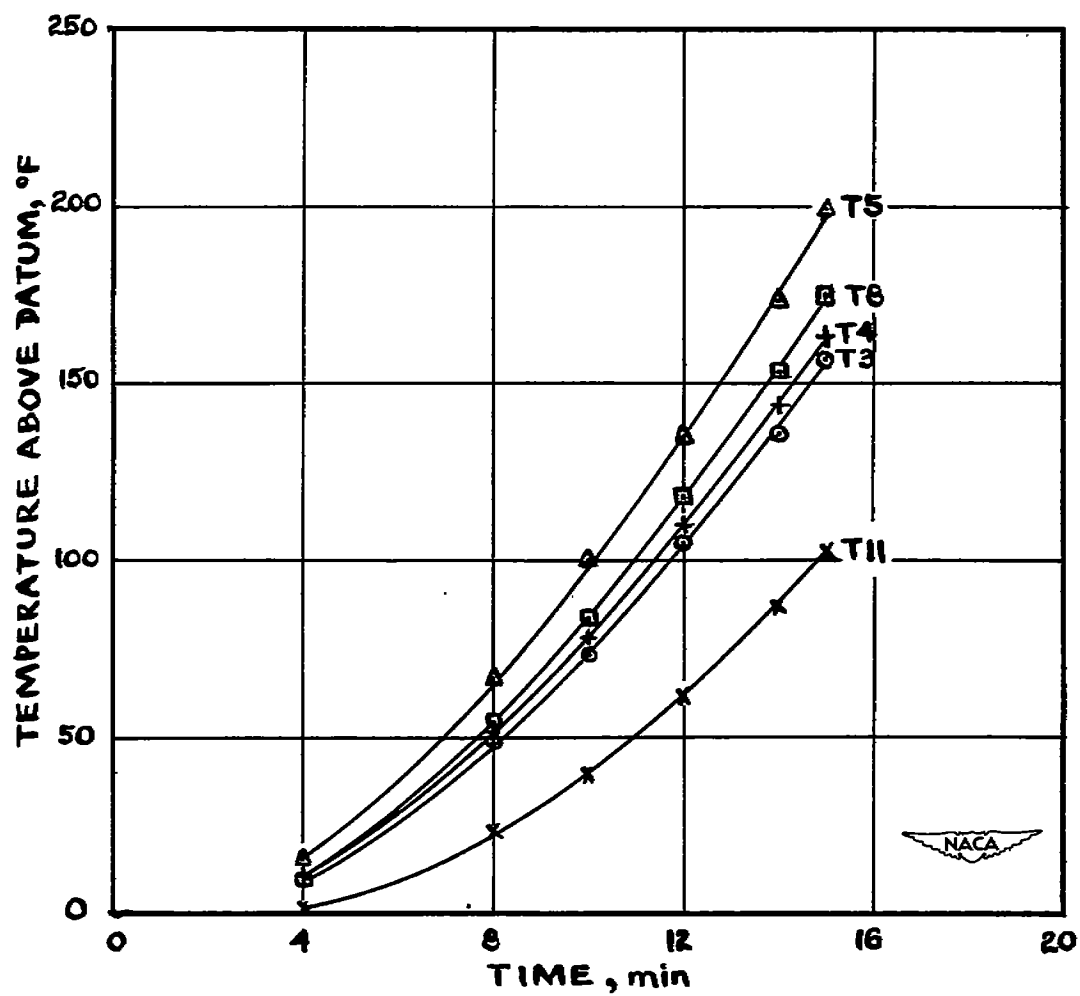
(c) Specimen 2, heating rate A.

Figure 10.- Continued.



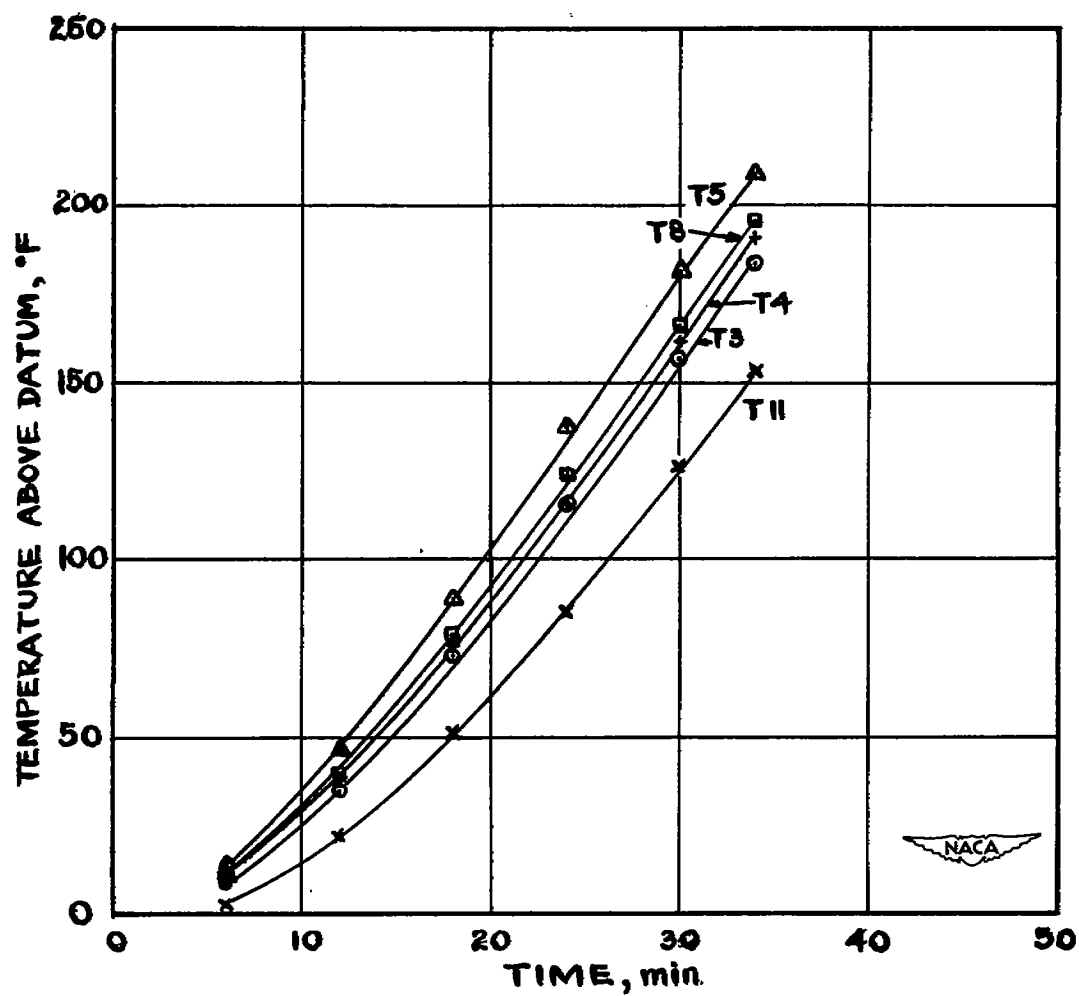
(d) Specimen 2, heating rate C.

Figure 10.- Continued.



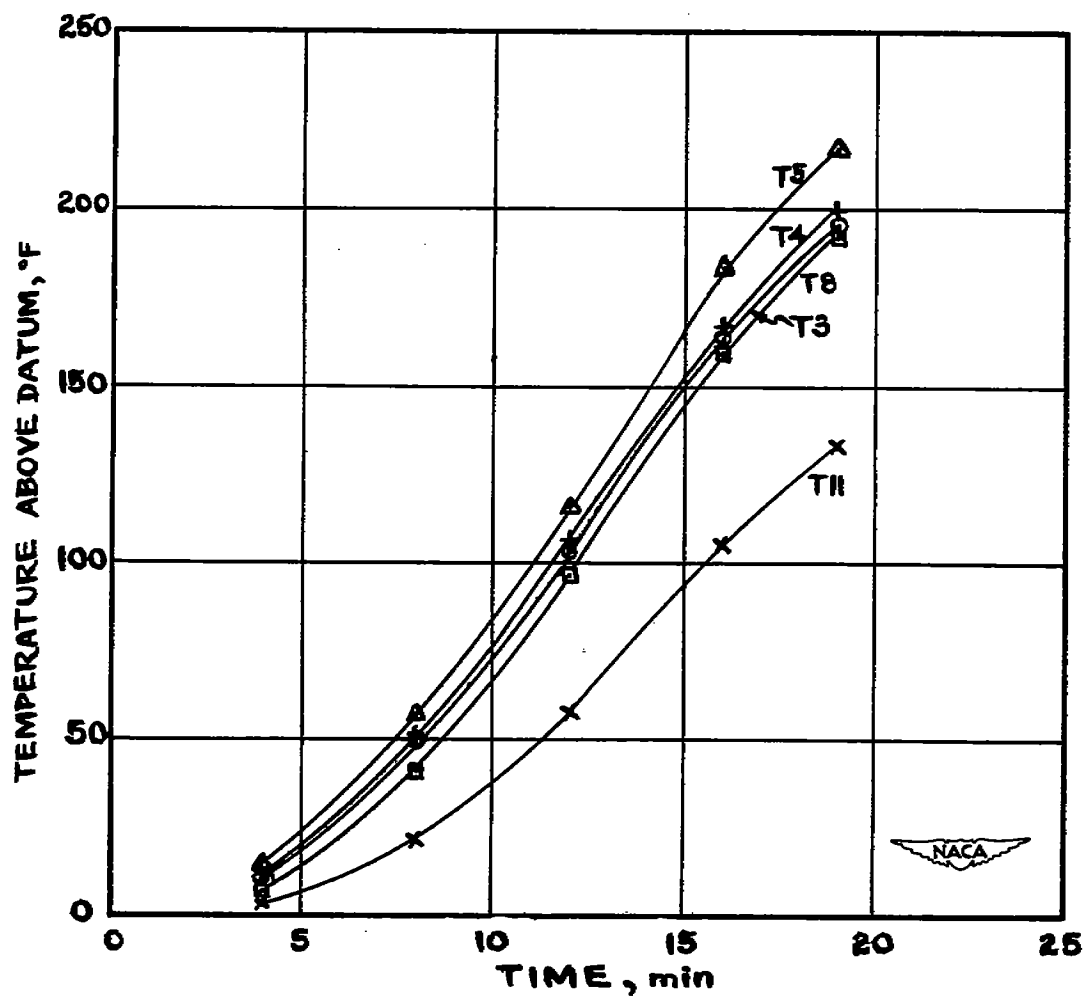
(e) Specimen 3, heating rate A.

Figure 10.- Continued.



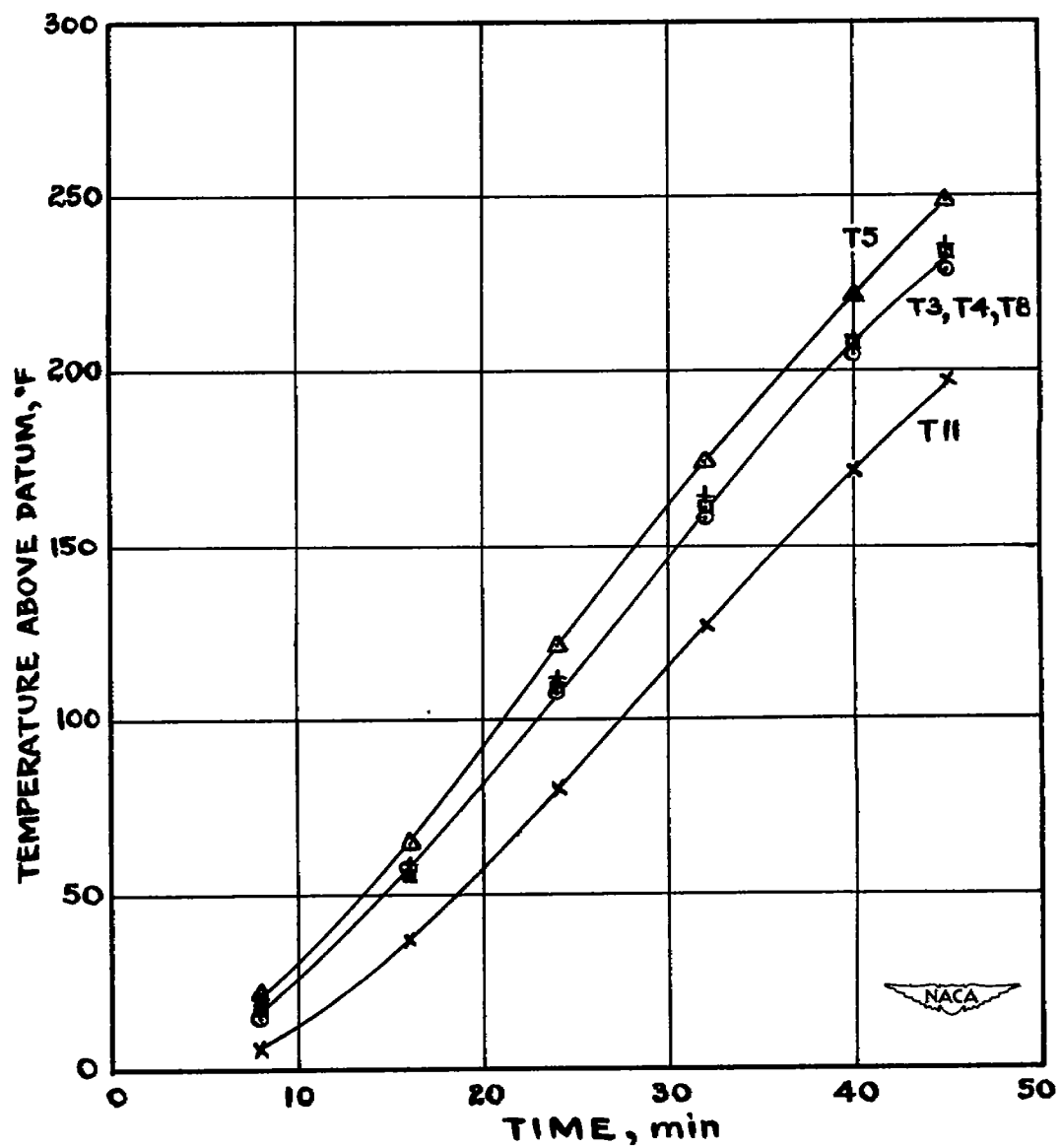
(f) Specimen 3, heating rate C.

Figure 10.- Continued.



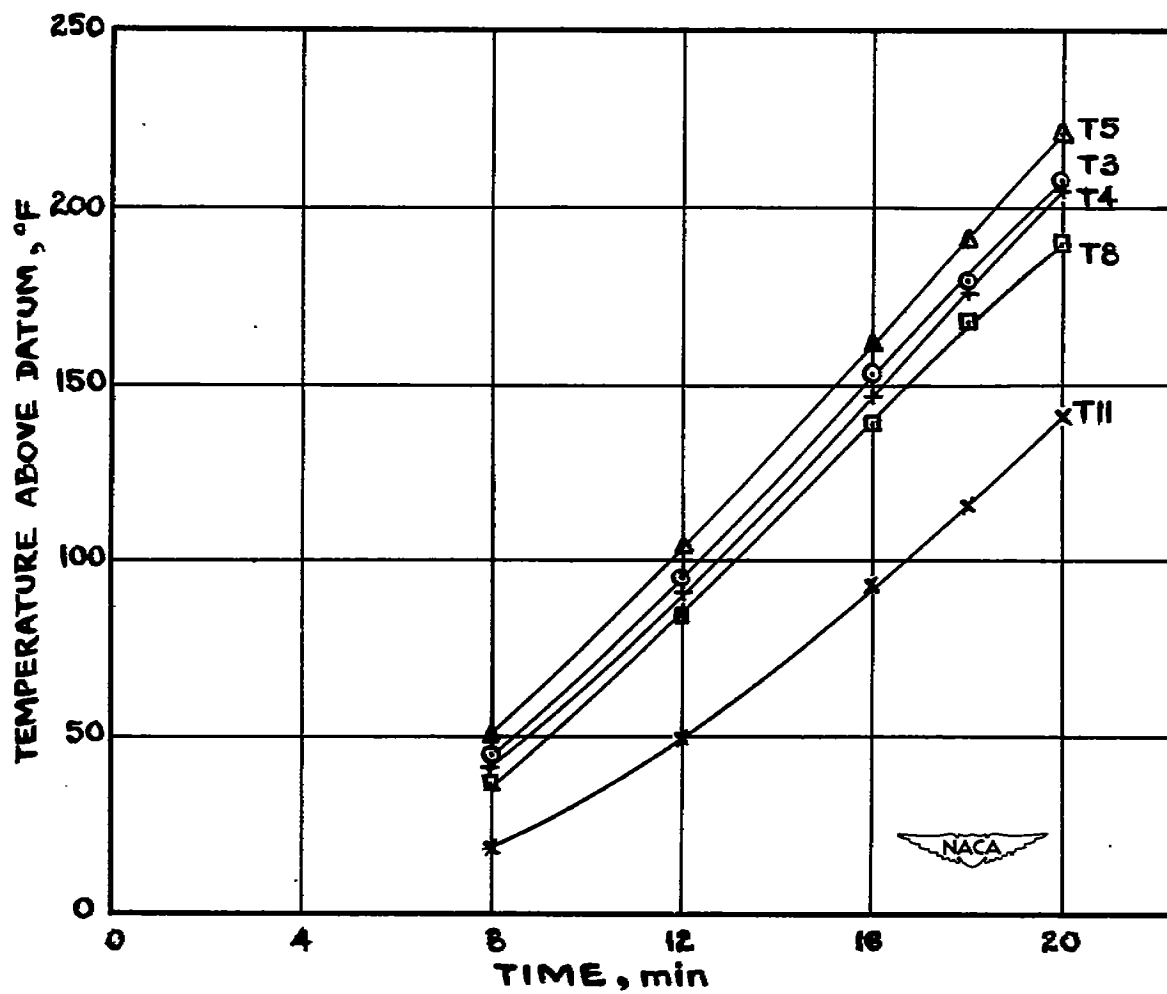
(g) Specimen 4, heating rate A.

Figure 10.- Continued.



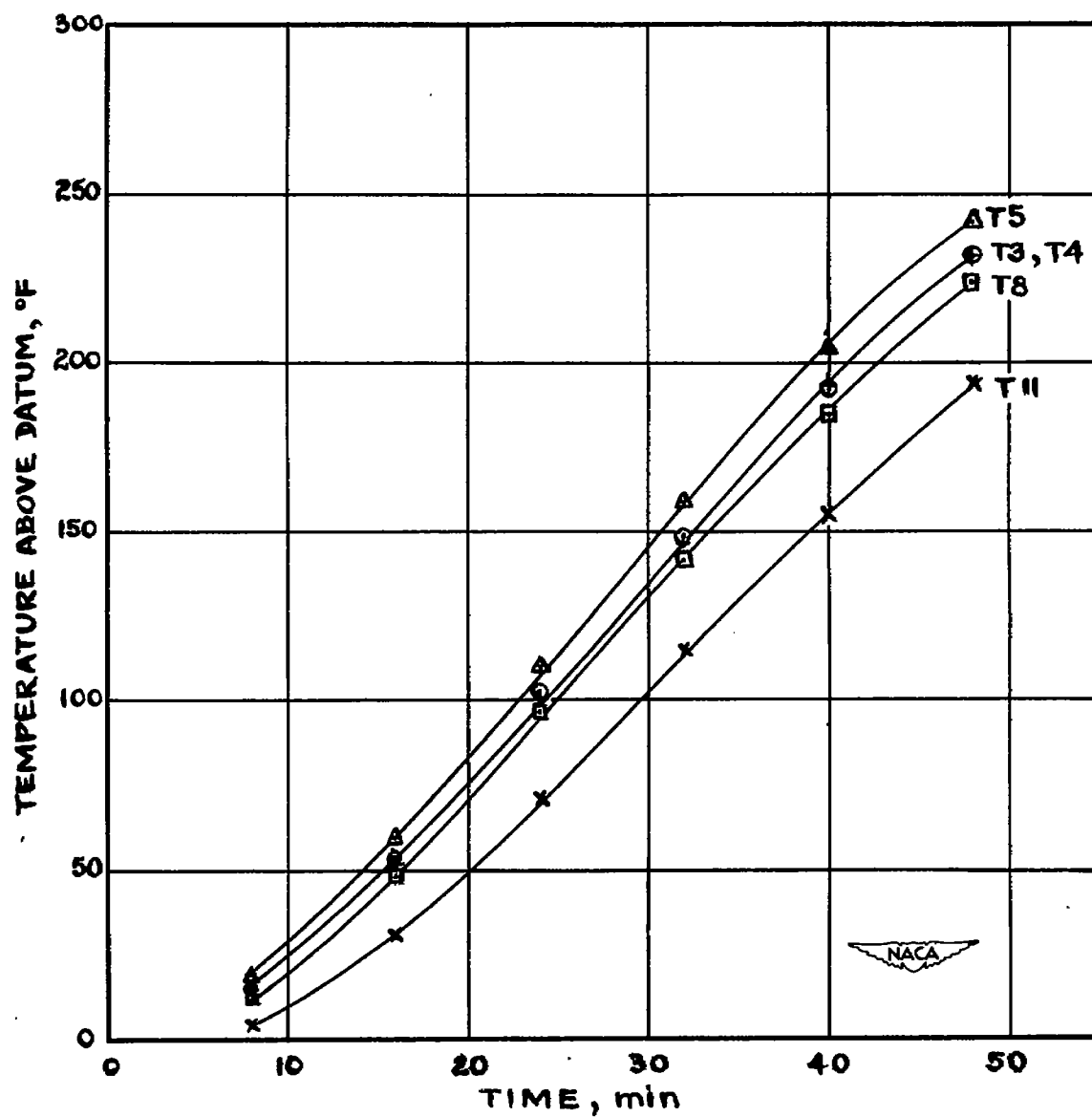
(h) Specimen 4, heating rate C.

Figure 10.- Continued.



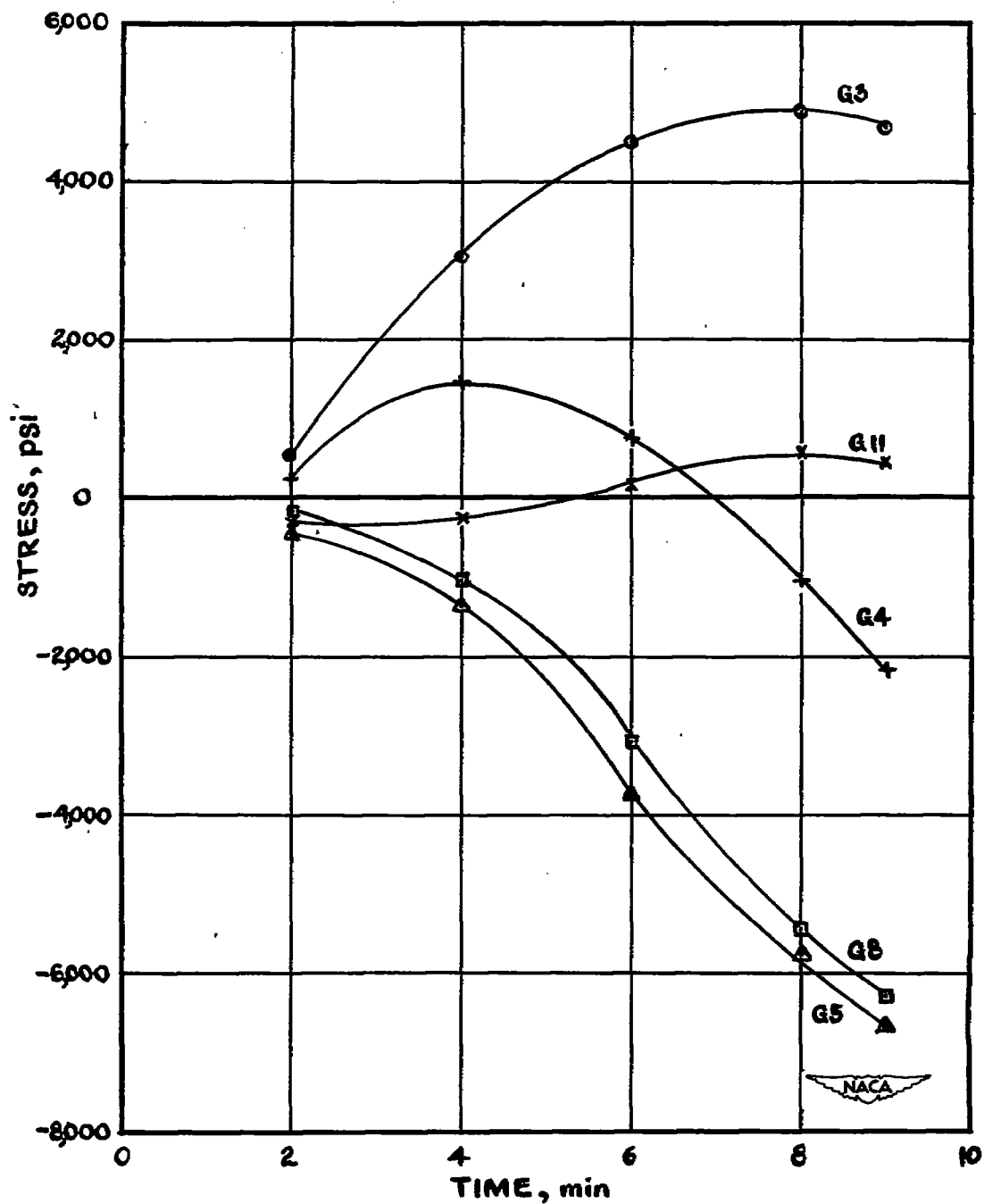
(1) Specimen 5, heating rate A.

Figure 10.- Continued.



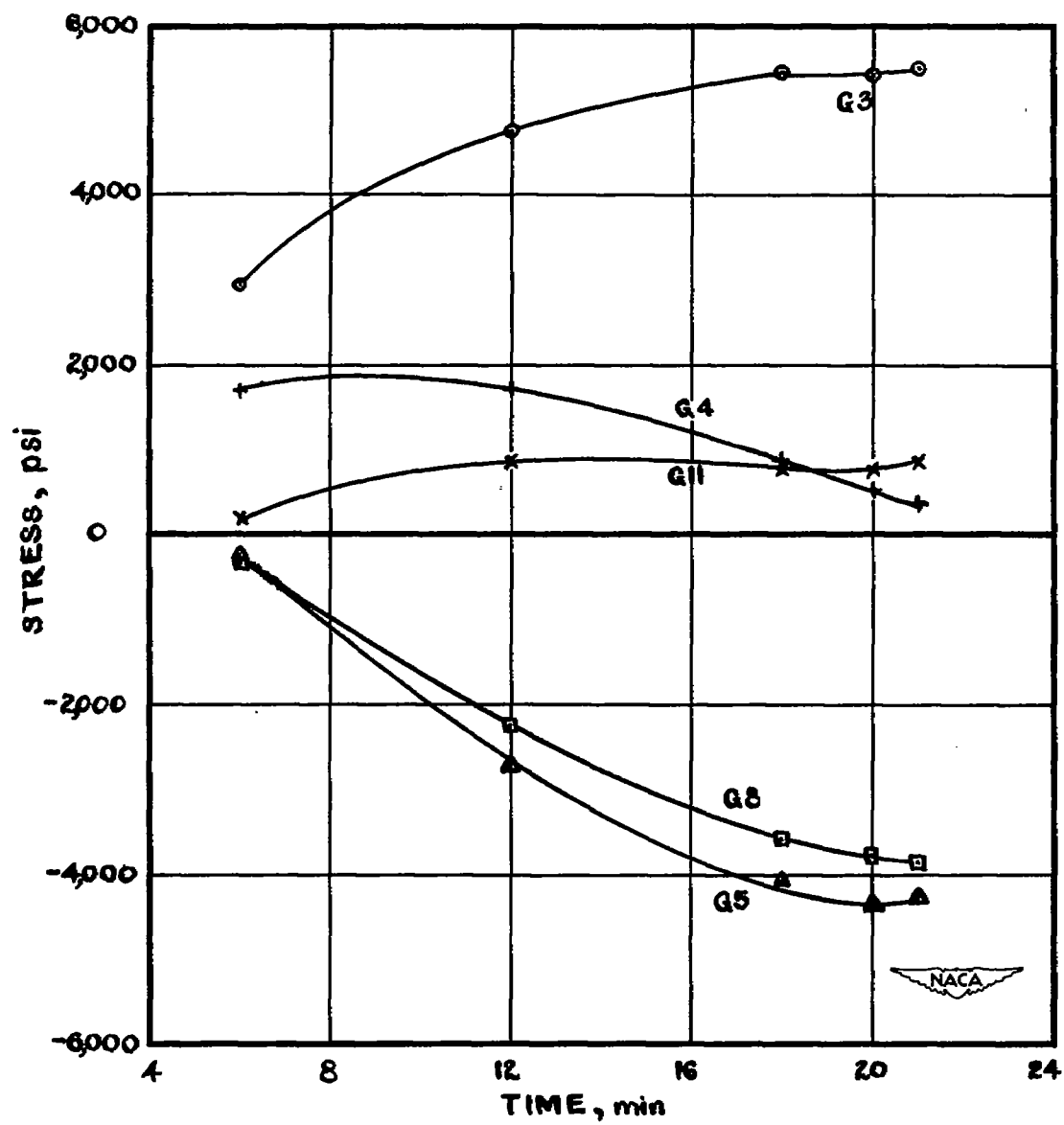
(j) Specimen 5, heating rate C.

Figure 10.- Concluded.



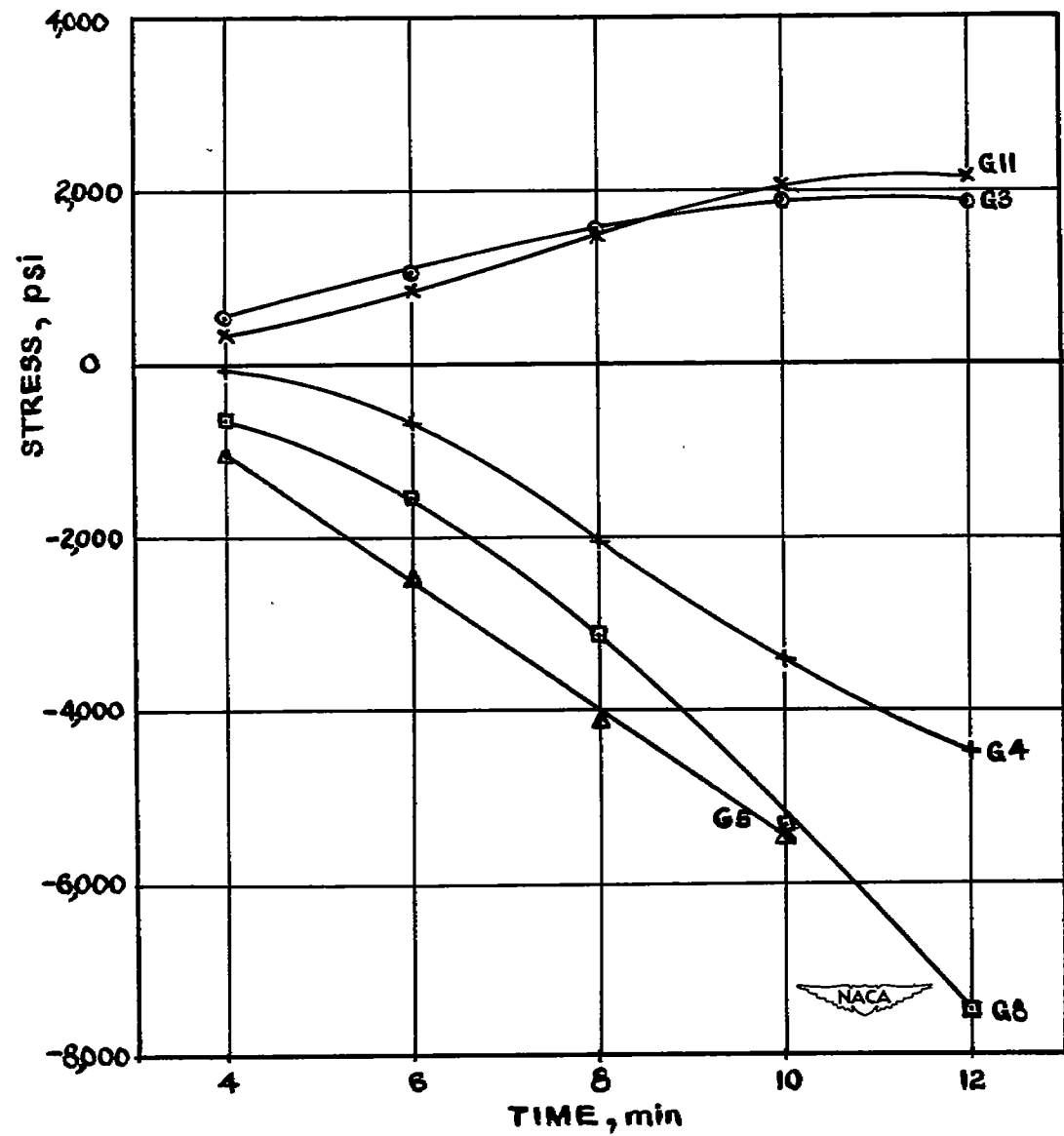
(a) Specimen 1, heating rate A.

Figure 11.- Time history of stress for selected points on specimen.



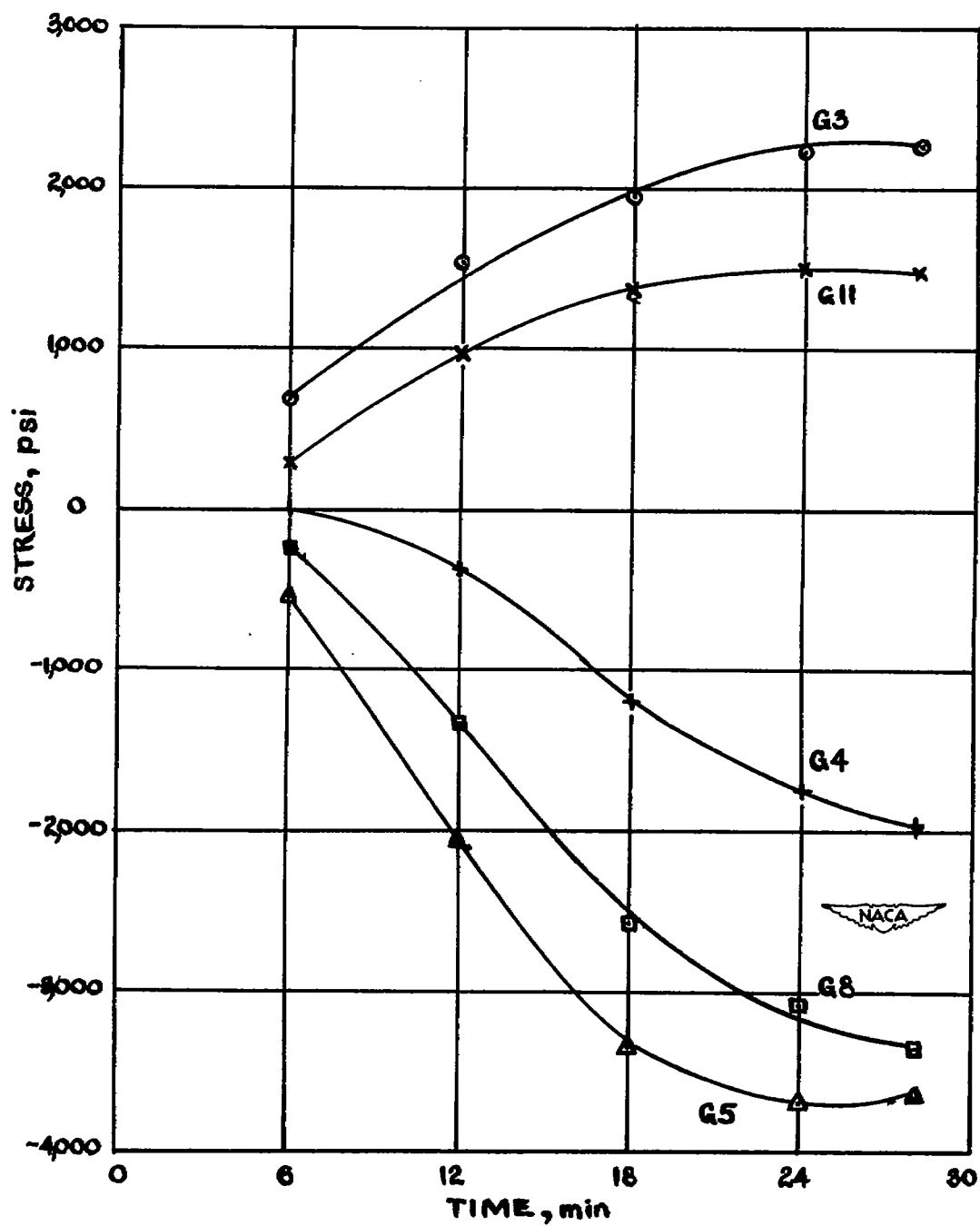
(b) Specimen 1, heating rate C.

Figure 11.- Continued.



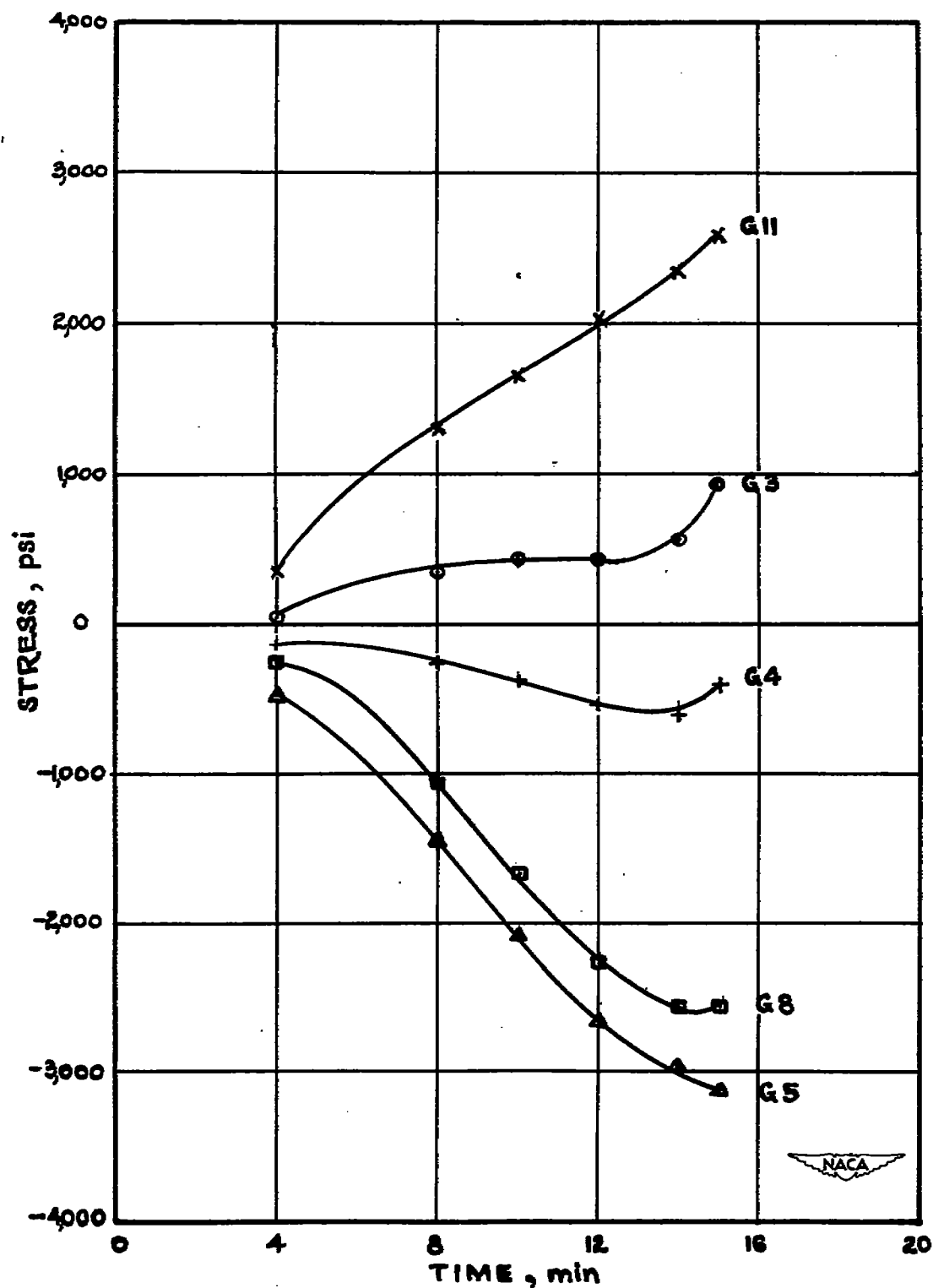
(c) Specimen 2, heating rate A.

Figure 11.- Continued.



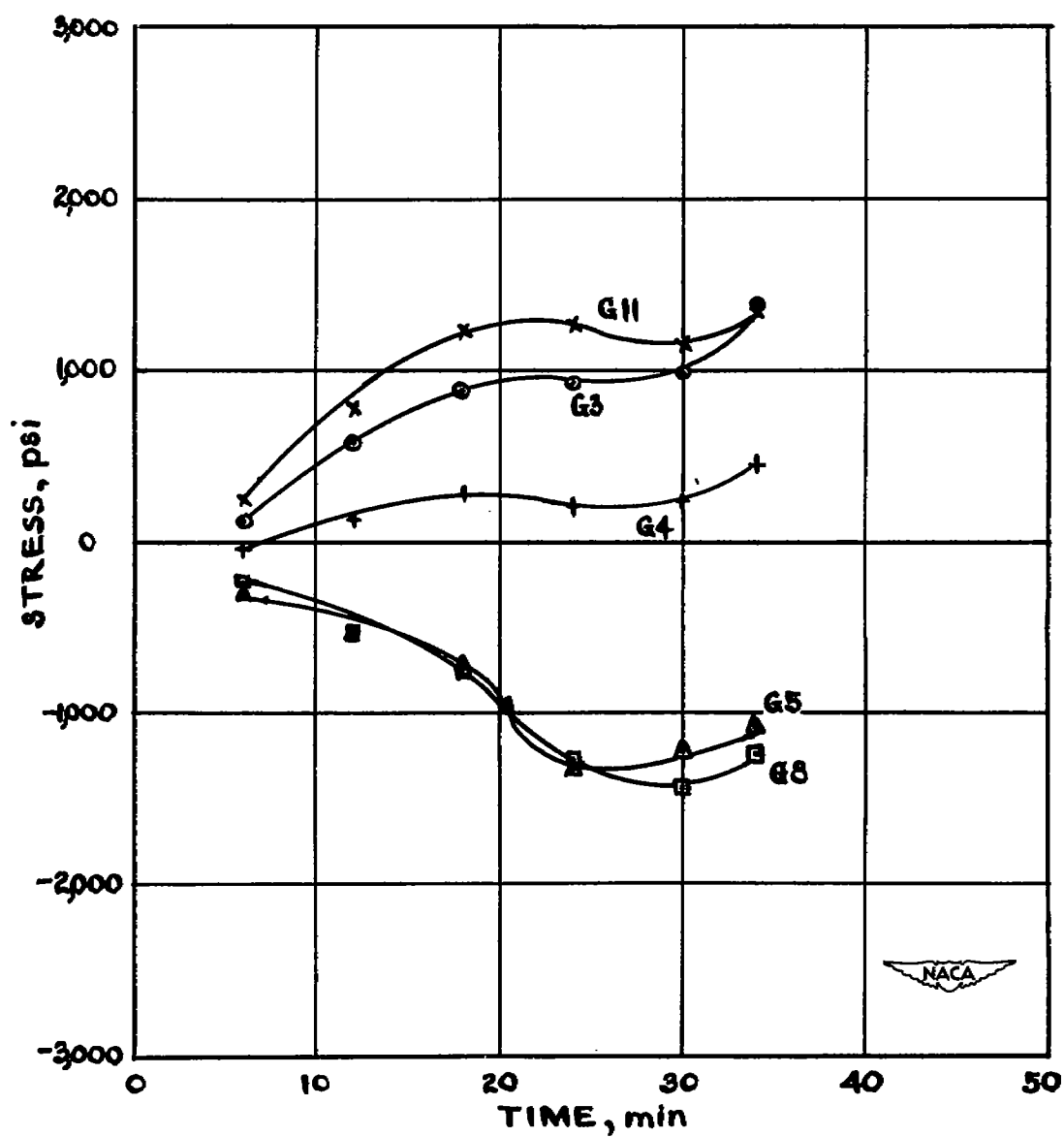
(d) Specimen 2, heating rate C.

Figure 11.- Continued.



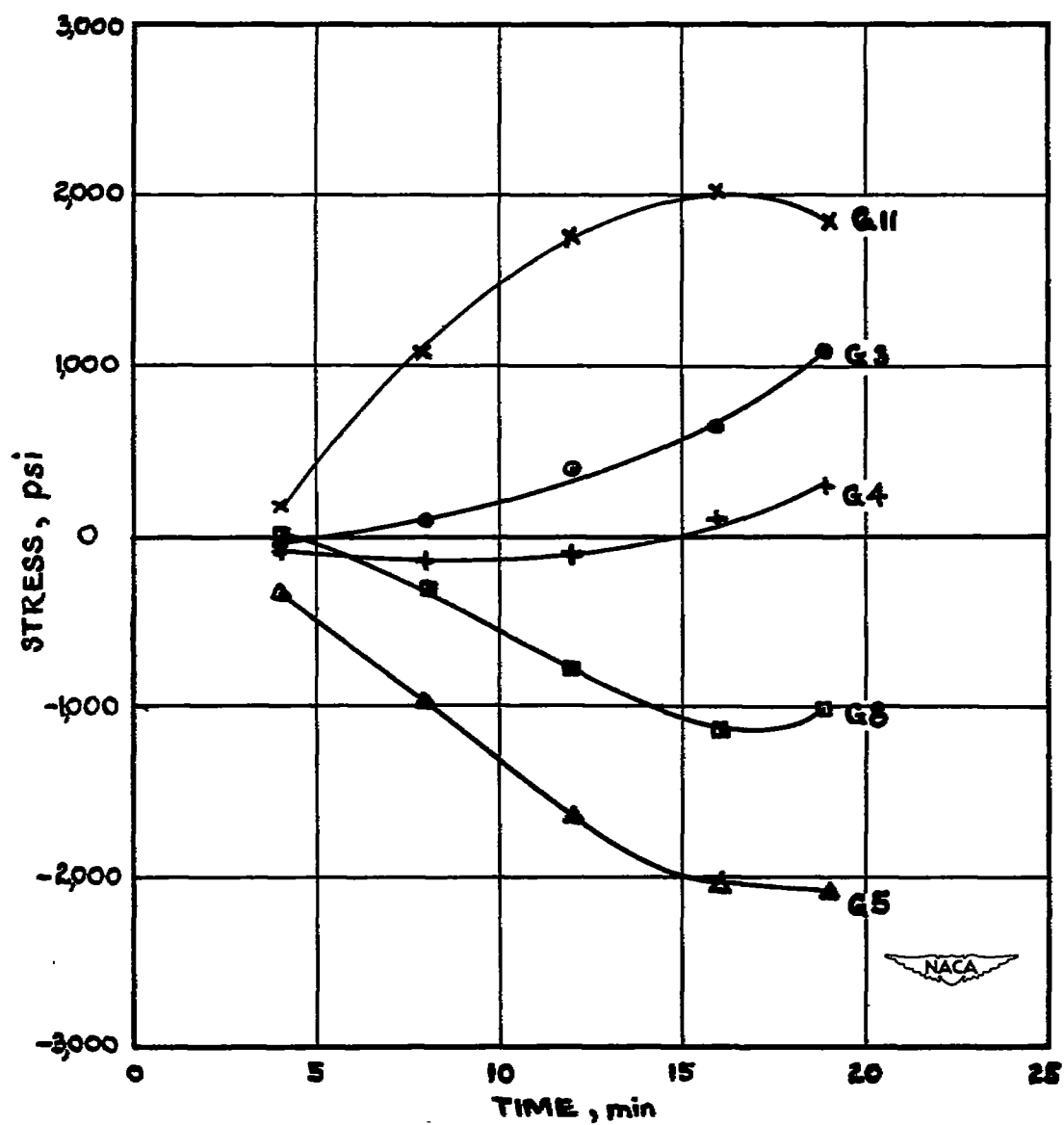
(e) Specimen 3, heating rate A.

Figure 11.- Continued.



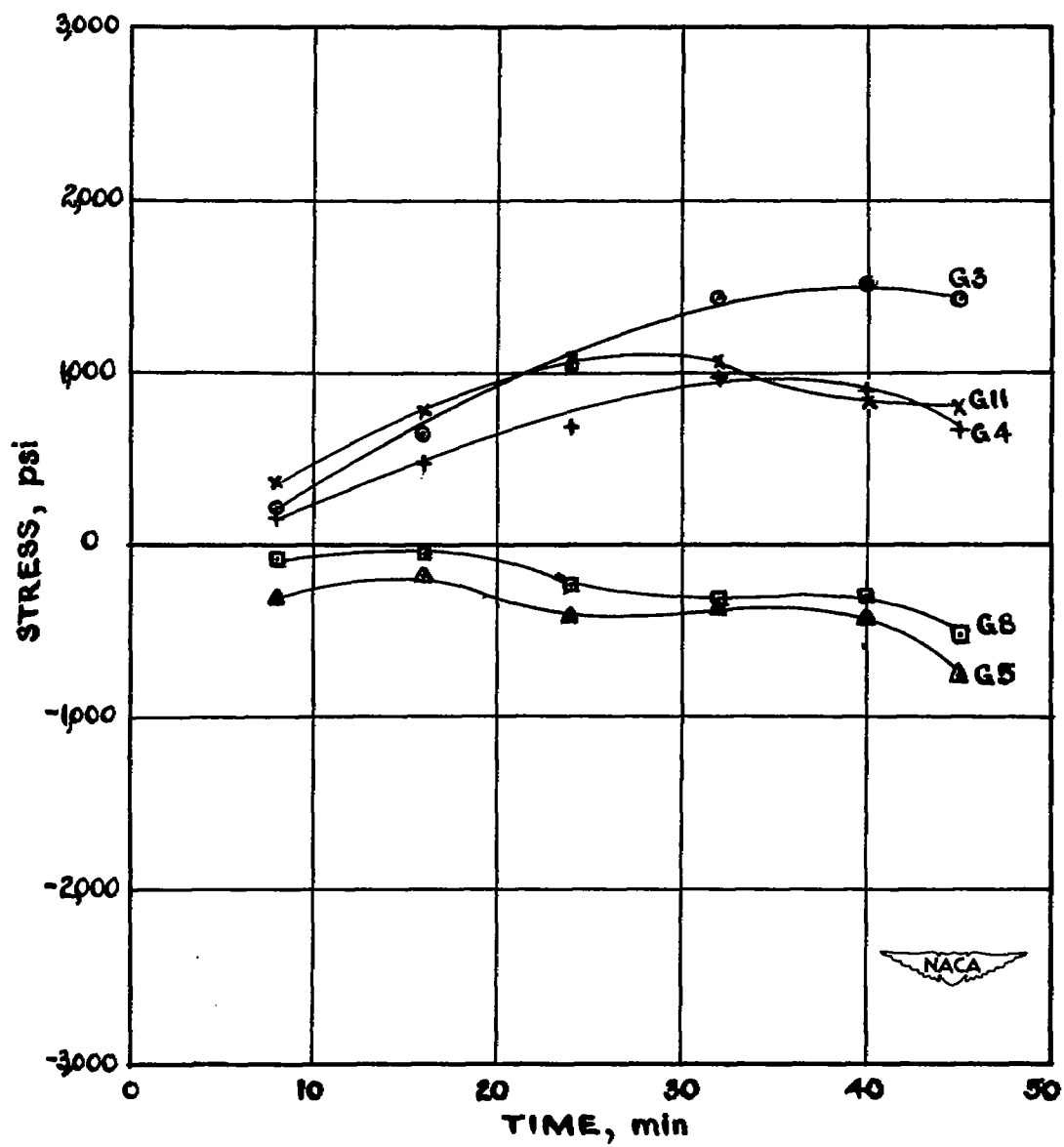
(f) Specimen 3, heating rate C.

Figure 11.- Continued.



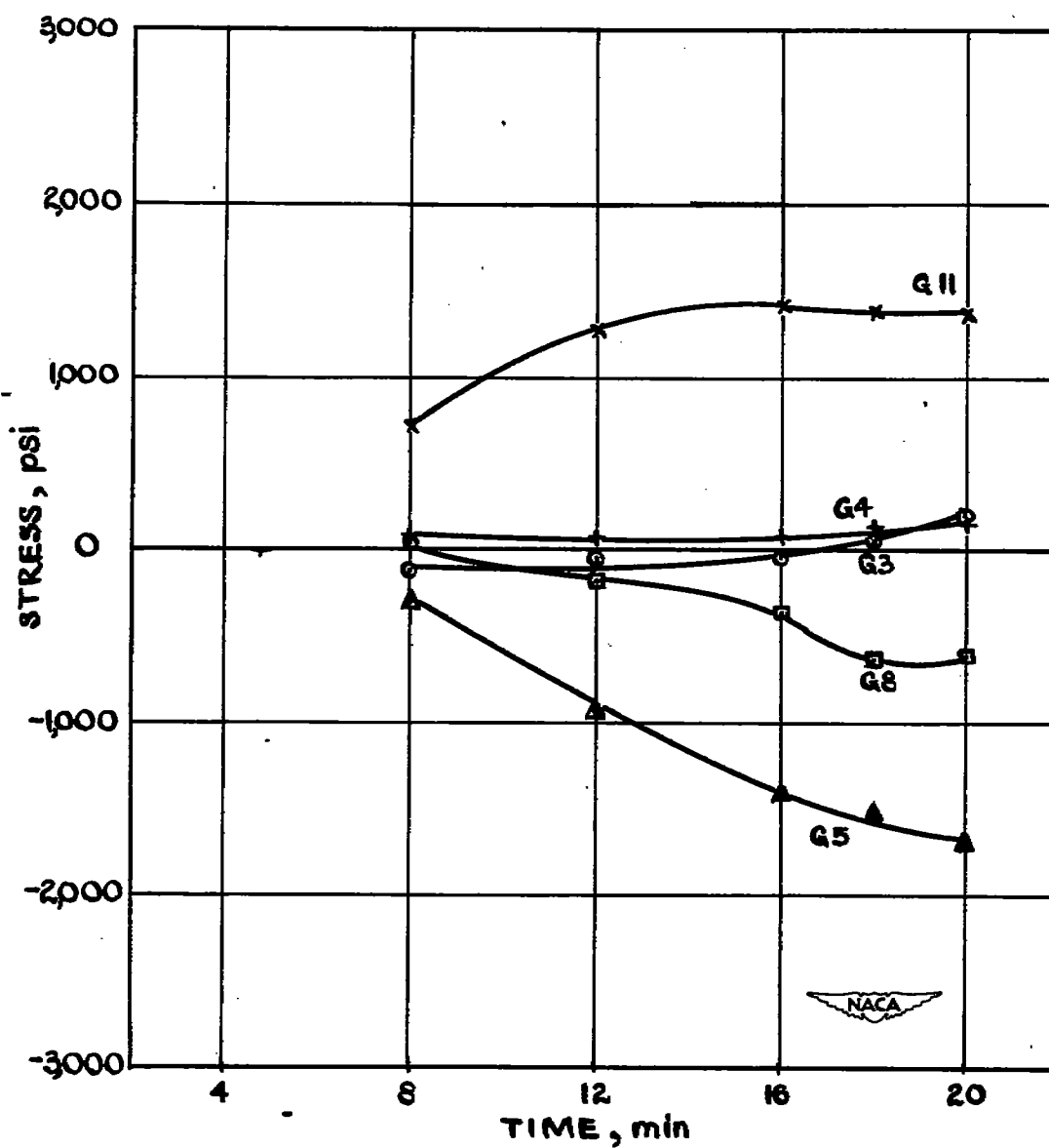
(g) Specimen 4, heating rate A.

Figure 11.- Continued.



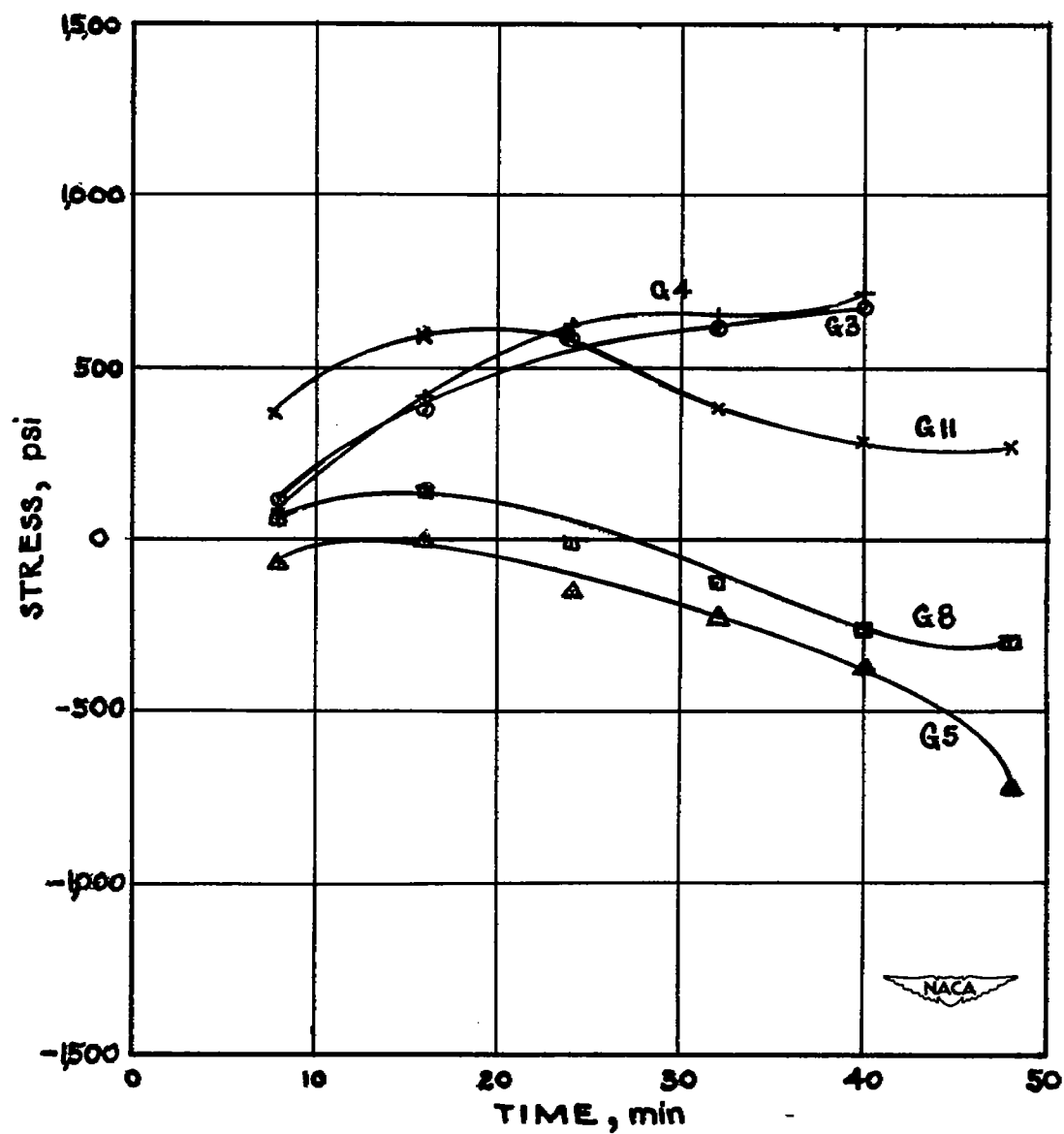
(h) Specimen 4, heating rate C.

Figure 11.- Continued.



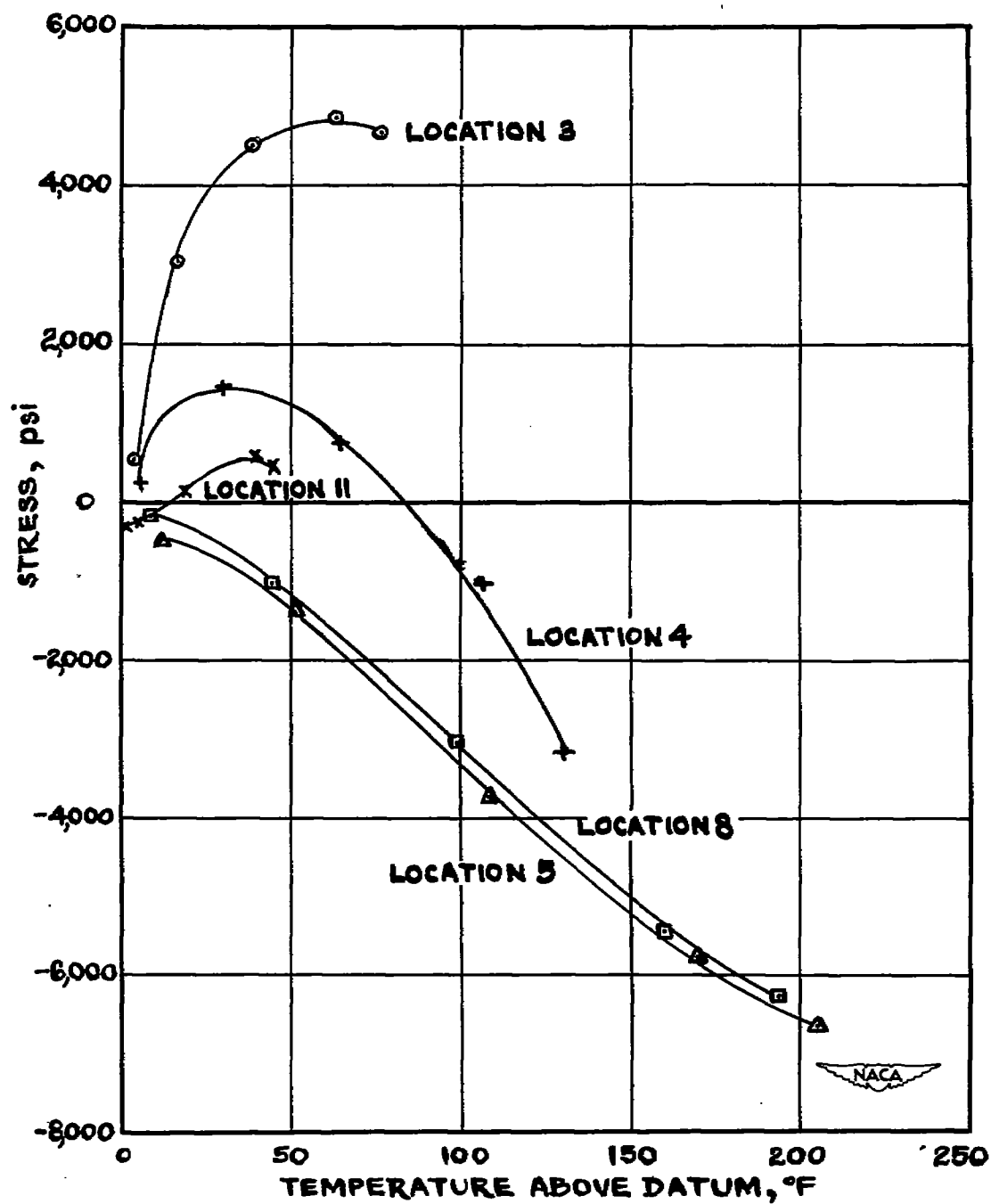
(i) Specimen 5, heating rate A.

Figure 11.- Continued.



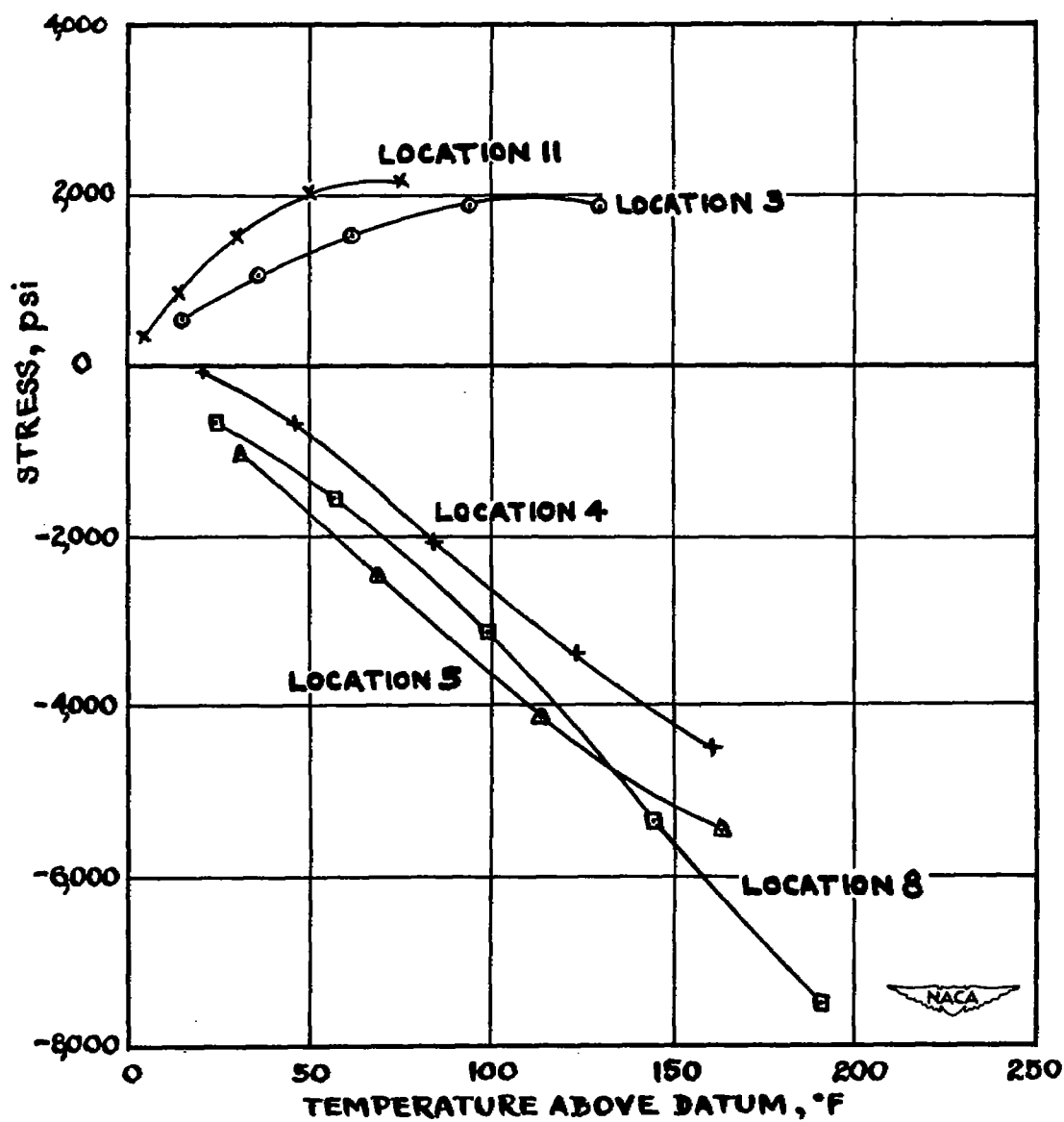
(j) Specimen 5, heating rate C.

Figure 11.- Concluded.



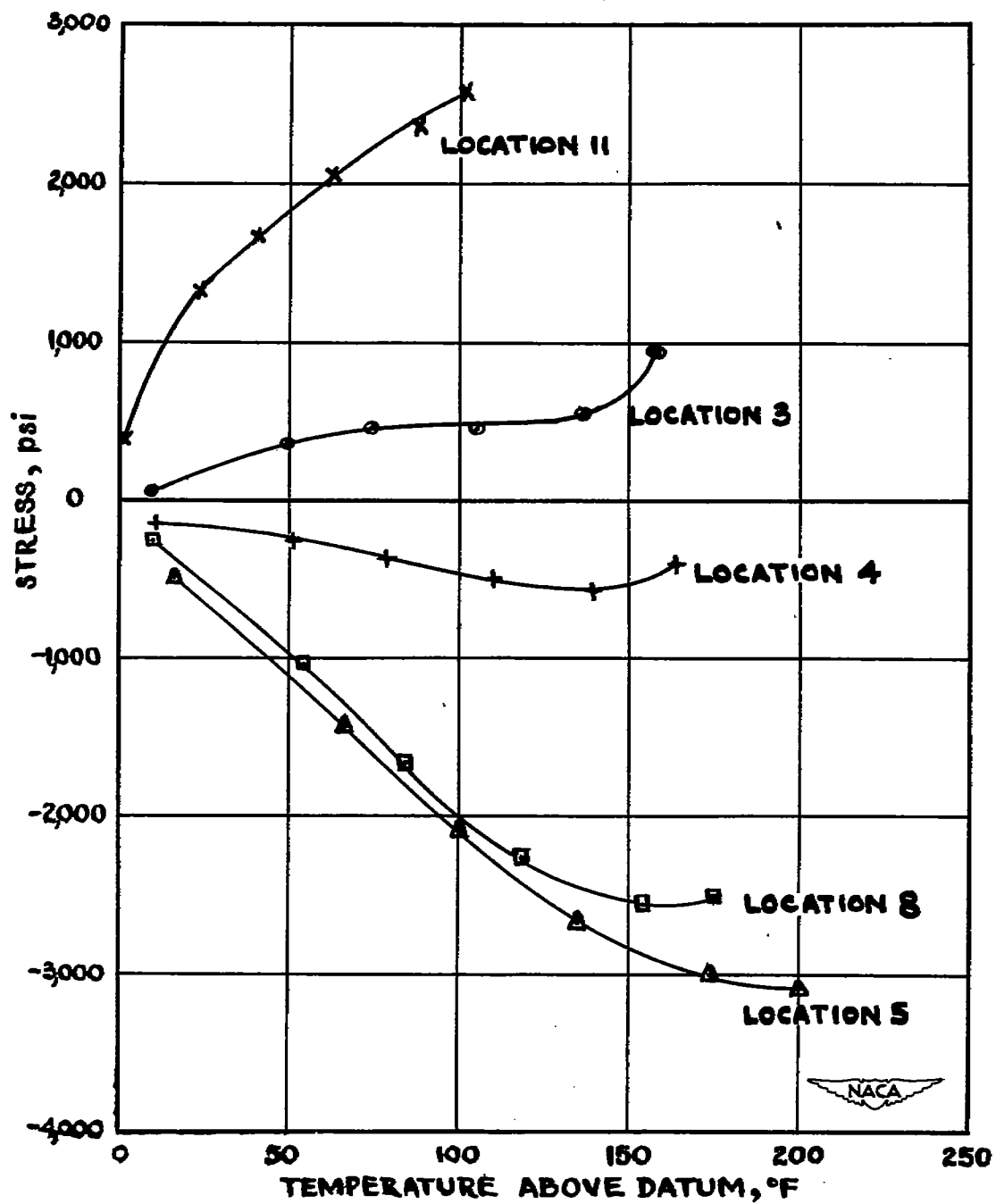
(a) Specimen 1.

Figure 12.- Stress against temperature at five locations on each specimen at heating rate A.



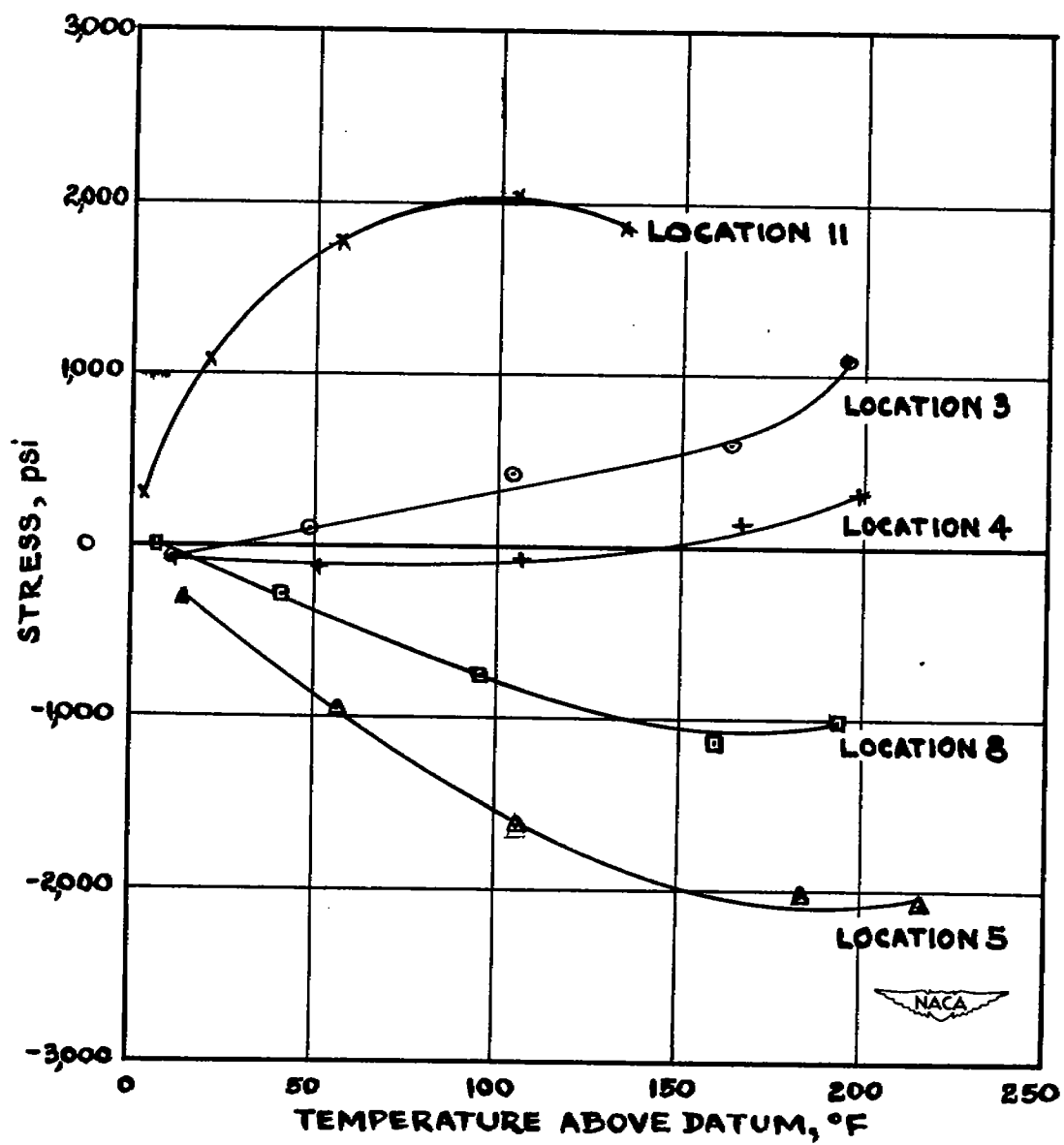
(b) Specimen 2.

Figure 12.- Continued.



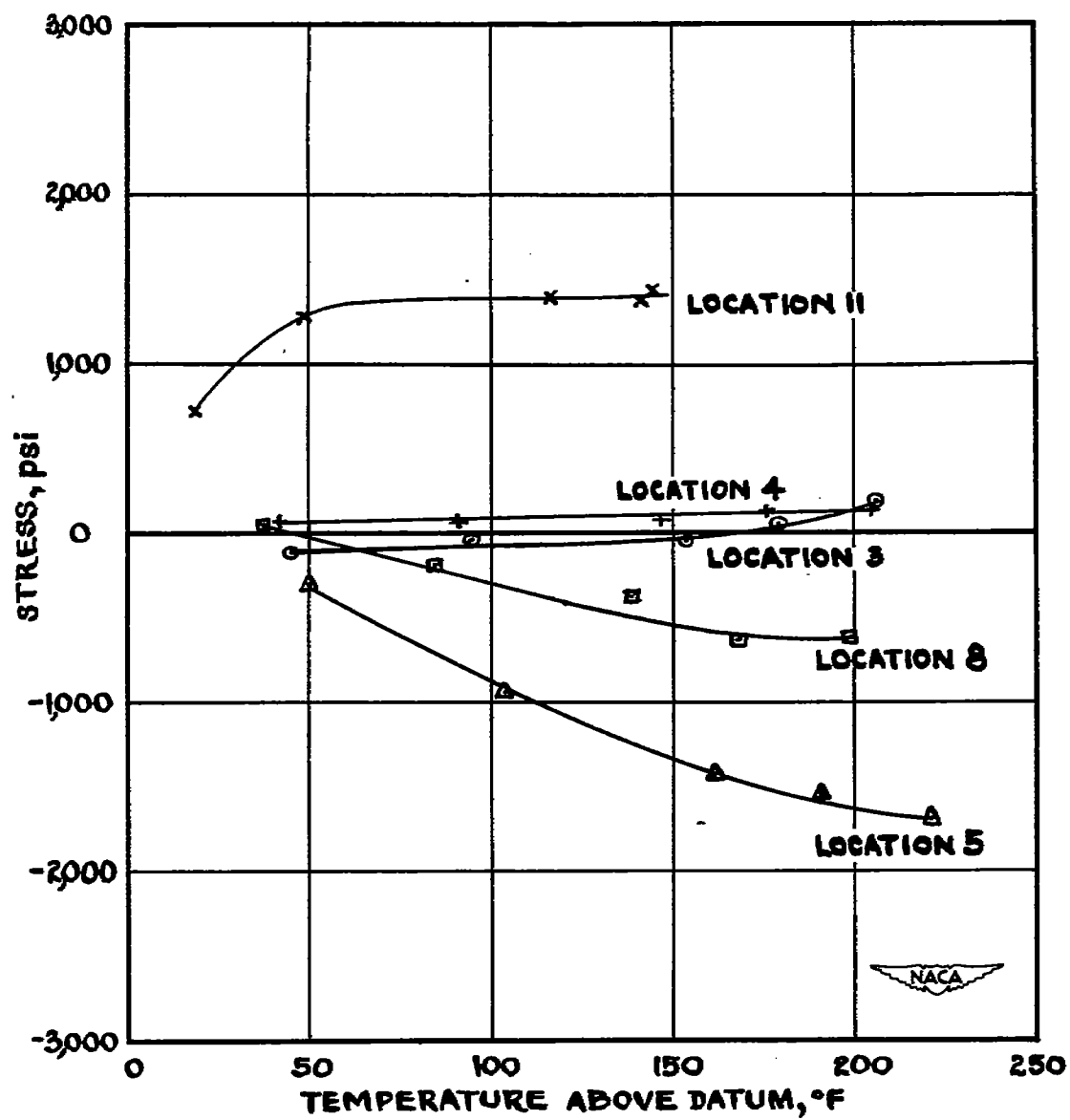
(c) Specimen 3.

Figure 12.- Continued.



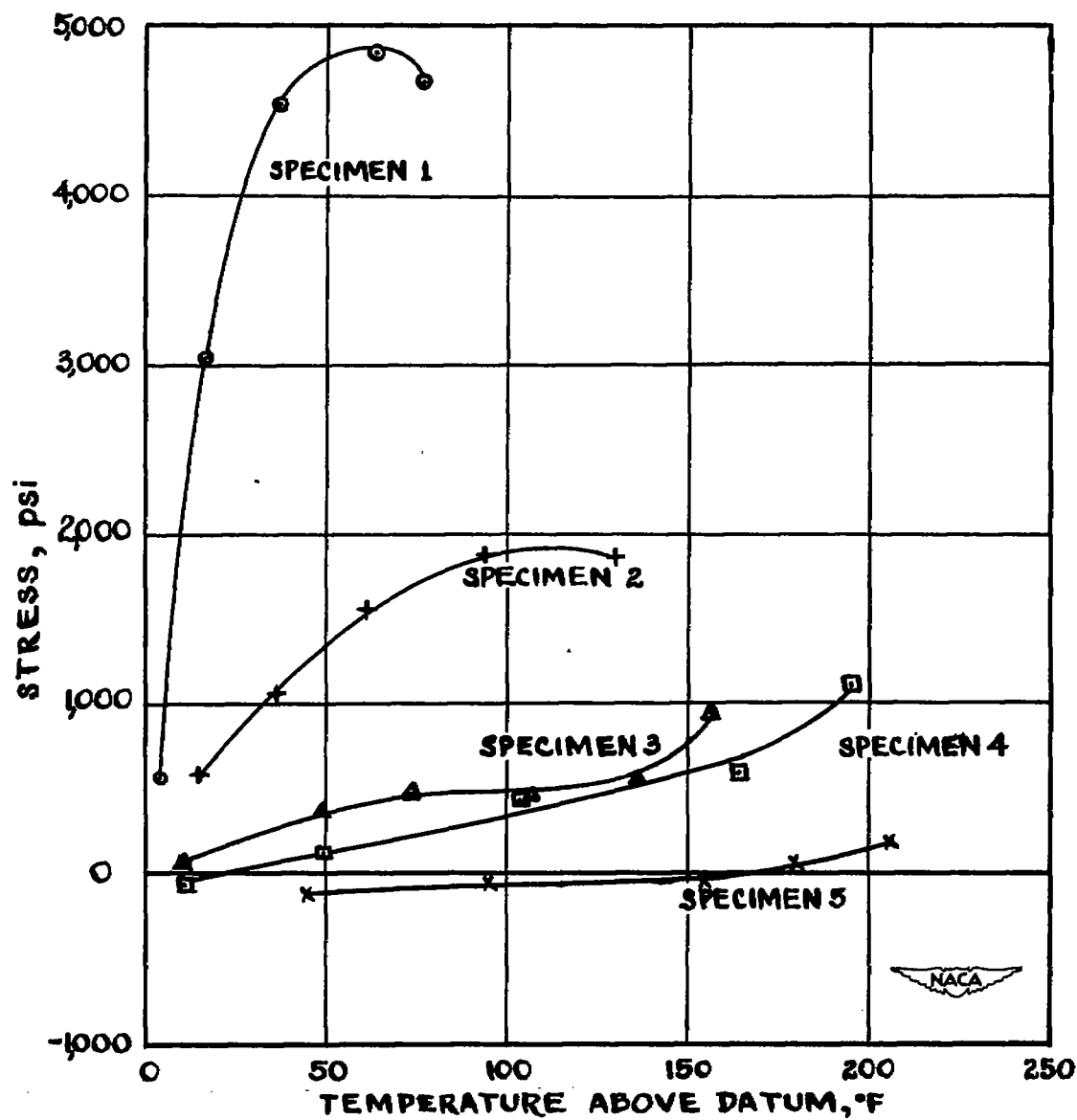
(d) Specimen 4.

Figure 12.- Continued.



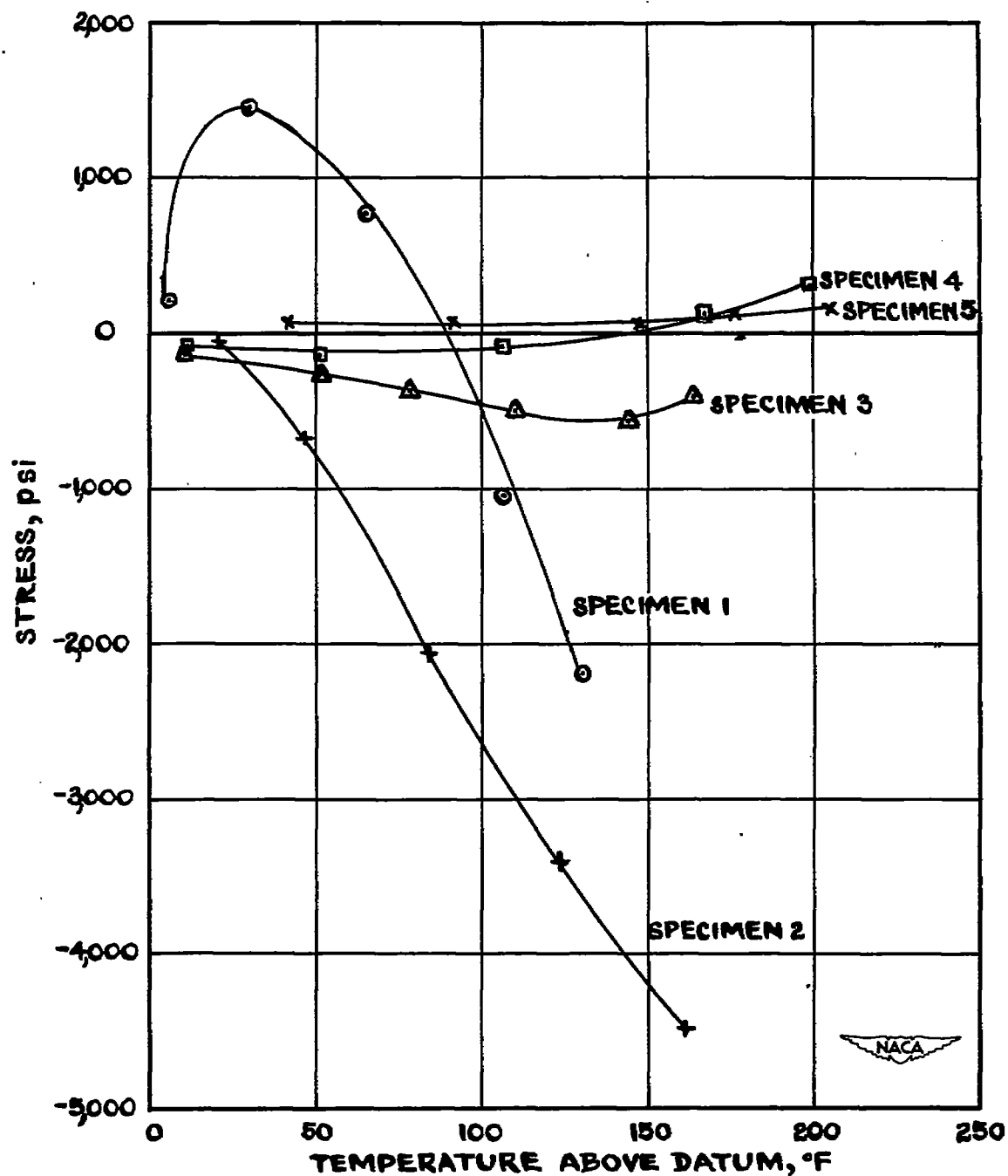
(e) Specimen 5.

Figure 12.- Concluded.



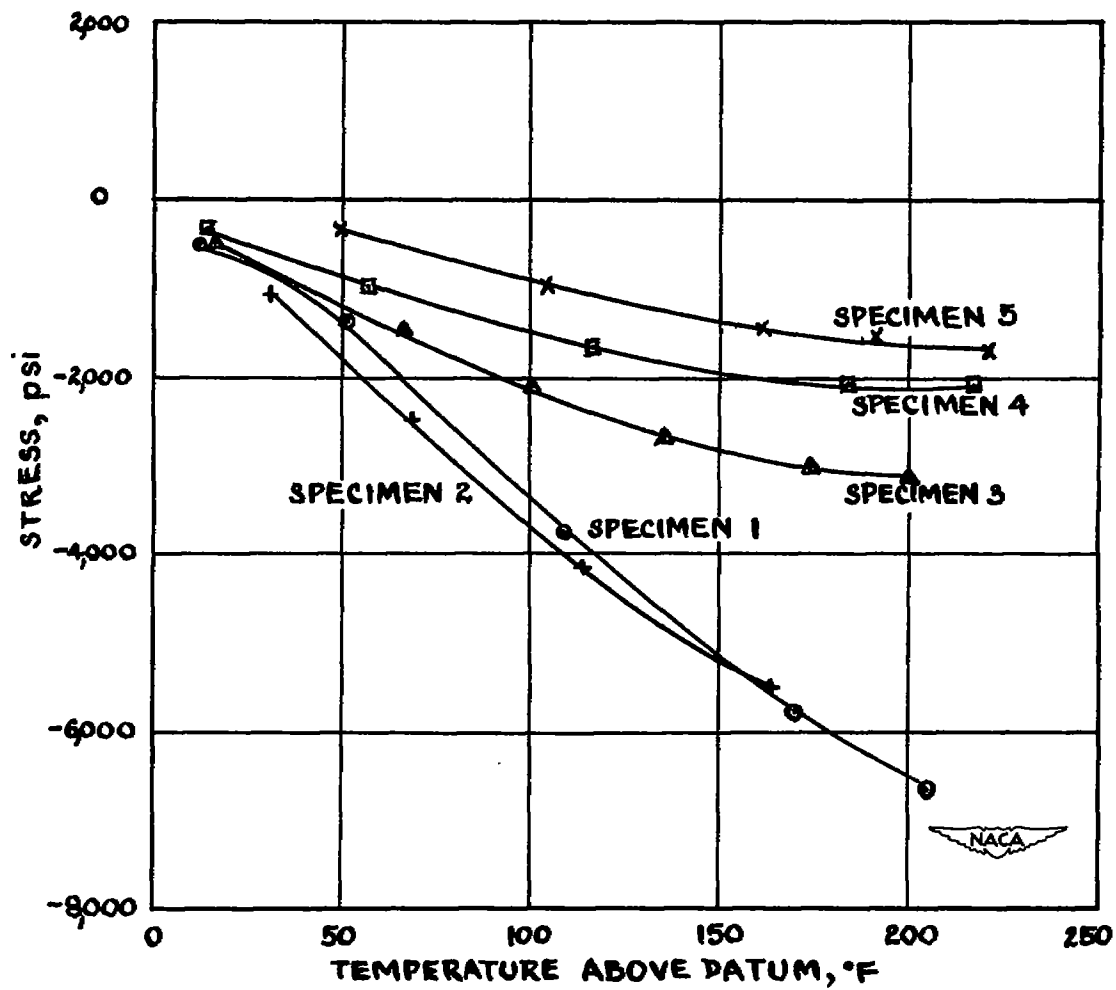
(a) Channel 3.

Figure 13.- Stress against temperature for five specimens at the same location for heating rate A.



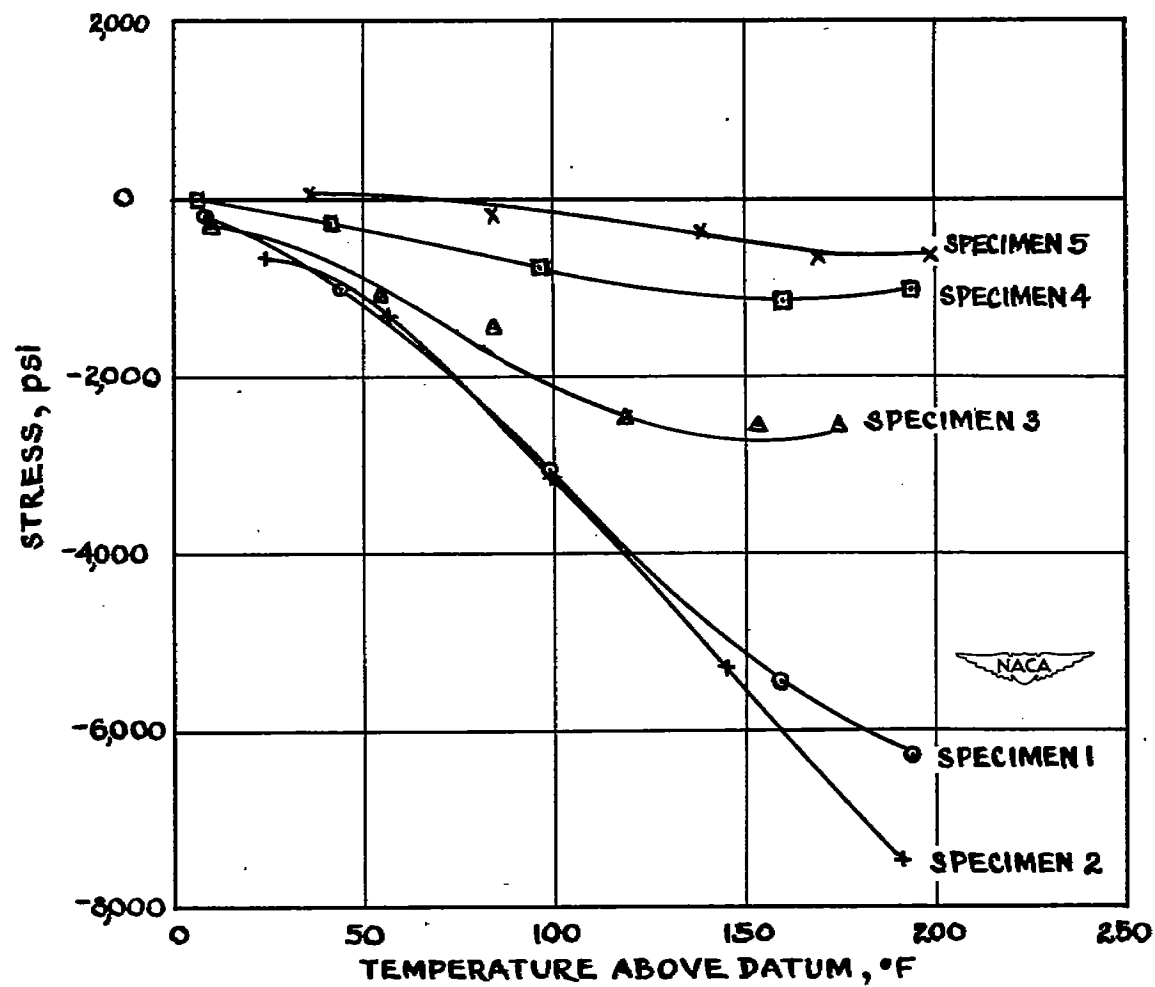
(b) Channel 4.

Figure 13.- Continued.



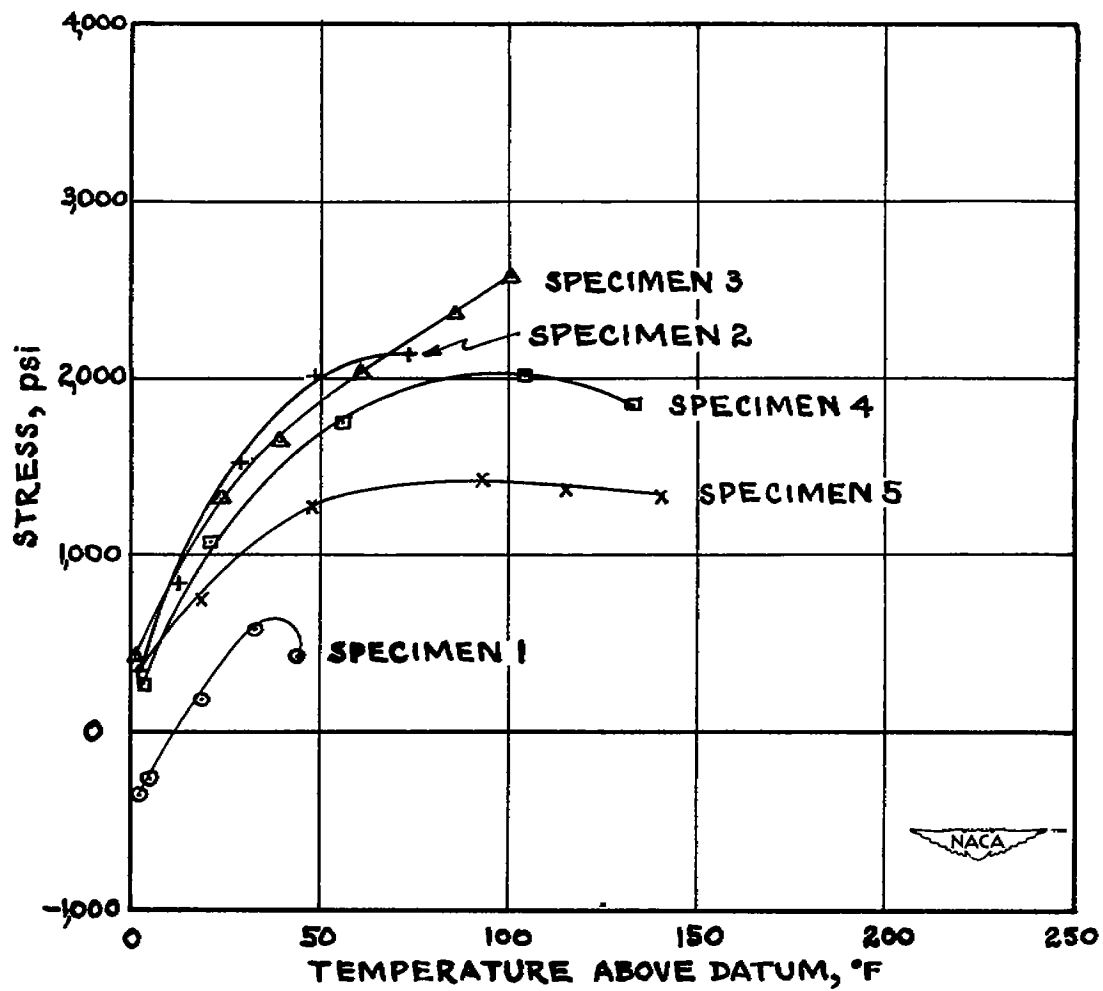
(c) Channel 5.

Figure 13.- Continued.



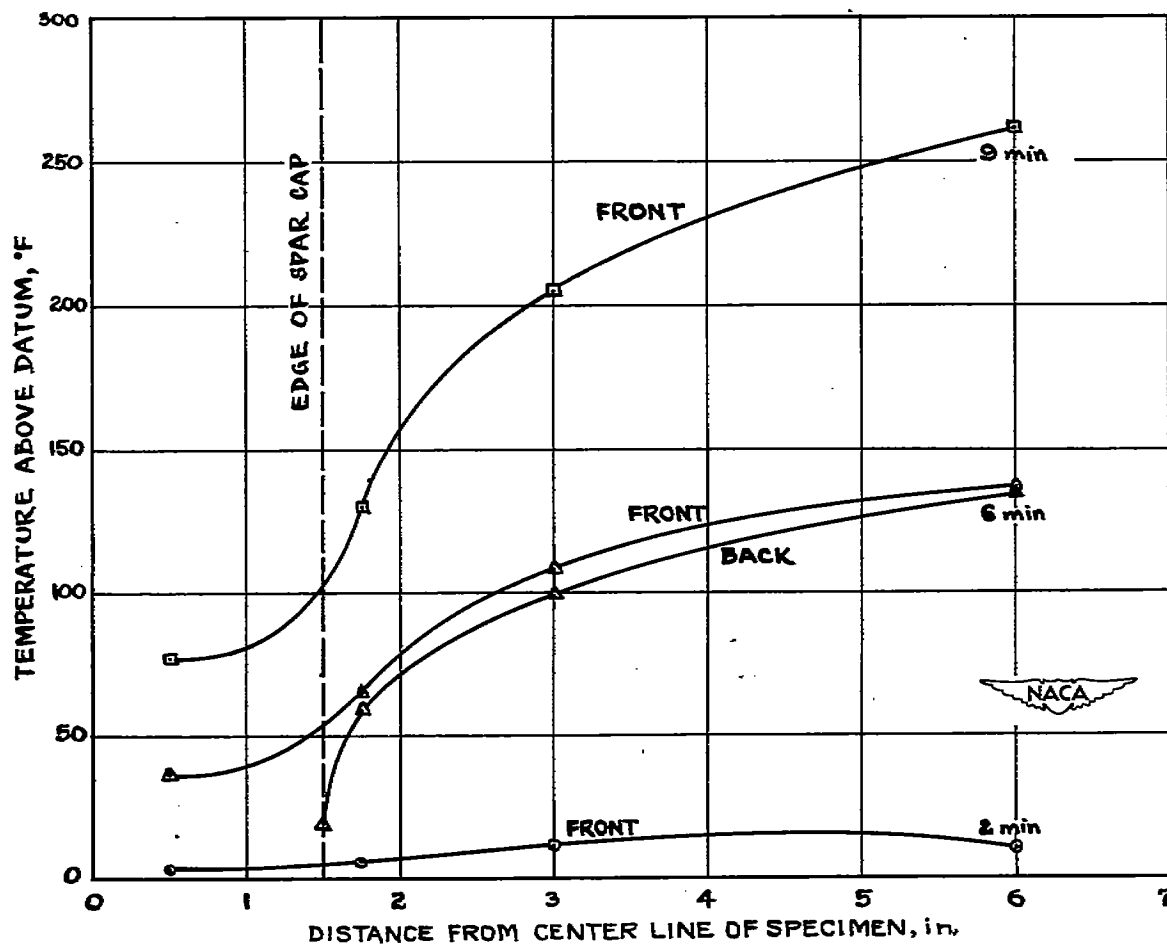
(d) Channel 8.

Figure 13.- Continued.



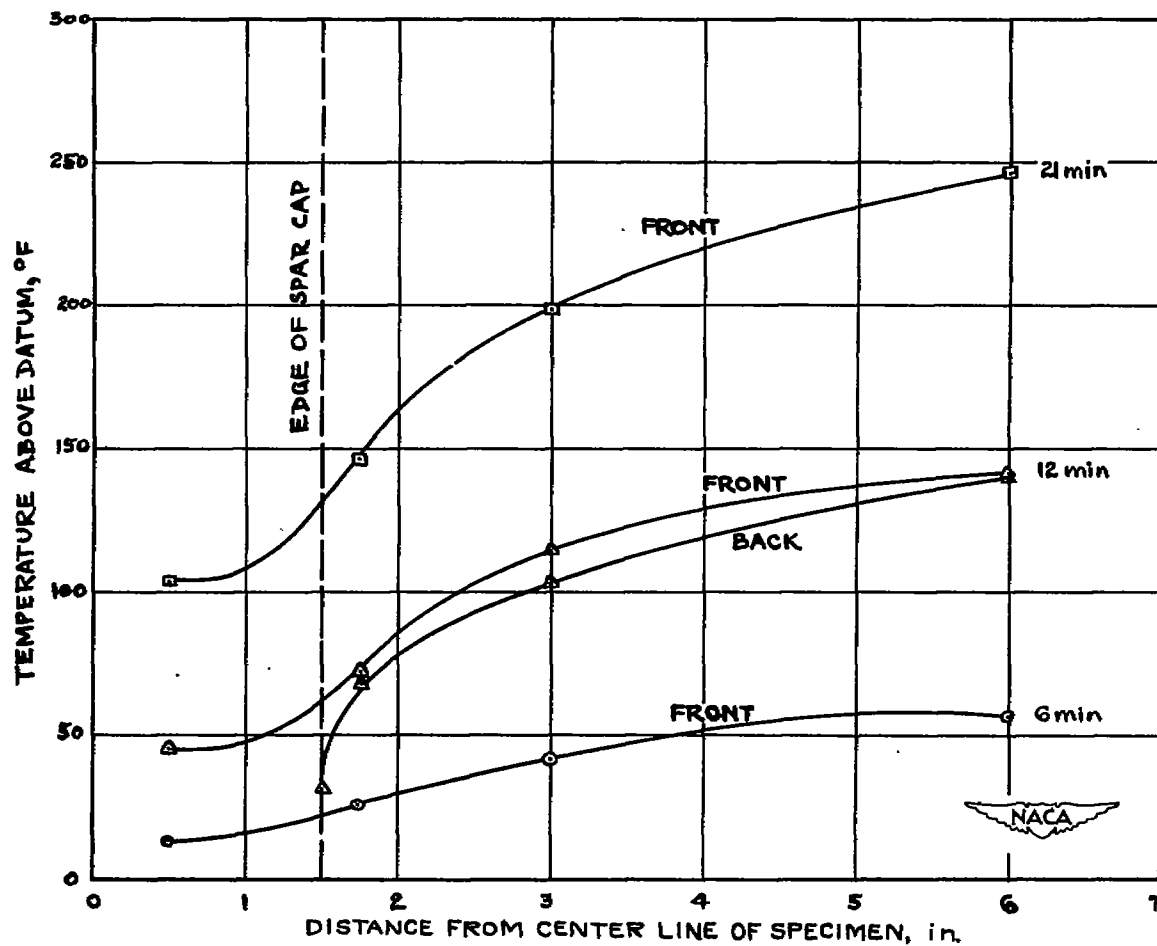
(e) Channel 11.

Figure 13.- Concluded.



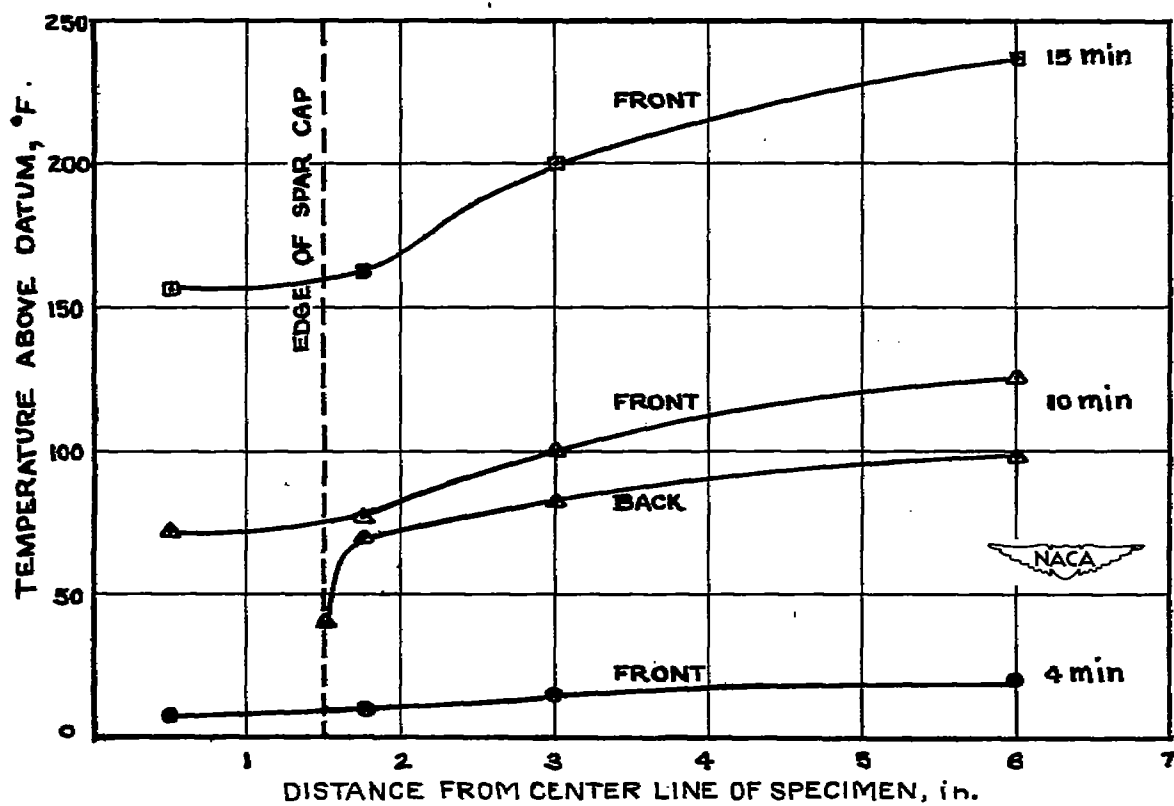
(a) Specimen 1, heating rate A.

Figure 14.- Chordwise temperature distributions for three specimens at heating rates A and C for three time intervals.



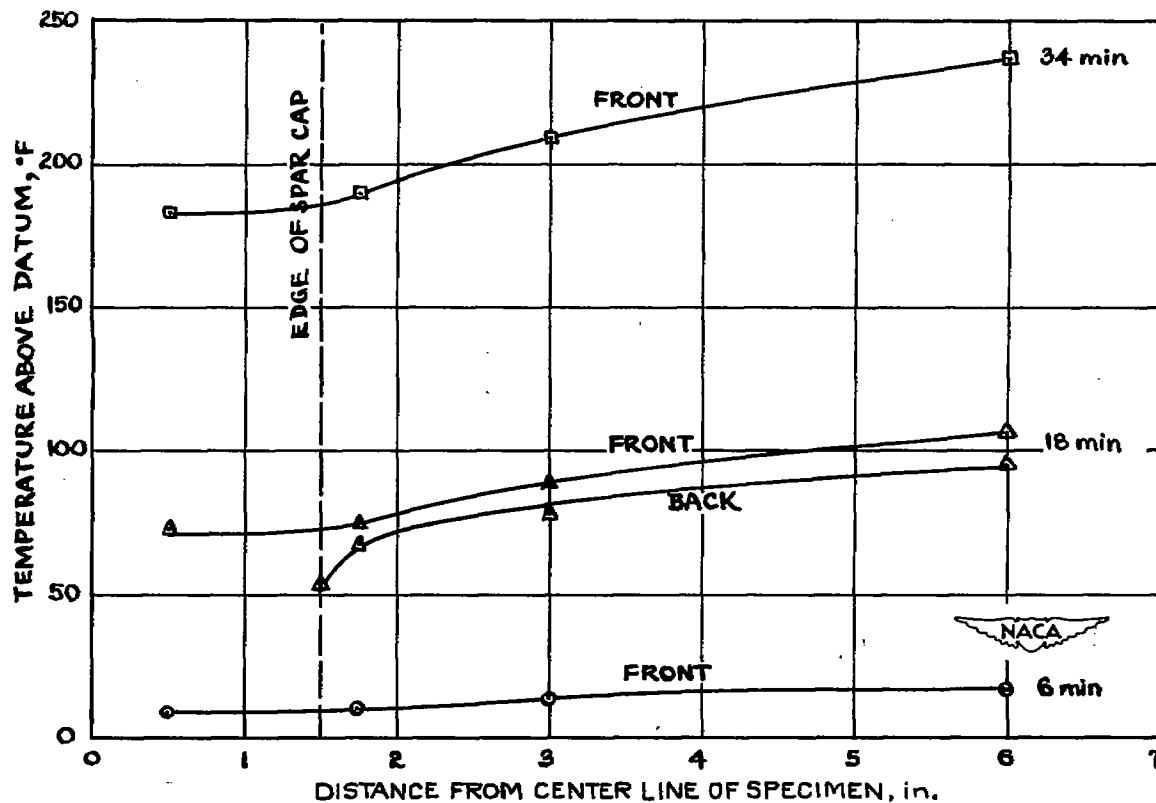
(b) Specimen 1, heating rate C.

Figure 14.- Continued.



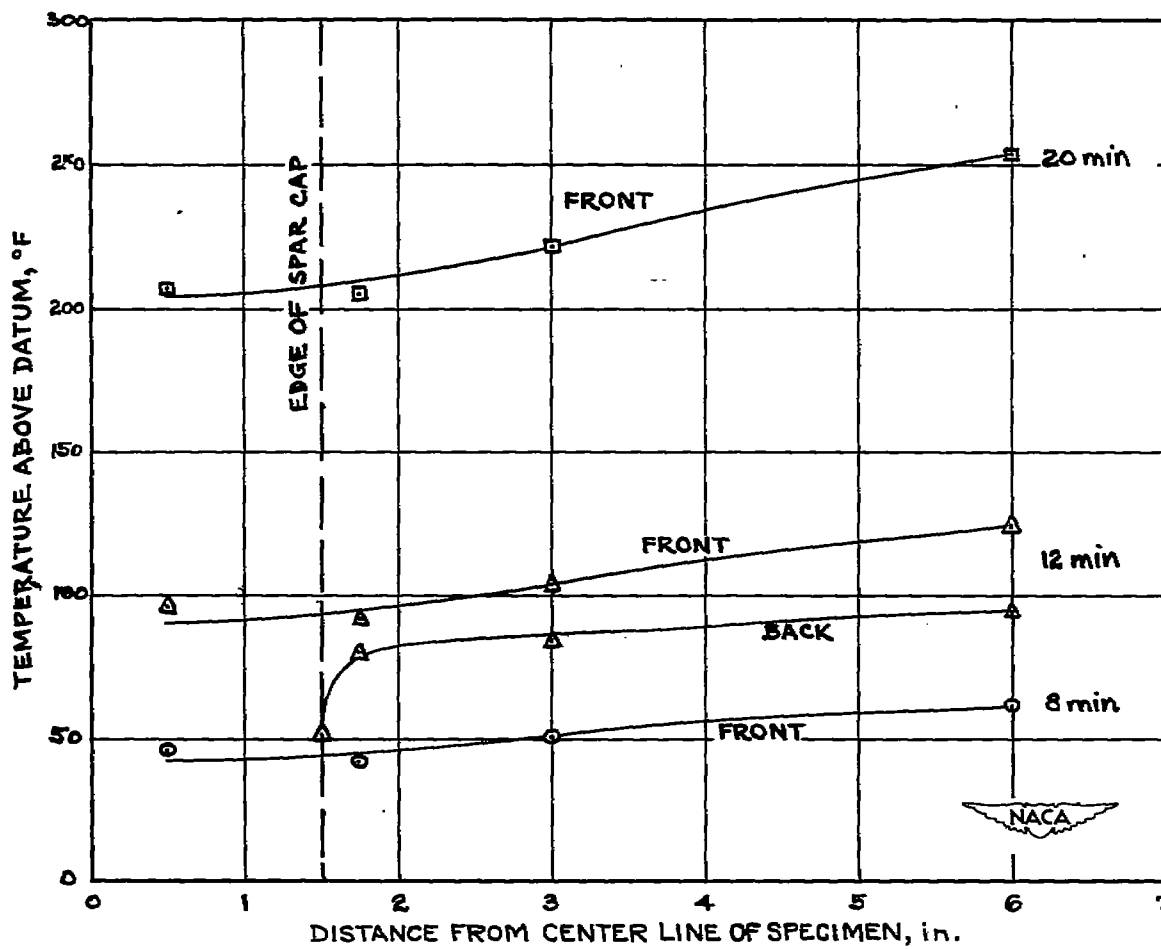
(c) Specimen 3, heating rate A.

Figure 14.- Continued.



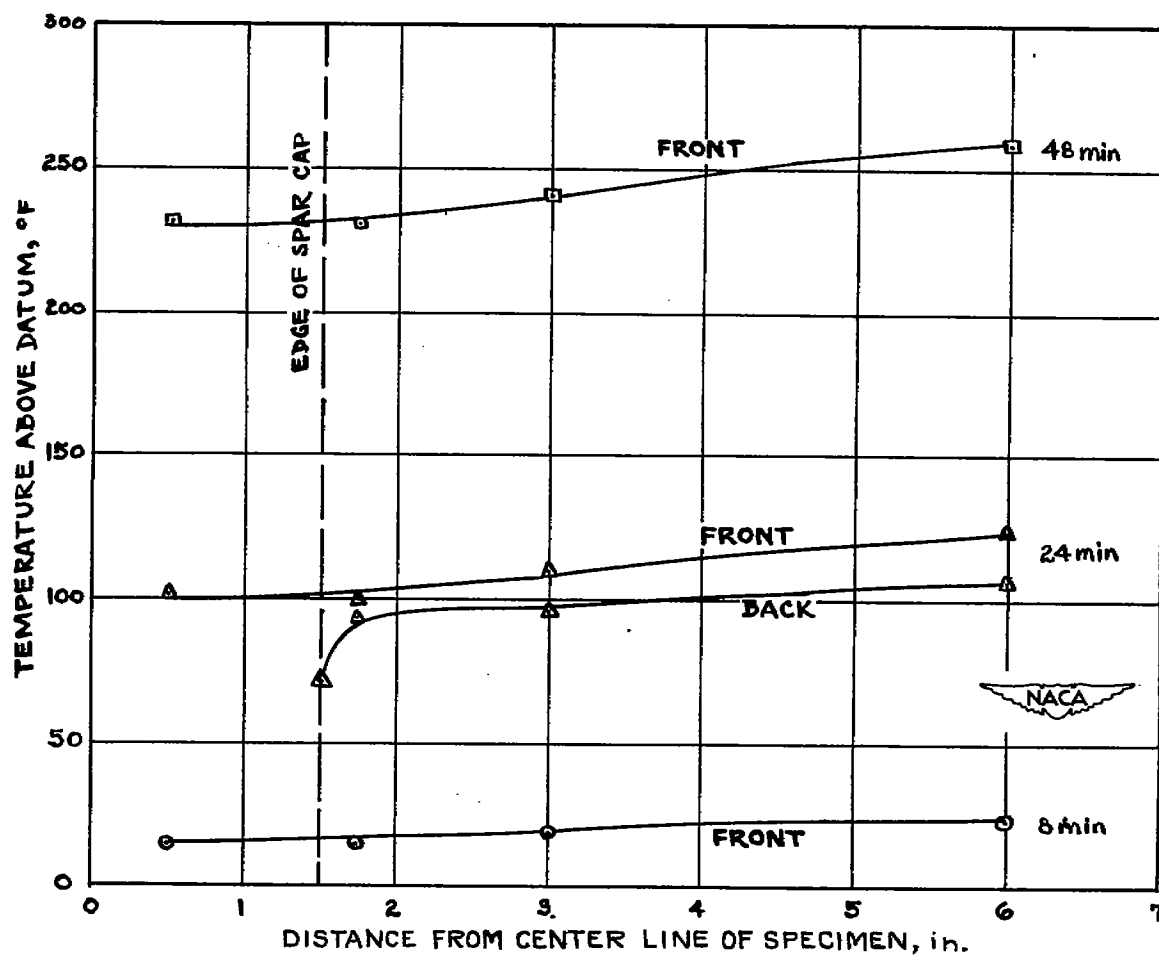
(d) Specimen 3, heating rate C.

Figure 14.- Continued.



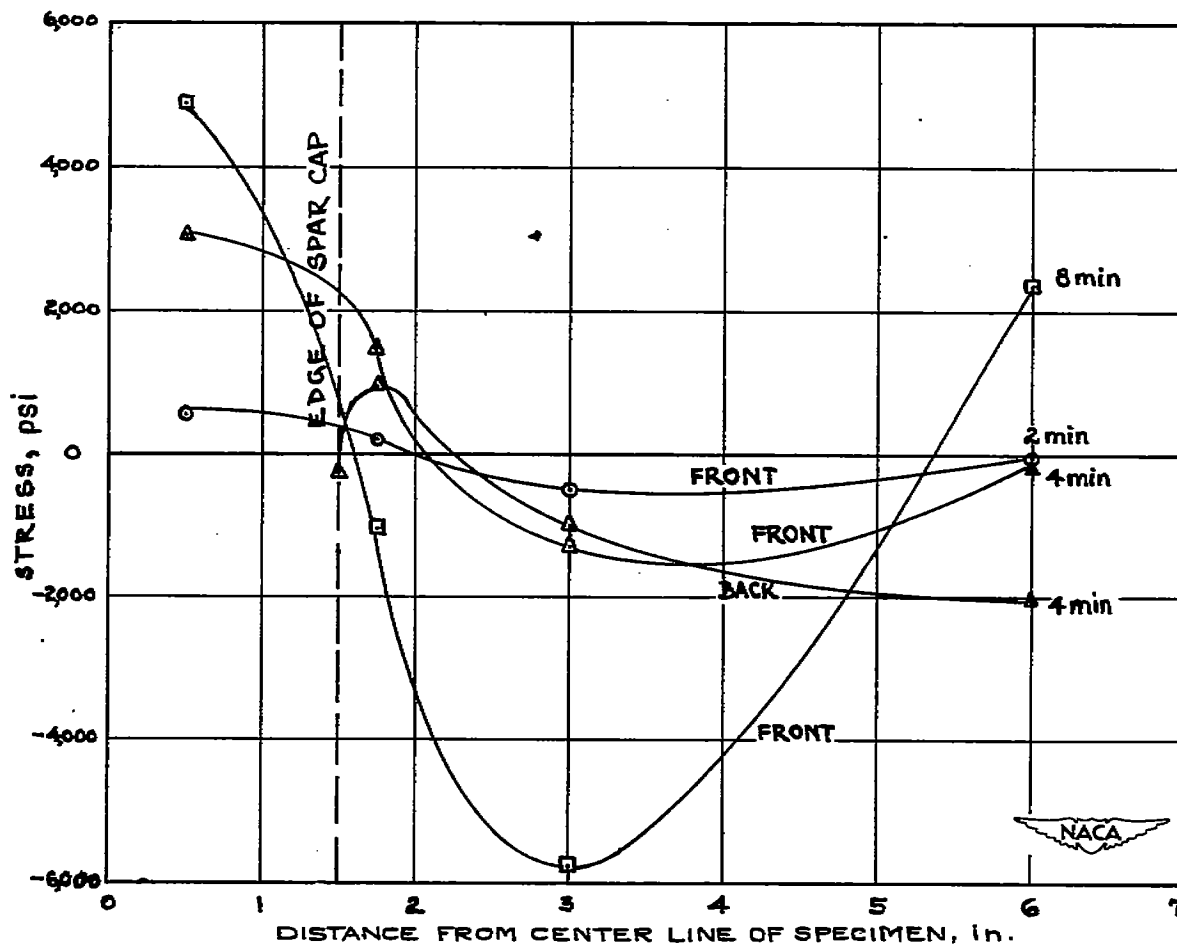
(e) Specimen 5, heating rate A.

Figure 14.- Continued.



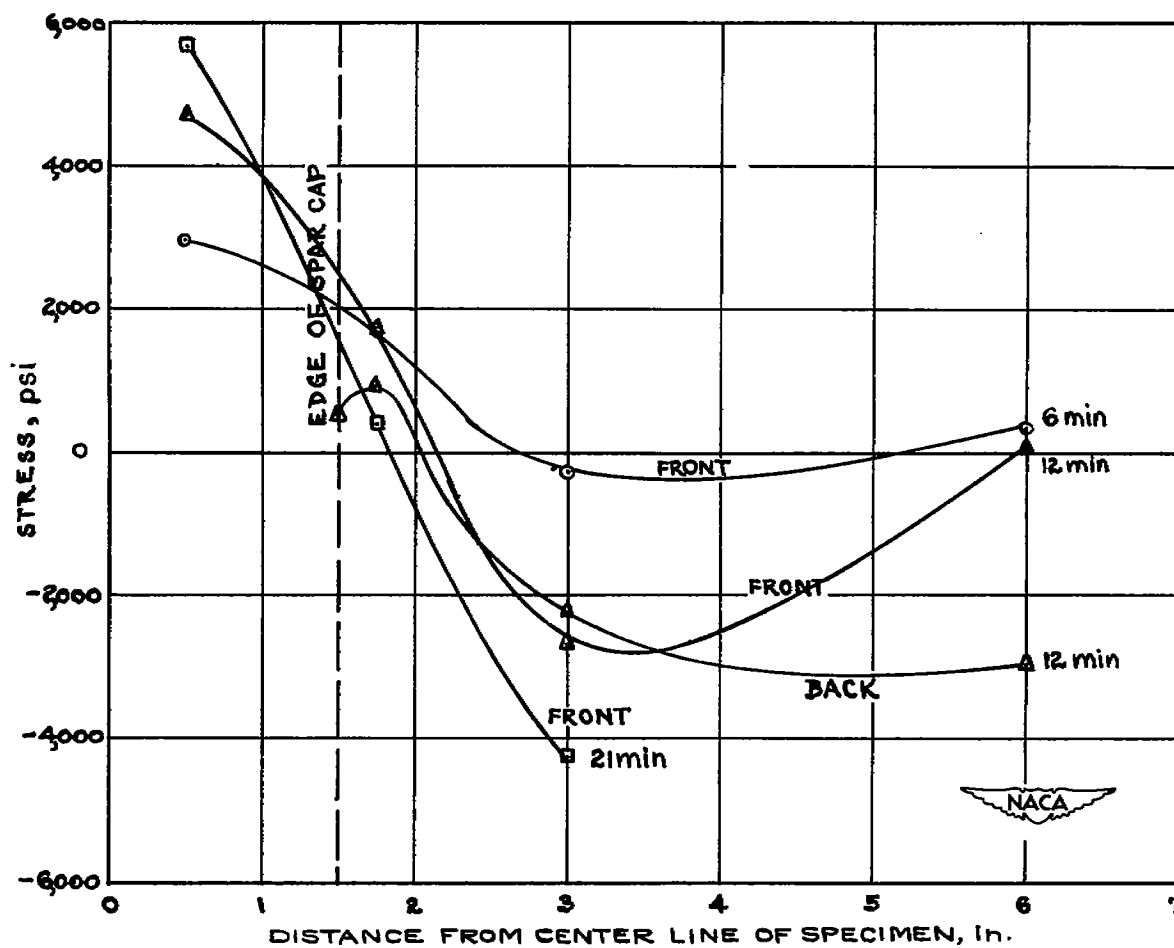
(f) Specimen 5, heating rate C.

Figure 14.- Concluded.



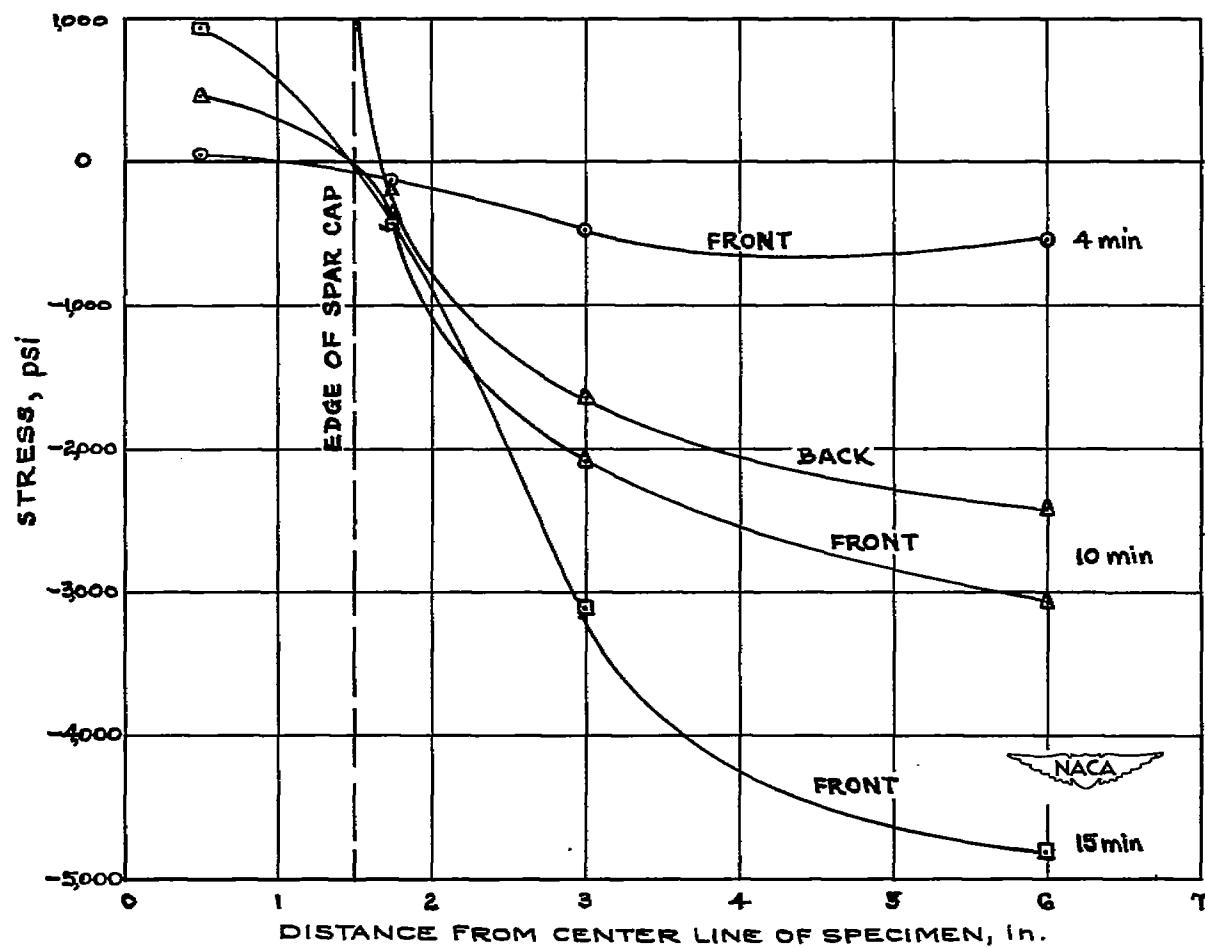
(a) Specimen 1, heating rate A.

Figure 15.- Chordwise stress distributions for three specimens at heating rates A and C for three time intervals.



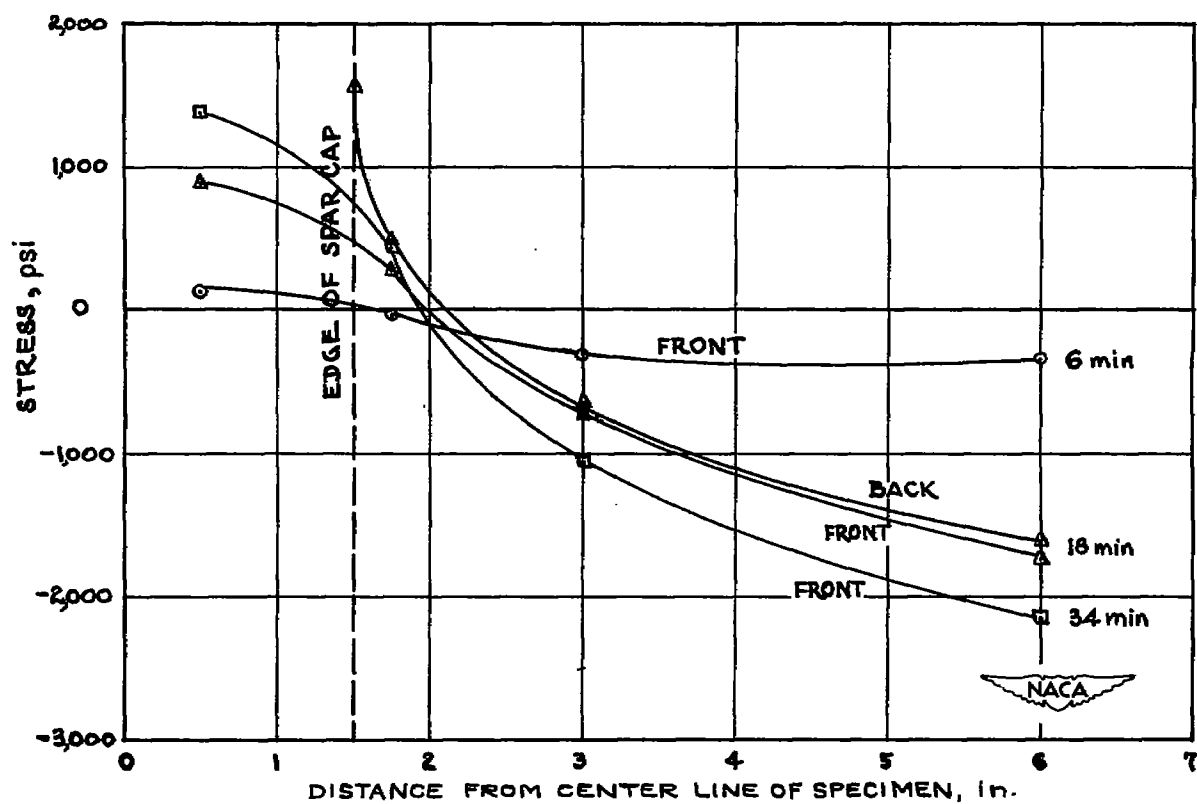
(b) Specimen 1, heating rate C.

Figure 15.- Continued.



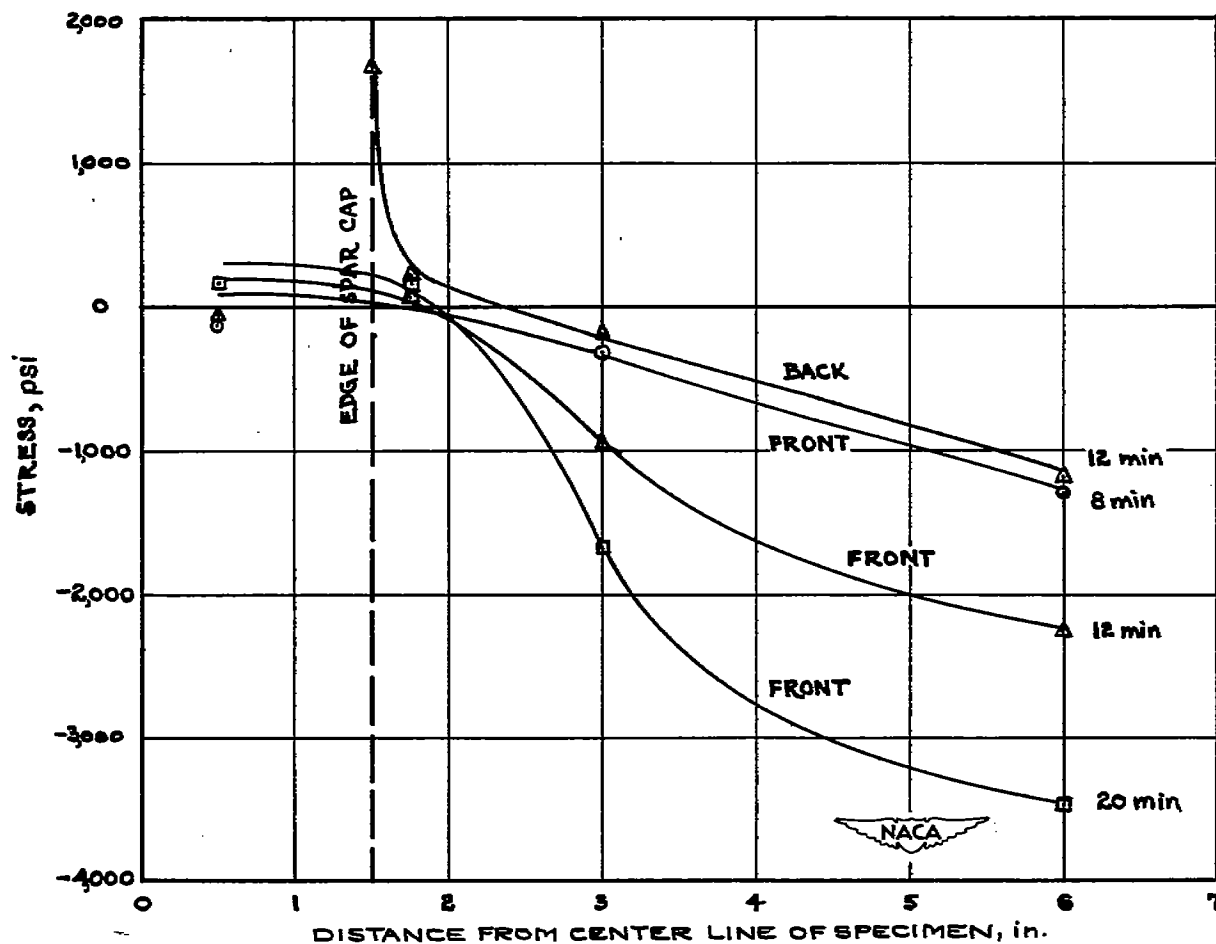
(c) Specimen 3, heating rate A.

Figure 15.- Continued.



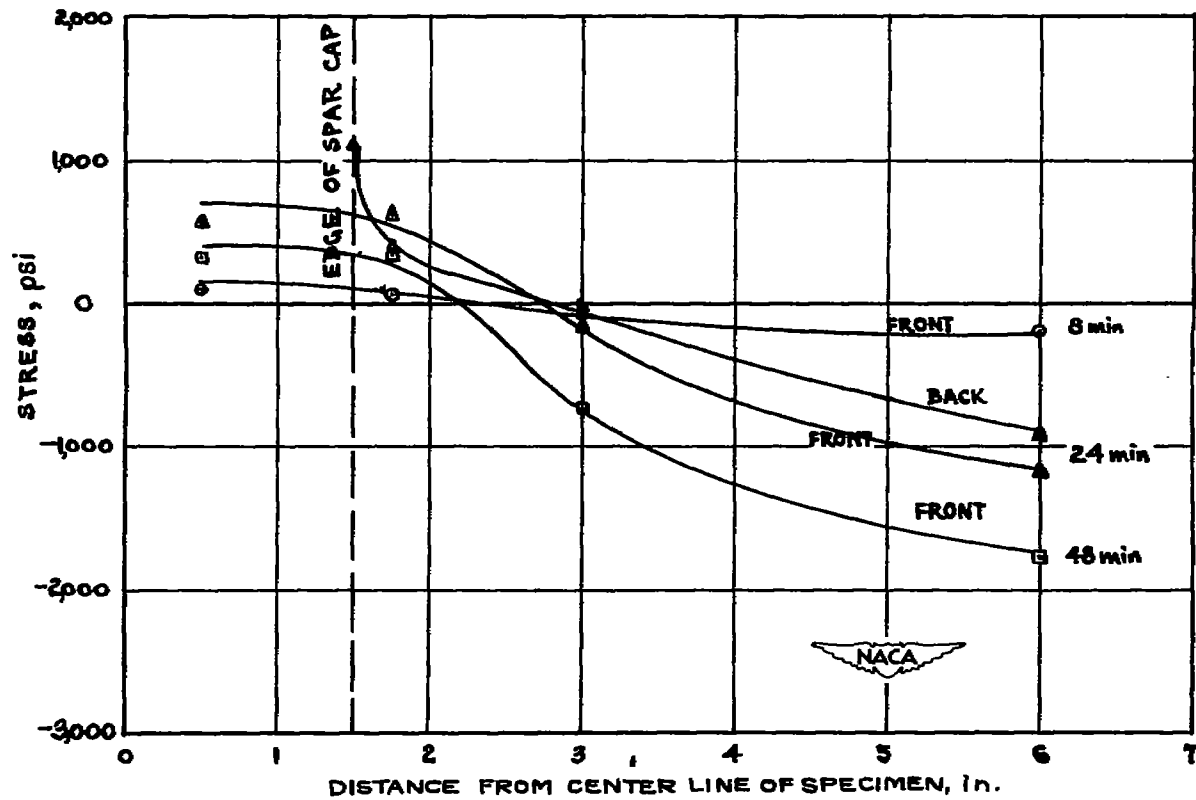
(d) Specimen 3, heating rate C.

Figure 15.- Continued.



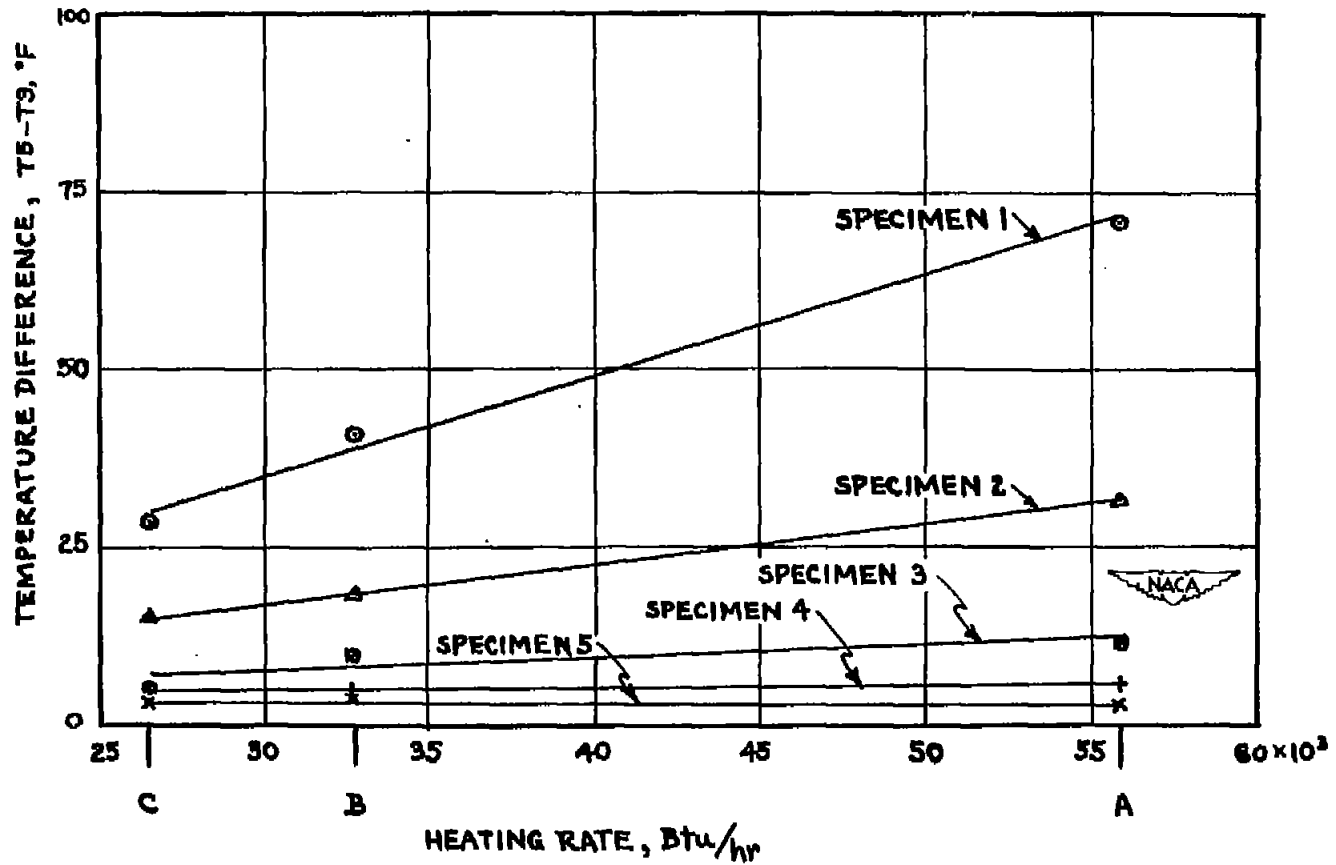
(e) Specimen 5, heating rate A.

Figure 15.- Continued.



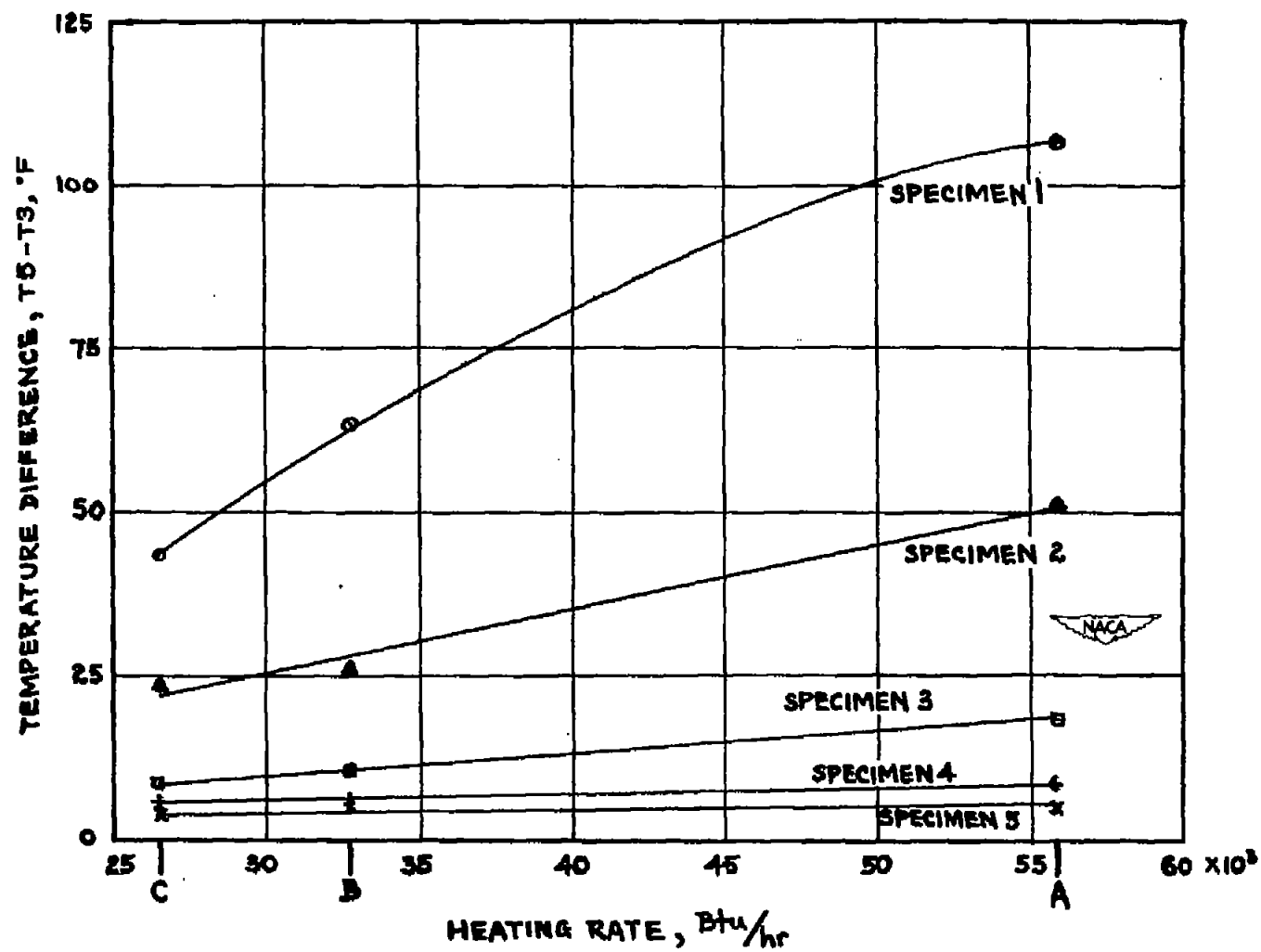
(f) Specimen 5, heating rate C.

Figure 15.- Concluded.



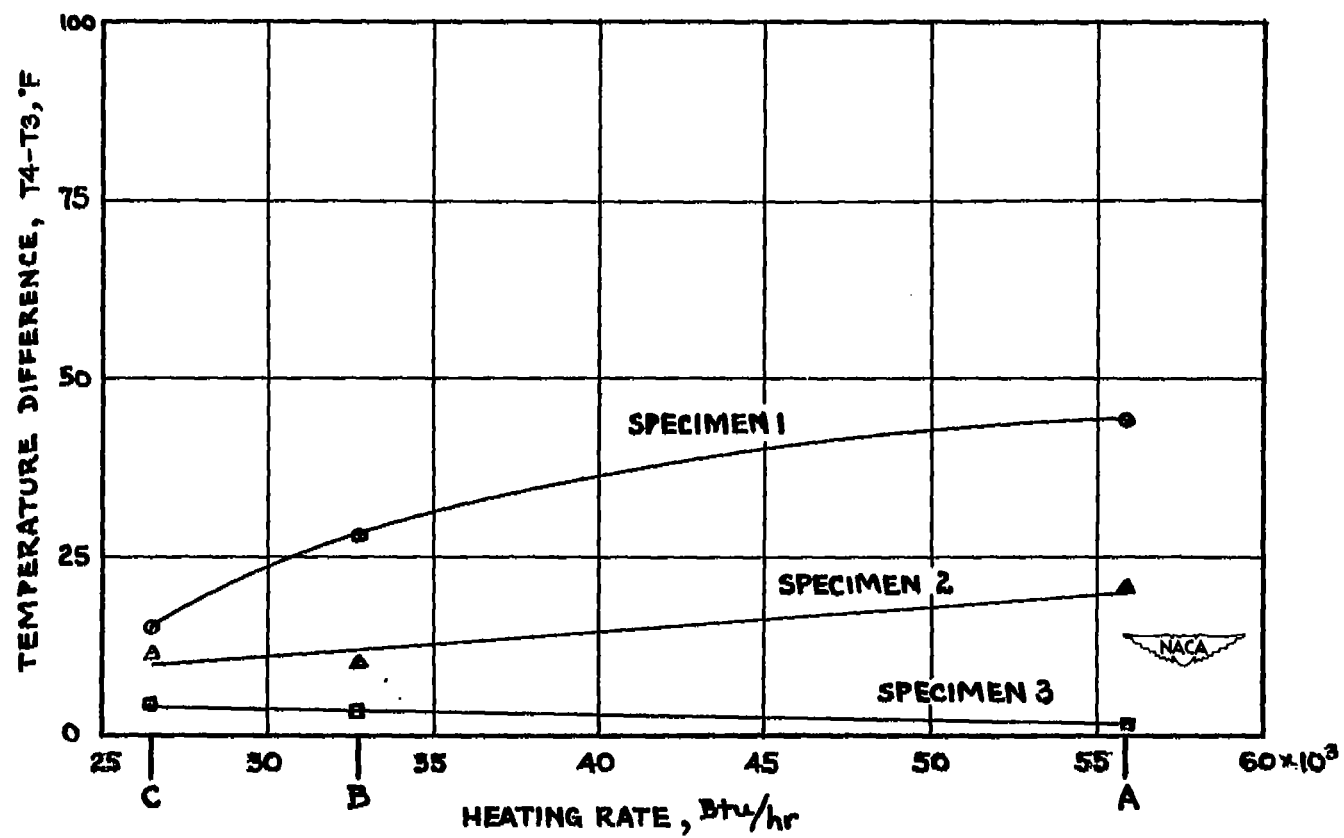
(a) Six minutes, $T_5 - T_3$.

Figure 16.- Temperature differences between skin and spar cap for various elapsed time intervals at three heating rates.



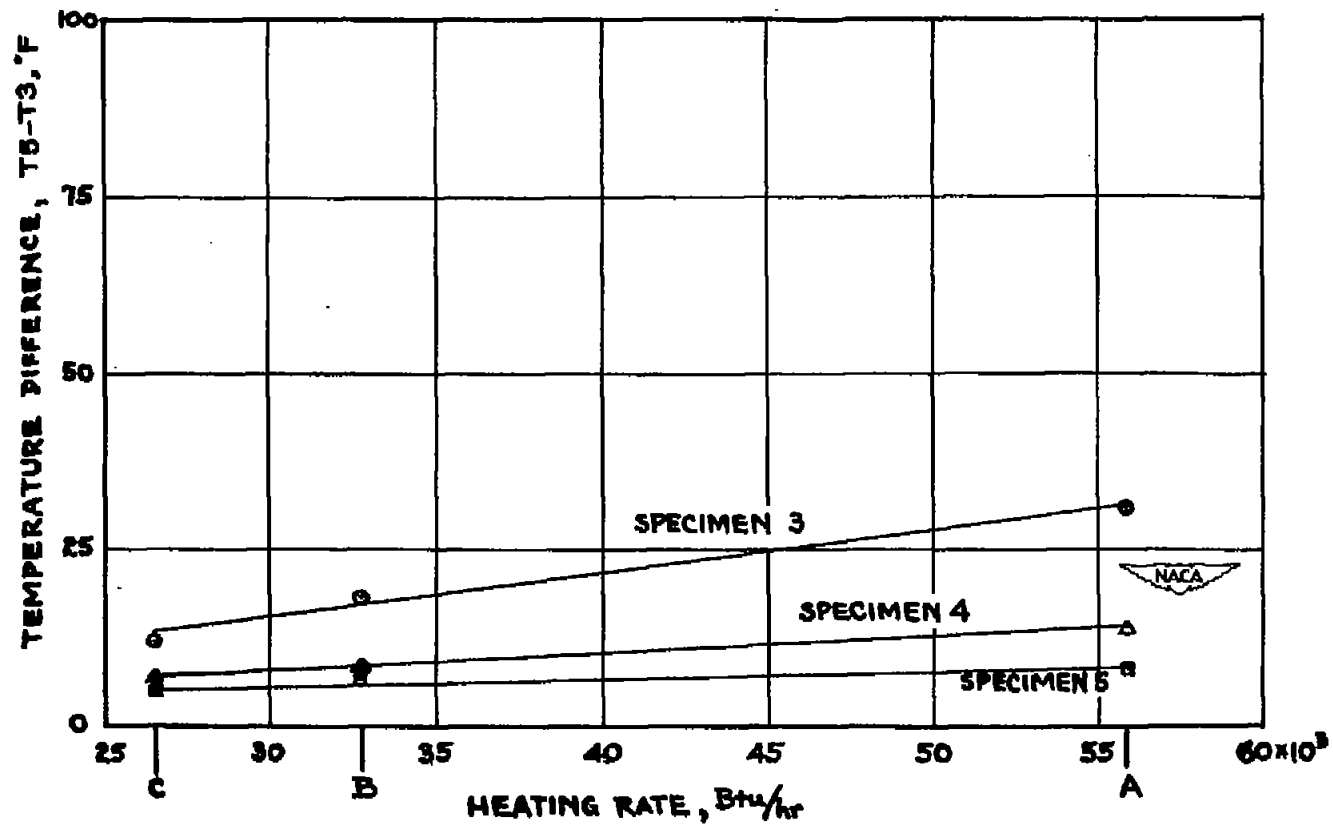
(b) Eight minutes, $T_5 - T_3$.

Figure 16.- Continued.



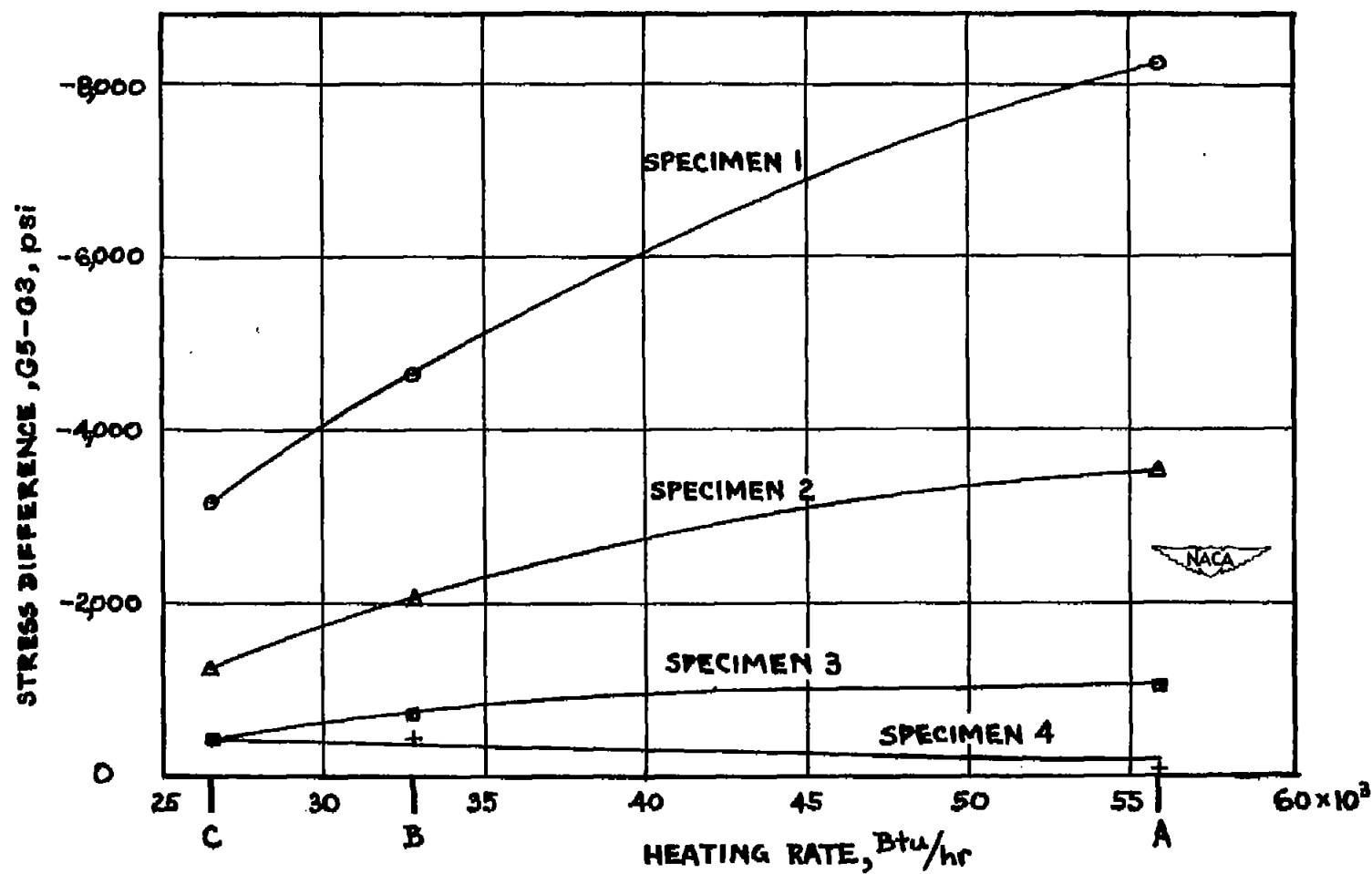
(c) Eight minutes, $T_4 - T_3$.

Figure 16.- Continued.



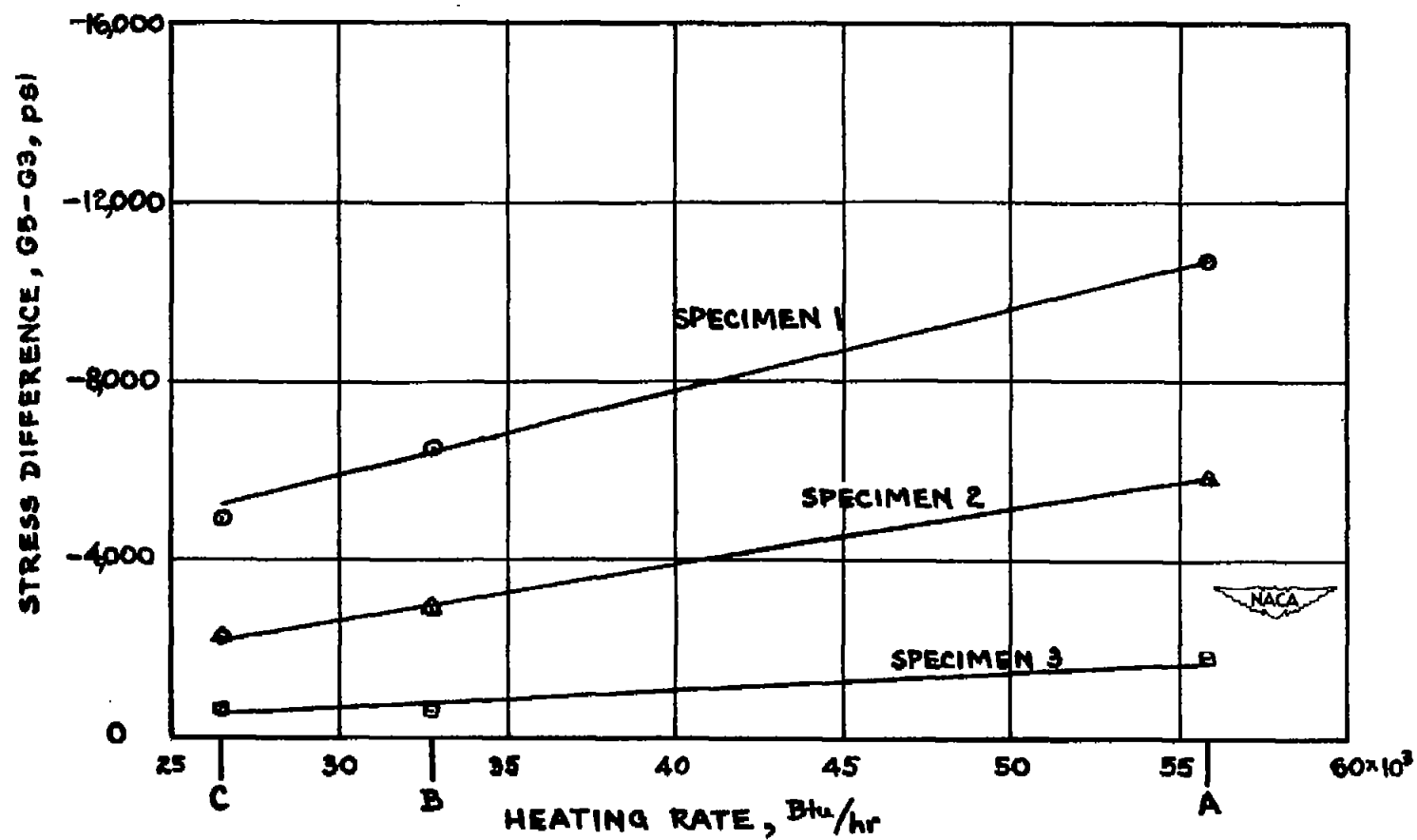
(d) Twelve minutes, T5 - T3.

Figure 16.- Concluded.



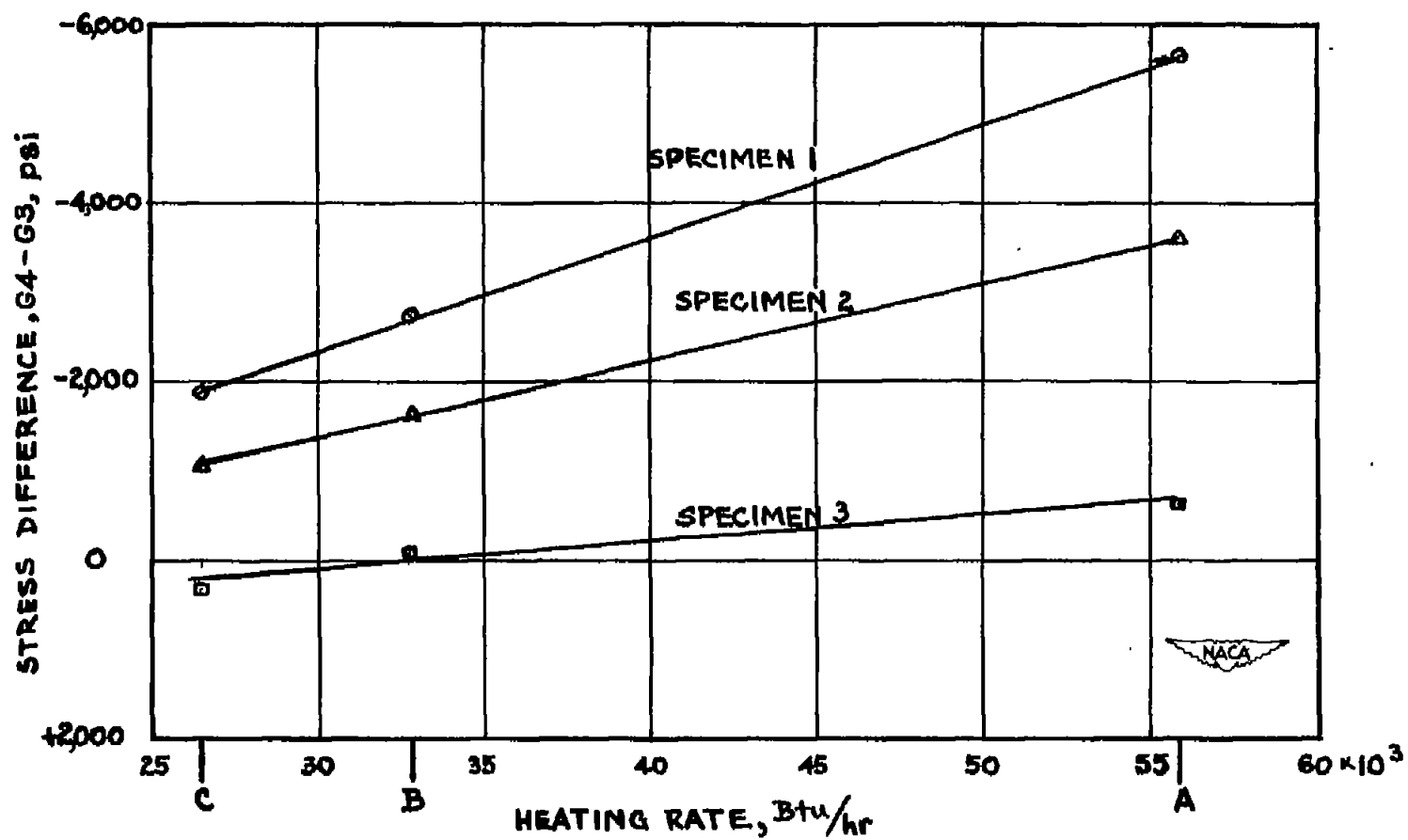
(a) Six minutes, G5 - G3.

Figure 17.- Stress differences between skin and spar cap for various elapsed time intervals at three heating rates.



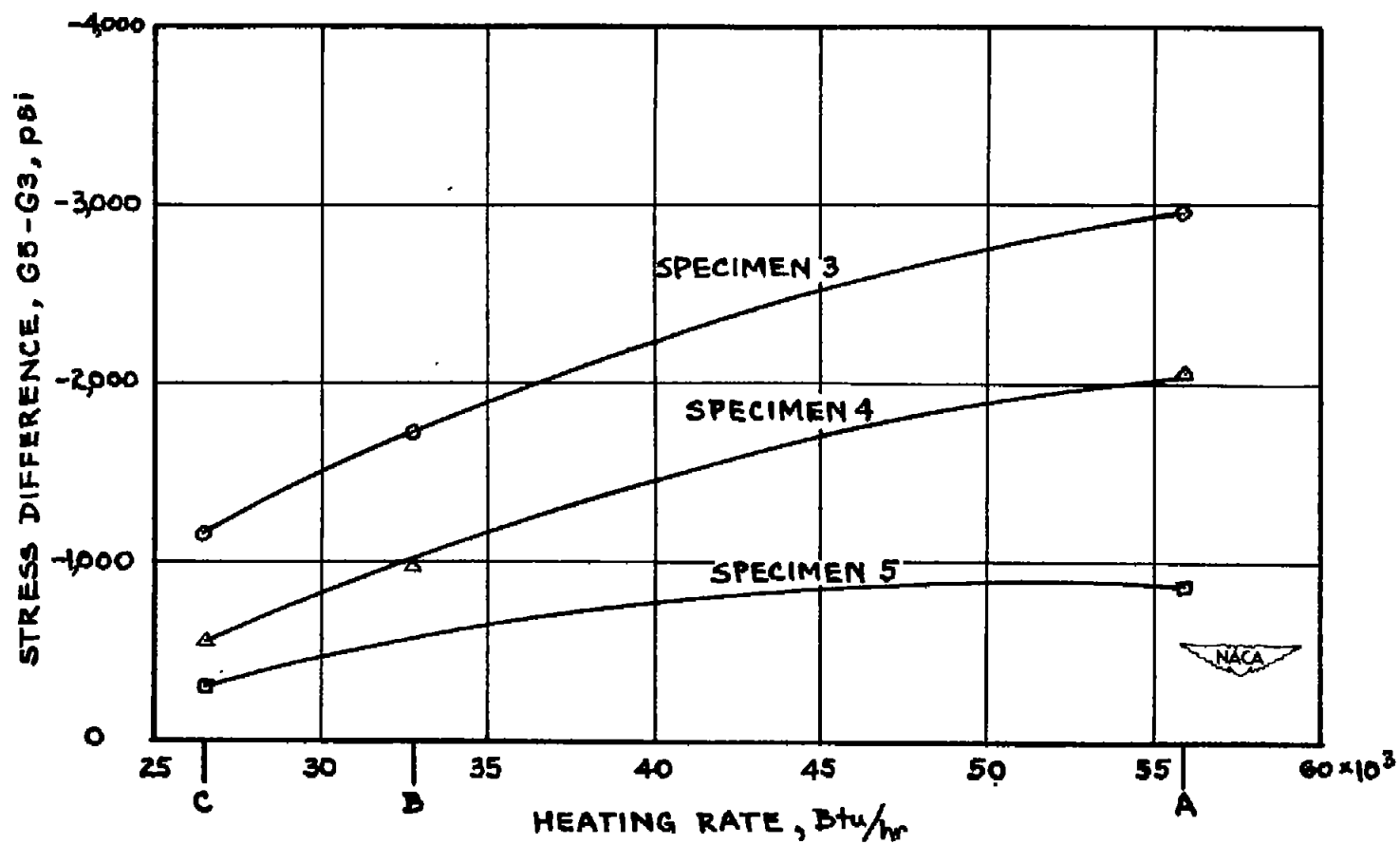
(b) Eight minutes, G5 - G3.

Figure 17.- Continued.



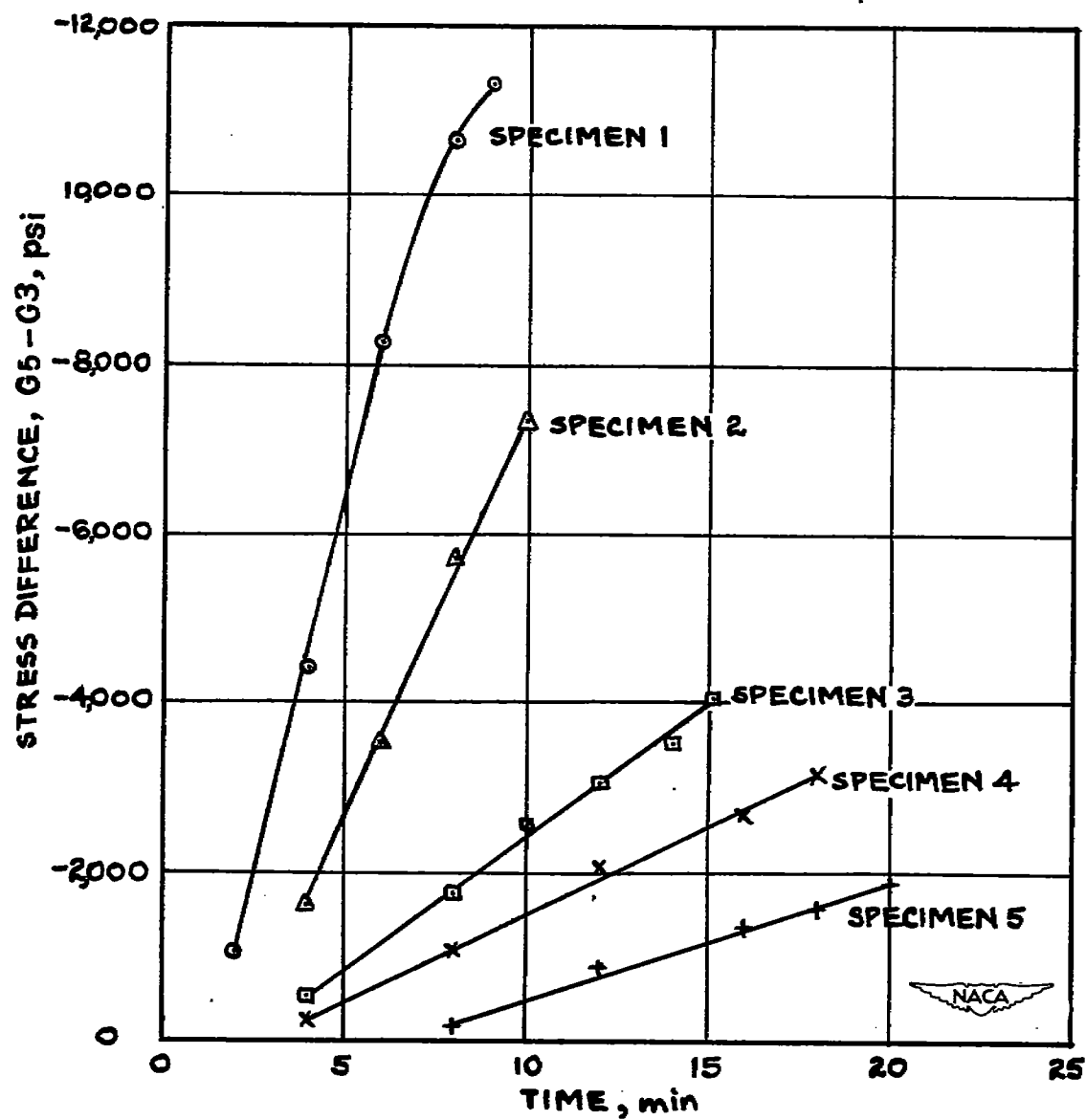
(c) Eight minutes, $G_4 - G_3$.

Figure 17.- Continued.



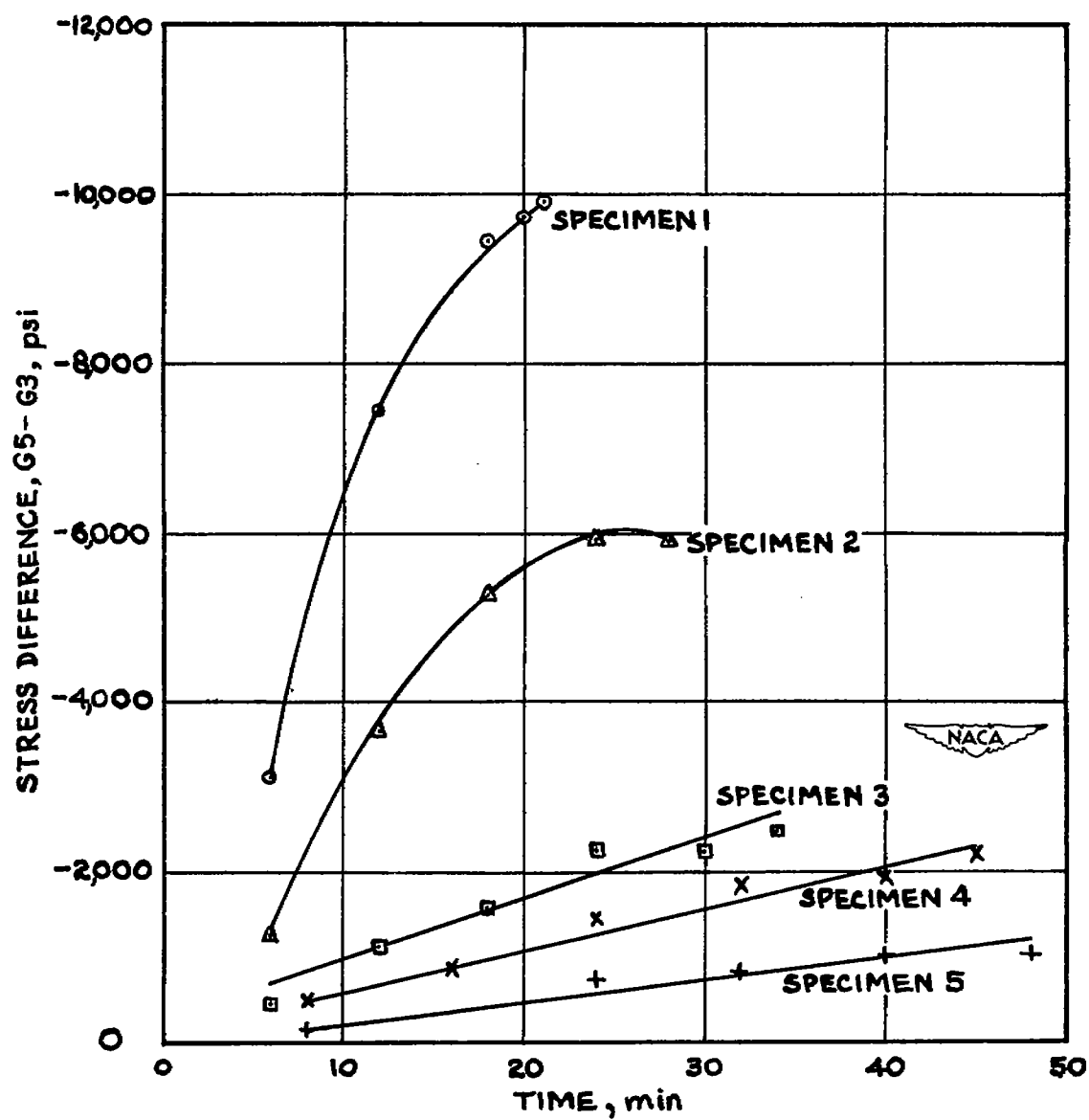
(d) Twelve minutes, G5 - G3.

Figure 17.- Concluded.



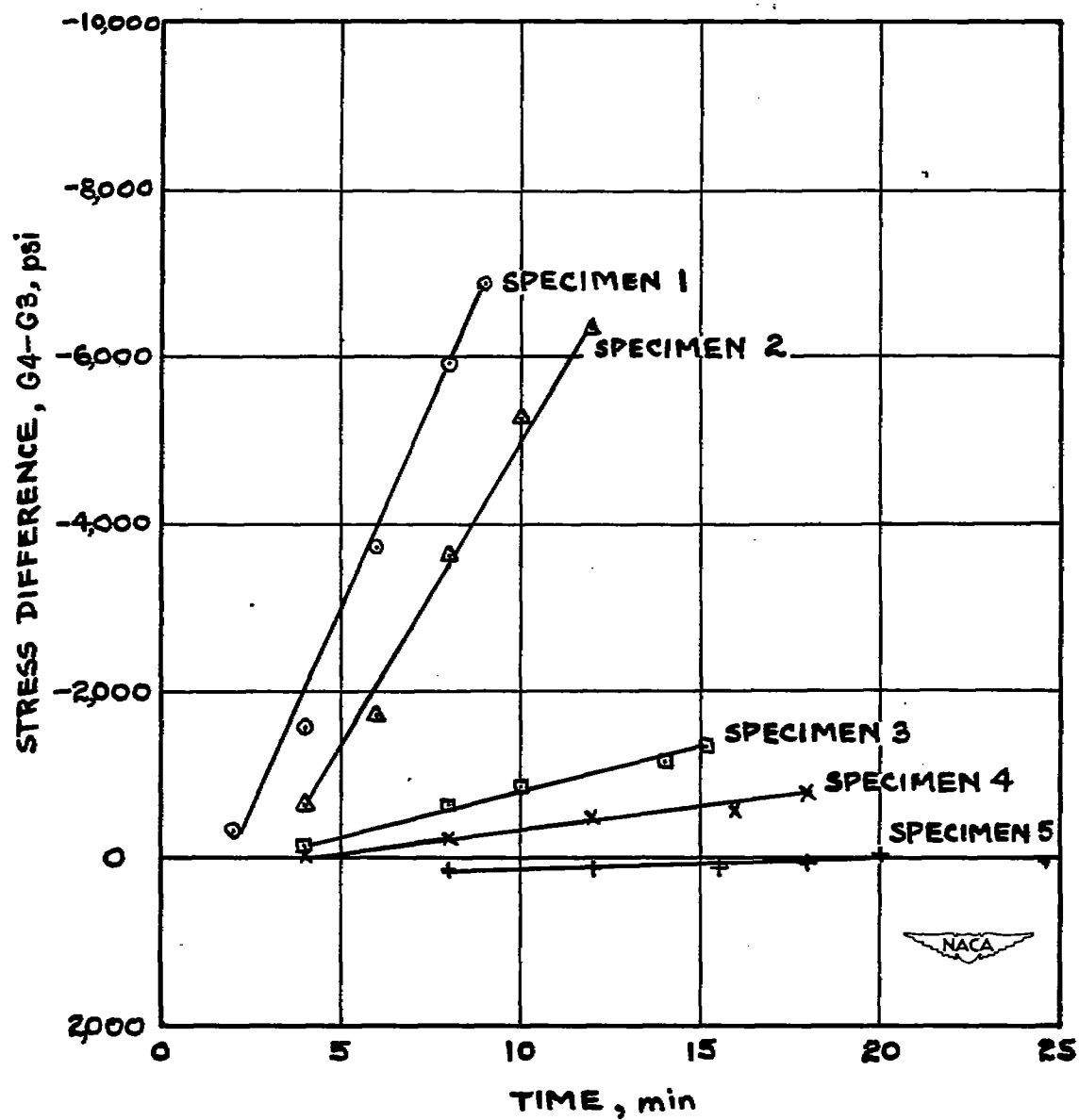
(a) Rate A, G5 - G3.

Figure 18.- Time histories of stress differences between skin and spar cap for five specimens at two heating rates.



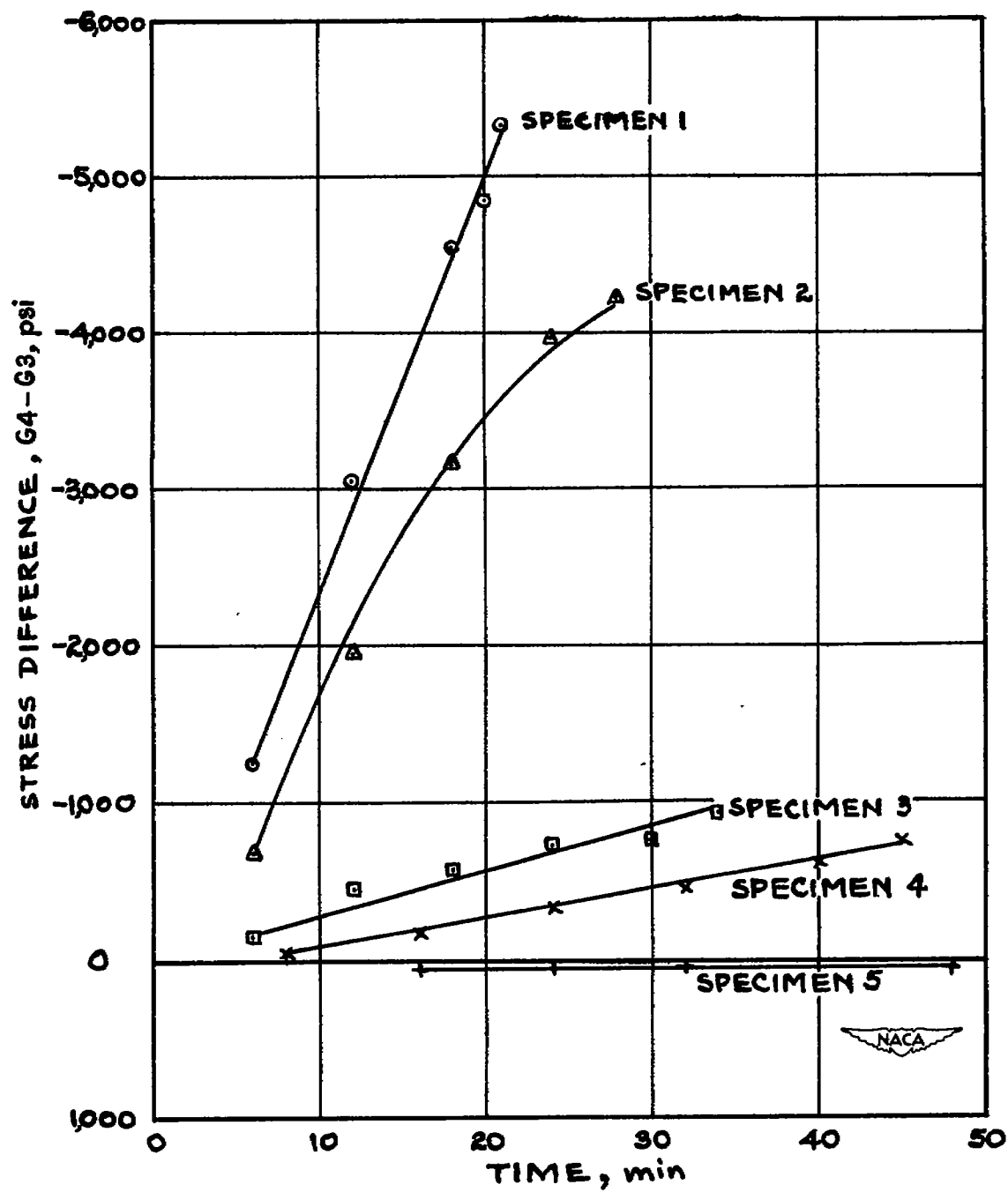
(b) Rate C, G5 - G3.

Figure 18.- Continued.



(c) Rate A, $G_4 - G_3$.

Figure 18.- Continued.



(d) Rate C, G4 - G3.

Figure 18.- Concluded.

NASA Technical Library



3 1176 01434 3777